ABSTRACT

Holtman, Kevin Matthew. An Investigation of the Milled Wood Lignin Isolation Procedure by Solution- and Solid-State NMR Spectroscopy. (Under the direction of Drs. Kadla and Jameel)

Milled wood lignin (MWL) is only a fraction of the total lignin in wood but is useful for lignin studies because it is isolated relatively free of carbohydrates. It is isolated from a finely milled wood powder by solvent extraction and is considered to be the isolated lignin most representative of native lignin. Because it is only a portion of the total lignin this study presents an extensive evaluation of all isolated lignin portions with the goal of studying the whole lignin structure intact in wood. In order to achieve this, solution-state NMR experiments and degradative techniques were performed on soluble lignins to make an estimation of the interunit linkages. The previously insoluble lignin portions were dissolved in a newly developed solvent system and examined by solution-state and solid-state NMR.

A systematic study of the MWL and cellulolytic enzyme lignin (CEL) found they were structurally similar with only minor differences. End groups were somewhat higher in MWL, especially the oxidized moieties. MWL was lower in β-aryl ether content and had a higher degree of condensation than CEL. Carbohydrate analyses indicated that MWL may derive from the middle lamella to a larger extent than CEL. These portions can be combined to create a higher yield of relatively carbohydrate-free lignin.

Lignin isolated from milled wood and REL are normally insoluble however they were dissolved using dimethyl sulfoxide (DMSO)/N-methylimidazole (NMI). Two-dimensional HMQC NMR showed that the milled wood, MWL, and REL were similar from the standpoint

of structural moieties present. Quantitative ^{13}C NMR however showed that MWL had a β-O-4' content lower than that of the wood. Dipolar dephasing solid-state NMR indicated that MWL had a higher degree of condensation. As a result, REL may be more similar structurally to the whole lignin in wood than MWL. The milled wood and REL contain a significant portion of high molecular weight material (~55,000 g/mol) while MWL (~10,000 g/mol) is lower molecular weight.

A solution-state NMR study of different milling techniques indicated that prolonged rotary ball milling results in more structural changes than the standard milling technique. It has been debated whether milling under N_2 results in more structural changes than milling in toluene. This study however clearly shows that there is little difference between these lignins. The wood milled under the N_2 atmosphere is more vigorously milled based on total MWL yield and contains higher aliphatic and phenolic hydroxyl contents.

The modified DFRC method for analysis of the uncondensed aryl ether structures in lignin is inefficient because it does not completely cleave all β-O-4' linkages. DFRC is more inefficient in higher molecular weight materials than in MWL indicating that molecular weight plays a role in either accessibility of chemicals or molecular mobility in the reductive cleavage step. Thioacidolysis completely degrades the β-aryl ether linkages in lignin and is therefore preferable for analysis of these structures.

Although lignin isolated from finely milled wood can be dissolved using the DMSO/NMI solvent system, structural changes still occur. As a result, it is preferable to develop solid-state NMR techniques to analyze lignin structure independent of milling. CP/MAS, DP/MAS, dipolar dephasing, and a newly developed technique to selectively retain methine carbons can be used to obtain in-depth information about lignin structure. Attempts in

the NCSU solid-state NMR facility were incomplete because we did not have the necessary pulse sequence to perform this last experiment. As a result, a collaboration between our group and a solid-state NMR group at Iowa State University has been established. Data obtained in the NCSU facility is presented here while the analysis of the data collected at ISU will be presented in publications.

An Investigation of the Milled Wood Lignin Isolation Procedure by Solution- and Solid-State NMR Spectroscopy

Kevin M. Holtman

A dissertation submitted to the Graduate Faculty of
North Carolina State University
in partial fulfillment of the
requirements for the Degree of
Doctor of Philosophy

Wood and Paper Science

Raleigh, NC, USA
2003

I would like to dedicate this dissertation to my wife, Gretchen, and my family all of whom had a major influence on my life, goals, and ambitions.

BIOGRAPHY

Kevin M. Holtman was born in Asheville, North Carolina on September 29, 1973. After graduating from West Florence High School in Florence, SC, in 1991, he entered North Carolina State University. In the spring of 1996 he received a B.S. degree in Pulp and Paper Technology and a B.A. degree in Chemistry.

After working full time for the Dept. of Wood and Paper Science for a year, he entered the graduate program under the guidance of Drs. John F. Kadla, Hou-min Chang, and Hasan Jameel. During his time in graduate school he interned at Nippon Paper Company in Tokyo, Japan, and Rayonier Corp., Inc., in Jesup, GA.

ACKNOWLEDGEMENTS

The author would like to express his sincere appreciation for the guidance and support he received from Dr. John F. Kadla and Dr. Hasan Jameel, co-chairs of his advisory committee. Their constant encouragement, invaluable advice and constructive criticism were always available when suggestions or stimulating discussions were needed. Their sincere friendship and guidance have made this study enjoyable and memorable.

Sincere gratitude is also extended to Dr. Hou-min Chang and Dr. Jeff L. White for their invaluable assistance and guidance. In addition the author would like to thank Dr. Thomas Joyce for the opportunity to perform research as an undergraduate, an experience which opened the door to graduate school. Finally, the author would also like to thank Dr. Ewellyn A. Capanema, Dr. Hanna S. Gracz, Dr. Mikhail Yu. Balakshin, Dr. Tsutomu Ikeda, and Dr. Satoshi Kubo for their suggestions, stimulating discussions and friendship.

The author expresses his deepest gratitude to Gretchen, for her love, patience, sacrifice and assistance have made this study an enjoyable experience. Special appreciation must also be given to the author's family for their constant support and encouragement throughout this study.

Finally, the author wishes to thank all those faculty members, colleagues and friends who in one way or another have contributed to making this study a successful experience.

TABLE OF CONTENTS

LIST OF FIGURES

LIST OF TABLES

1. Introduction

Lignin in the cell wall is an amorphous copolymer of phenylpropanoid units linked through both ether and carbon-carbon bonds. It provides mechanical support for the plant, as well as facilitating transport of water and nutrients, and providing defense against attack from microorganisms. [1-5] Therefore, elucidation of the complete structure and macromolecular characteristics of the lignin polymer is of interest from the biological perspective. In addition, lignin must be removed in order to produce high-quality printing and writing paper. [6] As a result, the structure of lignin is of great importance for optimizing the processes and understanding the reactions involved in its removal.

For decades, lignin chemists have been attempting to completely isolate lignin from wood in an unaltered form. However polymerization of monolignols occurs within the cell wall, embedded in a polysaccharide gel, producing molecular association and possibly covalent bonds. [4, 7, 8] Therefore quantitative isolation of the complete lignin polymer has proven impossible.

Milled wood lignin (MWL) is isolated after milling disrupts the crystallinity of the cellulose in the cell wall and depolymerizes the lignin and polysaccharide polymers to some extent. [9-12] Solvent can then penetrate the cell wall and extract some low molecular weight lignin at maximum yields of less than 50 % of theoretical. [13] Due to an inability to isolate the whole lignin, MWL has been typically considered to be representative of the structure of native lignin.

Conclusions about the structure of lignin have been largely deduced based upon biosynthetic, spectral, and degradative studies of MWL. One drawback of the study of MWL is that its isolation varies slightly from laboratory to laboratory from the standpoint of the

impact of milling. As a result, it is essential to perform an in-depth study of different milling techniques to determine the extent of structural changes that occur during MWL isolation.

While degradative techniques have proven invaluable in the study of the structure of lignin, they suffer the drawbacks that they supply only partial information about the macromolecule itself. Additionally, it is not known whether the conditions involved in the degradation procedure causes changes in the lignin structure resulting in artifacts that complicate analysis of the data.

The advent of high field nuclear magnetic resonance (NMR) spectrometers and multidimensional NMR techniques has allowed extensive characterization of lignin structure in the solution-state. The advantage of NMR spectroscopy is that the entire soluble lignin polymer can be studied in great detail.

Solution-state NMR spectroscopy has been used to identify several minor components in lignin. [14-17] It has also shown many of the conclusions made by earlier wood chemists to be very accurate. Solution-state NMR thus far has suffered a drawback that all conclusions are based upon only soluble lignins such as MWL, which represents only the easily isolatable lignin in wood.

There have been many reports on the heterogeneous nature of lignin in wood [18-20] and therefore anything less than quantitative isolation of lignin cannot be considered representative. A recently documented technique has been reported which allows for dissolution of the entire cell wall from a finely milled wood by acetylation in DMSO/N-methylimidazole in preparation for characterization by solution-state NMR. [21, 22] Therefore we will attempt to apply this technique to the quantitative estimation of interunit linkages in our milled woods.

The impact of milling on the structure of lignin in wood is not precisely known, limiting the effectiveness of studying even the lignin in a finely milled wood. It is widely held that Wiley wood meal is not milled extensively enough to alter the structure of the lignin in wood. As a result, we will attempt to perform an in-depth analysis of the structure of lignin in Wiley wood meal and later in solid wood by solid-state NMR. Solid-state NMR has not received a lot of interest in the study of lignin because signals in the spectrum are very broad and little detailed information about the lignin structure can be obtained. Recently developed techniques however will enable us to study the structure of lignin in wood meal by means of quantitative selection of different types of carbons in the NMR spectrum. [23-27]

As a result this document will report on the evaluation of the different milling techniques and their effects on the lignin structure. Additionally, all isolated lignin fractions will be evaluated where possible with solution-state NMR. Finally, the progression of experimental techniques towards the development of a protocol for analysis of the total lignin in wood will be detailed.

2. Introduction to Lignin

The term lignin is derived from the Latin word *lignum* meaning wood and while it is not the major component of wood, it nonetheless serves an essential function in the cell wall of all vascular plants. [1] In 1838, Anselme Payen observed that upon treatment of wood with nitric acid, a portion disappeared leaving solid, fibrous residue. He explained the soluble portion, which contained a higher carbon content than the solid residue, as being an encrusting material. [28] In 1907, Klason proposed that lignin is a polymer consisting of coniferyl alcohol units joined together by ether linkages. Thus the idea of the lignin macromolecule had been born and the era of modern lignin chemistry had begun. [29]

Lignin comprises from 15 -36 % of the total weight of wood and is arguably the second most common biomass component found on Earth. [30] While Payen's assertion that the acid-soluble portion is an encrusting material is correct, lignin serves several vital functions in vascular plants. Lignin provides mechanical strength and structural support, particularly in the case of trees, to the growing plant. Lignin prevents the permeation of water across the cell wall, thus facilitating conduction of water and nutrients in the xylem tissue. Finally, lignin provides the plant a natural defense in the form of a barrier against the penetration of microorganisms into the tree. [1]

2.1 The Phenylpropane Unit

Lignin is formed by polymerization of *p*-hydroxycinnamyl alcohol units. **Figure 2.1** depicts the three primary precursors of lignin, *p*-coumaryl alcohol, coniferyl alcohol, and sinapyl alcohol. As a result, lignin is an aromatic biopolymer with propane sidechains which are referred to as phenylpropanoid units. **Figure 2.2** illustrates the correct terminology for

the labelling of the aromatic and sidechain carbons. Structural information about lignin is often reported on a C_9 basis, indicative of this typical phenylpropanoid structure. While wood chemists have adopted their own nomenclature, **Figure 2.2(a)**, the more correct IUPAC labelling is shown in **Figure 2.2(b)**. Henceforth in this manuscript the traditional wood chemistry nomenclature will be used to convey structural information. [31]

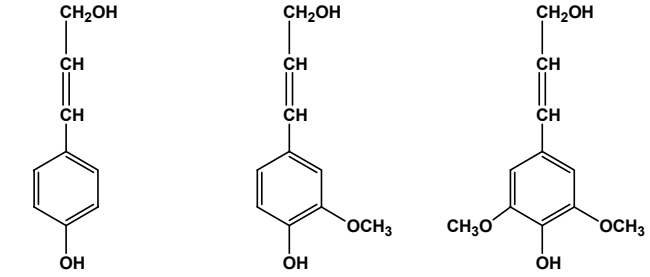

PRECURSORS			
GYMNOSPERMS	-	+	-
ANGIOSPERMS			
Dicotyledons	-	+	+
Monocotyledons	+	+	+

Figure 2.1 The primary lignin precursors.

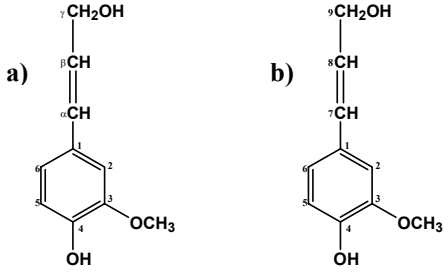

Figure 2.2 Labelling convention for monolignols, a) wood chemistry terminology and b) IUPAC nomenclature.

2.2 Lignin Biosynthesis

2.2.1 Introduction

Vascular plants have the ability to absorb CO_2 and water, and with the energy gained through photosynthesis, convert these basic compounds into simple sugars. The simple sugars can be then either be used to fuel various biosynthetic processes or stored for later use. This process is called carbon fixation and is key in the biosynthesis of lignin. [32]

Plants convert a significant portion of the sugars produced by photosynthesis into the phenylpropanoid precursors in lignin polymerization described in **Figure 2.1**. Early plants did not produce lignin and there is evidence that the evolution of these pathways was a major step in plant evolution and played a fundamental role in the adaptation of plants to living on land. It is likely that lignin initially functioned as an antimicrobial agent based upon the detection of lignin in ancient algae. [5]

Sugars such as glucose are converted into the lignin precursors, the *p*-hydroxy cinnamyl alcohols, by a two-step sequence of reactions known as the shikimic acid pathway and the lignin precursor pathway. The shikimic acid pathway involves the conversion of glucose into L-phenylalanine, an aromatic amino acid produced by all higher plants. This is a primary metabolic process and the L-phenylalanine produced is used in many different metabolic pathways in plants.

Lignin is a product of secondary metabolism and shares a common precursor, phenylalanine, with other metabolites including flavonoids, coumarins, stilbenes, and lignans. (**Figure 2.3**) At this point the pathways to the production of these different metabolites split. In the case of lignin, the L-phenylalanine is converted to the three *p*-hydroxycinnamyl alcohols and is known as the lignin biosynthetic pathway.

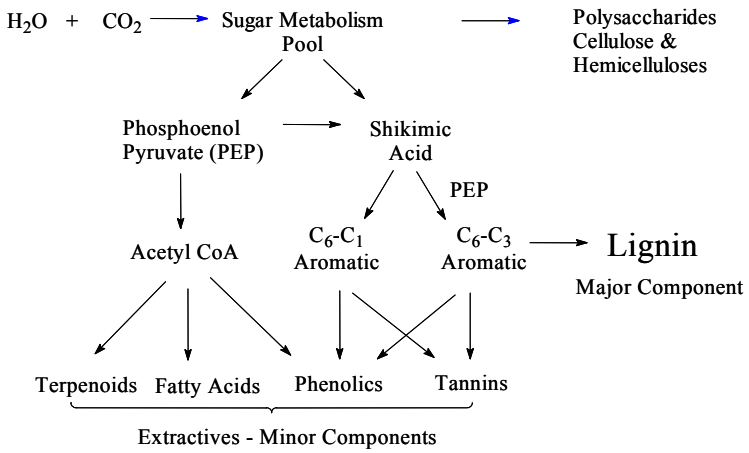

Figure 2.3 Primary and secondary metabolic pathways leading to the biosynthesis of lignin and wood components.

Recently, lignin and lignification have become very active areas for research of biological processes. Many of the new studies have involved either identification of new, alternate pathways in lignin biosynthesis, and/or attempts to genetically manipulate lignin structures based upon these pathways. [33-37]} New reports indicate that a facile change in the lignin biosynthetic pathway may have a dramatic effect on lignin structure. [38] Furthermore, manipulation may cause different monomers to be introduced into the lignifying zone. As a result, the lignification may be a much more flexible process than originally believed. [39-41] If this is true, there may be many interesting applications of genetic modification of lignin structure.

2.2.2 Shikimic Acid Pathway

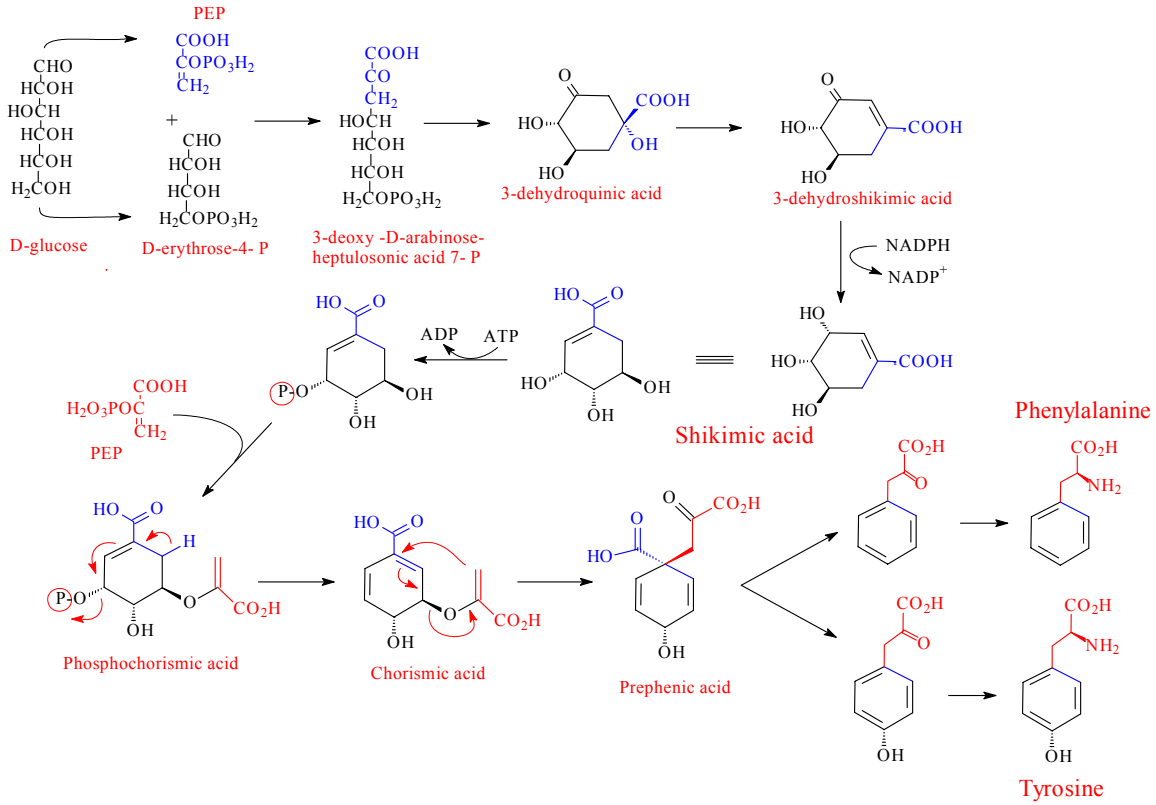

Figure 2.4 Shikimic acid pathway.

Figure 2.4 outlines the steps in the shikimic acid pathway. The first step in the shikimic acid pathway is the formation of 3-deoxy-D-arabino-heptulosonate-7-phosphate (DAHP) via condensation of phosphoenol pyruvate (PEP) and erythrose-4-phosphate (ery-4-P) mediated by DAHP synthase. PEP and erythrose-4-phosphate are each formed from glucose via the glycolytic and pentose phosphate pathways, respectively. As a result, even though the lignin precursors will eventually be formed from glucose, the pathway is not straightforward but rather the combination of several pathways. The glycolytic and pentose phosphate pathways will not be discussed in detail, however, all steps of these pathways are known and can be easily referenced. [32]

DAHP cyclizes and is then reduced by 3-dehydroquinate synthase to 3-dehydroquinic acid. The next step, formation of 3-dehydroshikimic acid, involves 3-dehydroquinate dehydratase and creates one of the three double bonds that will eventually be incorporated into the aromatic ring. Reduction of the ketone by shikimate dehydrogenase to an alcohol produces shikimic acid. The next three steps serve to form a second double bond and to introduce the sidechain. A phosphate group is added at the C_3 position by shikimate kinase forming shikimate-3-phosphate and a PEP group at the C_5 position to form 5-enolpyruvylshikimate 3-phosphate (EPSP) by the enzyme EPSP synthase. The PEP group will eventually be modified to become the propane sidechain. Finally, the phospo group is eliminated by a process mediated by chorismate synthase to create the second double bond, and the product is known as chorismate. In the field of biochemistry, chorismate is the final step in the shikimic acid pathway as chorismate is the precursor for other metabolites such as quinates and folates. [42] However, in the case of wood chemistry, the shikimic acid pathway is considered to involve production of the aromatic amino acids.

The final three steps convert chorismate to L-phenylalanine. Chorismate mutase catalyzes a rearrangement with the sidechain carbons migrating from the C_5 to C_1 is the first step and produces prephenic acid. A transamination step at the carbon destined to become C_β, followed by a reduction involving the loss of CO_2 from the C_1 position and water completes the biosynthesis of L-phenylalanine. This is a two-step process with the first step mediated by an enzyme known as aromatic aminotransferase to form L-arogenic acid. The second step then forms L-phenylalanine via the enzyme arogenate dehydratase. [43]

Brown and Neish were the first to demonstrate the incorporation of glucose via the shikimic acid pathway using radioactive glucose labelled at the C_1 and C_6 positions. [44] As

mentioned above, glucose is not directly incorporated into the shikimic acid pathway, instead it is incorporated through PEP and erythrose-4-phosphate. Therefore DAHP carries the radioactive labels at C_3 and C_7 as the C_3 in PEP and C_4 in erythrose-4-phosphate are derived from C_1 and C_6 in glucose. (**Figure 2.4**) Cyclization would then dictate that the eventual labels on the aromatic ring will be at the C_2 and C_6 carbons. In addition, the incorporation of the additional PEP will introduce another radioactive label at the eventual C_α position on the phenylpropane sidechain.

2.2.3 Biosynthetic Pathway for Primary Lignin Precursors

The shikimic acid pathway to L-phenylalanine described above is a primary metabolic pathway. The lignin biosynthetic pathway however is an example of secondary metabolism. L-phenylalanine is transformed in higher plants to the main lignin precursors discussed previously through a series of enzyme-mediated reactions. It should also be noted that some grasses also employ L-tyrosine in the lignin biosynthetic pathway, probably as a shortcut to *p*-coumaryl alcohol.

Figure 2.5 outlines in red the classical biosynthetic pathway from L-phenylalanine to the main lignin precursor in gymnosperms, coniferyl alcohol. The first step is deamination via the enzyme phenylalanine ammonia lyase to produce cinnamic acid. This is followed by a hydroxylation at the *para* position on the aromatic ring. This is facilitated by the enzyme cinnamate-4-hydroxylase (C4H) and results in the creation of *p*-coumaric acid. This is the first point at which the lignin precursor pathway can branch. A series of alternating hydroxylation and methylation steps can convert the *p*-coumaric acid into the mono- and dimethoxylated analogs, ferulic acid and sinapic acid. This is achieved by hydroxylation of

the C_3 position by *p*-coumarate-3-hydroxylase (C3H) to form caffeic acid followed transmethylation of the C_3 hydroxyl group via O-methyl transferase (OMT) to produce ferulic acid. This step can be basically repeated by addition of a hydroxyl group at the C_5 position followed by transmethylation to produce sinapic acid. These reactions are facilitated by ferulate-5-hydroxylase (F5H) and OMT, respectively. [5]

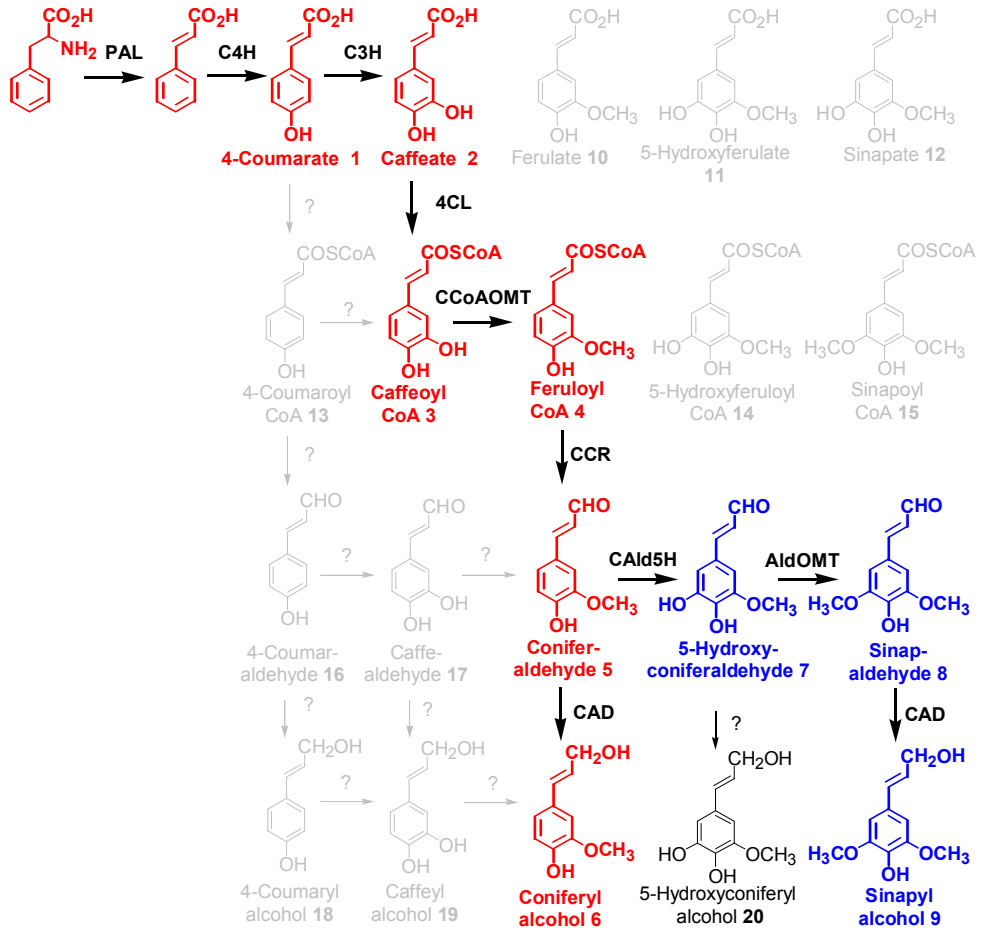

Figure 2.5 Biosynthetic pathway to lignin precursors.

As mentioned above, *p*-coumaric acid results in the first branching point in the lignin biosynthetic pathway. 4-coumarate:CoA ligase (4CL) catalyzes the formation of a thioester at the C_γ position on the side chain to form *p*-coumaroyl-CoA. Analogously 4CL can also

catalyze the formation of feruloyl-CoA from ferulic acid. It however shows little specificity to sinapic acid and the enzyme for formation of sinapoyl-CoA has not been identified. [45] The recent identification of the enzyme coniferaldehyde 5-hydroxylase, which has been shown to catalyze the hydroxylation coniferaldehyde, indicates that the lignin biosynthetic pathway instead prefers to follow the pathway highlighted in blue in **Figure 2.5** to produce sinapyl alcohol. [35-37] After hydroxylation, COMT catalyzes the methylation to form sinapaldehyde.

The final two steps in the lignin biosynthetic pathway involve the reduction of the various coenzyme thioesters to their cinnamyl alcohol counterparts. Cinnamoyl-CoA reductase (CCR) catalyzes the reduction of the thioesters to the corresponding aldehydes, *p*-coumaraldehyde, coniferaldehyde, and sinapaldehyde. CCR seems to show relatively the same specificity for all hydroxycinnamyl thioesters. The last step involves the reduction of the aldehyde to the final lignin precursors. This is achieved by cinnamyl alcohol dehydrogenase (CAD). CAD in gymnosperms is generally more responsive to coniferaldehyde whereas those in angiosperms react equally to coniferaldehyde and sinapaldehyde. [46] Chiang, et al., however have recently demonstrated that sinapaldehyde is reduced by the enzyme sinapyl alcohol dehydrogenase (SAD) in angiosperms. [37]

2.2.4 Transport of monolignol glucosides into the lignifying zone

Monolignols are not found in abundance in the lignifying zone but are found as monolignol glucosides, known as coniferin in gymnosperms. (**Figure 2.6**) The monolignol glucoside increases the solubility of the monomer as well as reducing its toxicity. [5] The monolignol

glucoside is cleaved in the lignifying zone by a β-glucosidase to free the phenolic hydroxyl allowing for dehydrogenative polymerization. [47]

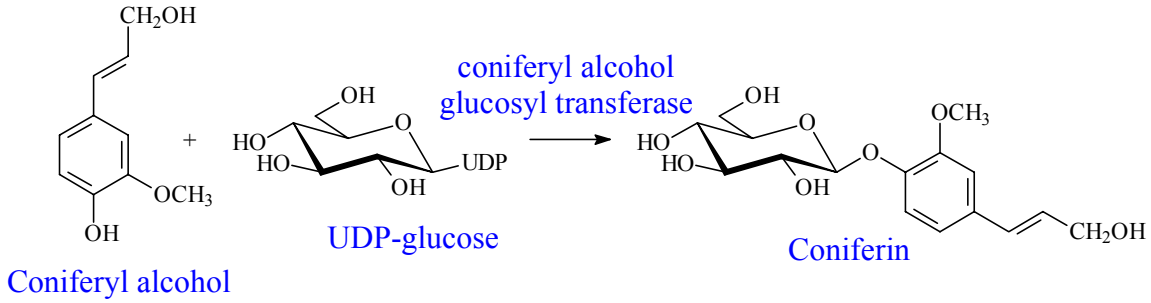

Figure 2.6 Monolignol glucoside formation.

2.3. Polymerization of Monolignols

In 1939, Erdtmann proposed that the lignin macromolecule is formed by a coupling reaction of phenoxy radicals of coniferyl alcohol formed by enzymatic dehydrogenation. [48] Freudenberg et al., confirmed this hypothesis and demonstrated that a system of laccase/O_2 or peroxidase/H_2O_2 can abstract an electron from the phenolic hydroxyl of coniferyl alcohol to form a phenoxy radical. (**Figure 2.7**) [49]

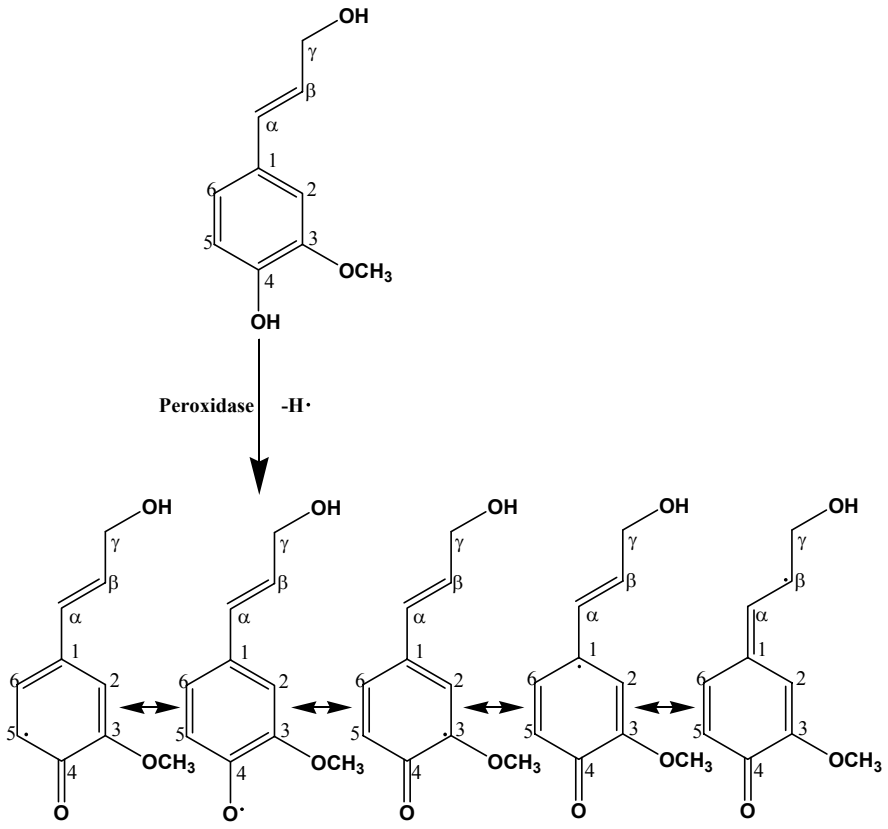

Figure 2.7 Dehydrogenative polymerization of lignin monomers.

This phenoxy radical has five resonance-stabilized mesomeric forms, depicted in **Figure 2.7**. The actual radical coupling process of monomers is not enzyme mediated and as a result, lignin lacks a true repeating unit. Therefore there are 15 possible intermonomeric

linkages that can be formed based upon the *p*-hydroxycinnamyl alcohol mesomers and the probability of formation of these linkages depends upon sterics, electronic effects, and solvation. [50] Radical coupling therefore occurs based upon the scheme shown in **Figure 2.8**. Coupling of two monomers results in the formation of a dimer, which can be further polymerized by addition of another monomer to form a trimer or another dimer to form a tetramer. This process continues to form oligomers and ultimately the three-dimensional lignin polymer. The most prominent of the interunit linkages in lignin are shown in **Figure 2.9**.

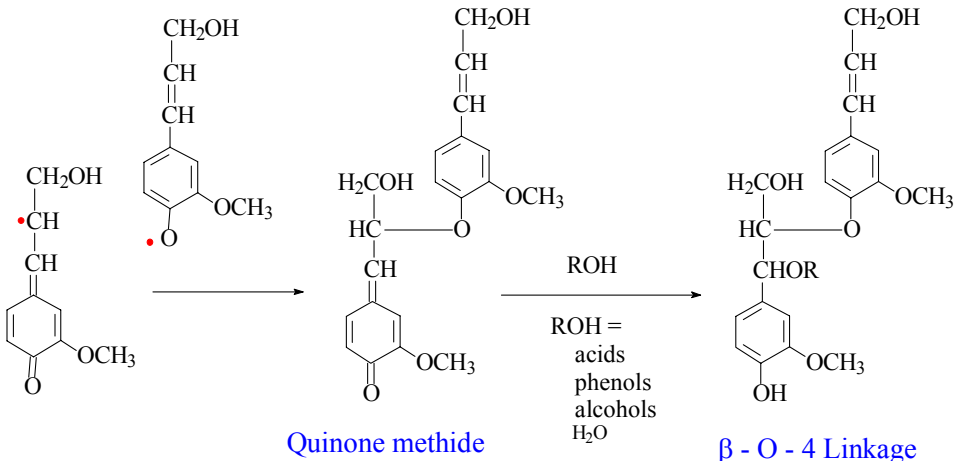

Figure 2.8 Radical Coupling in Lignin Polymerization.

Table 2.1 Relative frequency of interunit linkages reported per C_9 unit in some softwood lignins.

Linkage Type	Freudenberg [51]	Adler[198]	Sakakibara [52]	Glasser and Glasser[53]
β-O-4'	35	48	43	55
α-O-4'	20	6-8	11	
β-5'	15	9-12	14	16
β-1'	0	7	11	9
5-5'	15	9.5-11	21	9
4-O-5'	5	3.4-4	7	3
β-β'	10	2	14	2

The relative frequencies of the most common interunit linkages in some softwood lignins are shown in **Table 2.1**. Discrepancies between estimations may result from differences in species or techniques used to quantify these linkages.

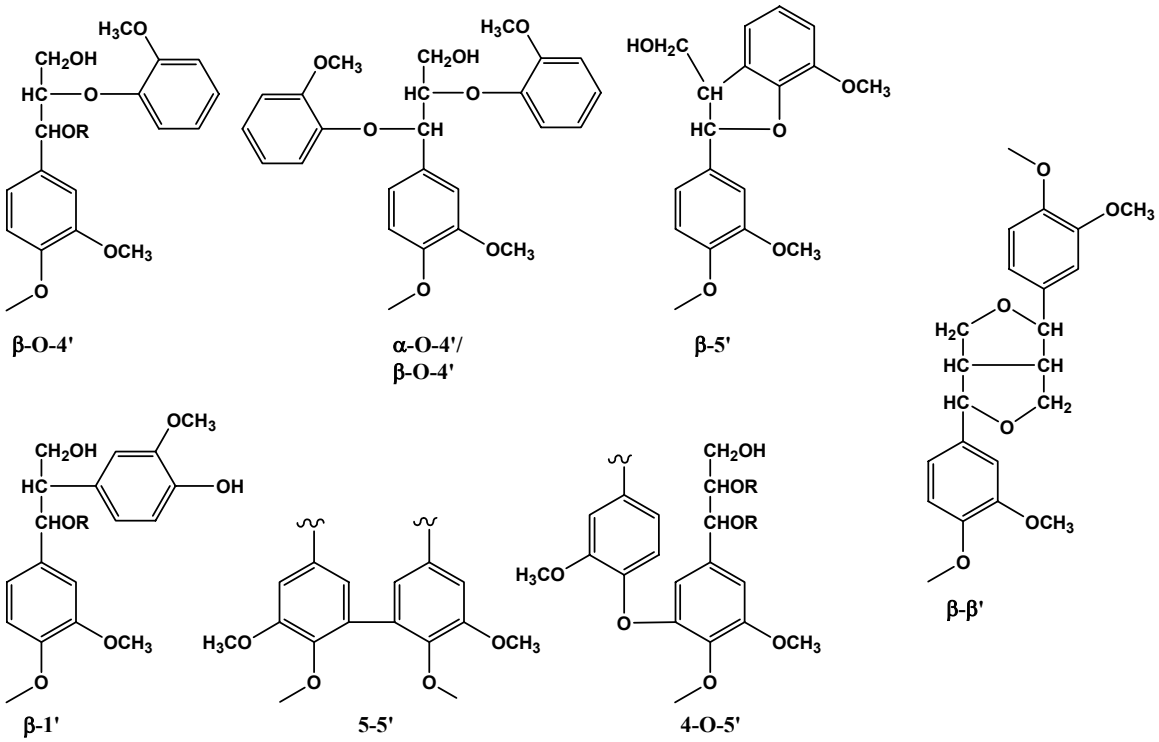

Figure 2.9 Prominent interunit linkages in lignin.

2.3.1 Classification of Lignin

As discussed in the previous section, the lignin polymer is formed from polymerization of the three lignin precursors depicted in **Figure 2.1**, further contributing to the complexity of the lignin polymer. The types of lignin are classified based upon their monolignol origin, i.e., lignin arising from primarily *p*-coumaryl alcohol are referred to as *p*-hydroxyphenyl (H) units, guaiacyl (G) units from coniferyl alcohol, and syringyl (S) units from sinapyl alcohol. The qualitative differences between the different types of lignin are

obvious; H units contain zero methoxyl groups, G units contain one methoxyl at the C_3 position, and S units 2 methoxyl groups at C_3 and C_5. While these differences may seem minor, they provide a dramatic difference in lignin polymer structure based on probability of interunit linkages.

Figure 2.1 also reveals some of the differences in the heterogeneity in lignins from different plant sources. Gymnosperms (softwoods) are comprised of primarily guaiacyl-type lignin with only small amounts of H and S units. A typical structural model for a typical softwood is given in **Figure 2.10**.

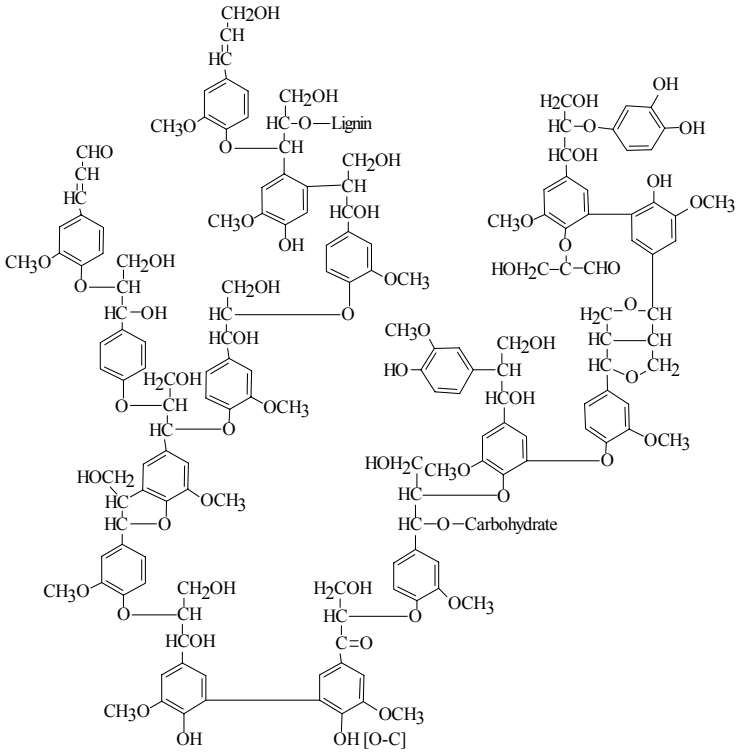

Figure 2.10 A structural model for softwood. [52]

Angiosperms (hardwoods) are often referred to as guaiacyl-syringyl lignins, meaning that they contain significant proportions of each type of lignin. Hardwoods will also contain

small amounts of *p*-hydroxyphenyl lignin. **Table 2.2** shows the relative differences in distribution of interunit linkages between lignins from spruce (softwood) and birch (hardwood). As can be seen there are higher levels of uncondensed, etherified structures such as β-O-4' linkages and lower levels of condensed structures, i.e., 5-5' and β-5', in hardwoods. This is directly attributable to the increased C_5 methoxyl units in syringyl units. During polymerization, this site is not readily available for radical coupling and as a result a higher incidence of particularly β-O-4' linkages are observed.

Table 2.2 Frequency of interunit linkages per C_9 unit for spruce and birch wood lignins.[31]

	β-O-4'	α-O-4'	β-5'	β-1'	5-5'	4-O-5'	β-β'
Spruce	48	6-8	9-12	7	9.5-11	3.5-4	2
Birch	60	6-8	6	7	4.5	6.5	3

2.3.2 The Ultrastructure of Wood

Wood consists mainly of cellulose, hemicellulose, and lignin. The cellulose is composed of microfibrils and the hemicellulose and lignin are deposited in the spaces between the microfibrils. Cellulose contains both crystalline and amorphous regions while the hemicellulose and lignin are amorphous.

2.3.3 Distribution of Components in the Cell Wall

The cell wall consists of several layers which are depicted in the classical representation in **Figure 2.11**. The layers of the cell wall from outer to inner are as follows: middle lamella (ML), the primary wall, the secondary wall (divided into the S_1, S_2, and S_3 layers), and the hollow inner region called the lumen. The layers of the secondary wall differ

based on the thickness of the cell wall layer and the microfibril angle. Both of these aspects will be discussed below.

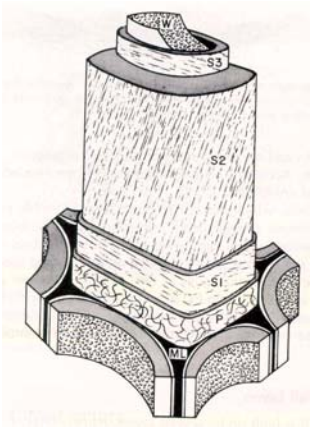

Figure 2.11 Structure of the cell wall in wood showing the middle lamella (ML), the primary wall, the outer (S_1), middle (S_2), and inner layers (S_3). [29]

As the cell divides it initially forms a cell plate, which is made of primarily pectic substances such as 1,4-α-polygalacturonic acid. The new cells enclose upon themselves to form primary walls. Next the cells grow to their final size after which the secondary wall begins to thicken. As the secondary wall forms, deposition of cellulose and hemicellulose begins first in the middle lamella and primary wall. While the secondary wall is still thickening, cellulose and hemicellulose deposition begins in the S_1 layer. Lignification also begins in the cell corners and middle lamella and then proceeding to the primary wall. Lignification begins in the S_1 layer before cellulose deposition is complete in the S_3 layer. Once lignification is complete in the S_3 layer, the cell dies.

The middle lamella and cell corners are highly lignified with the concentration of lignin ranging from 50-60 % in the middle lamella to 85-100 % in the cell corners in a softwood. (**Table 2.3**) The thickness of this region on average is only 0.2-1.0 μm and as a

result the middle lamella and cell corners contain only 19-28 % of the total lignin in gymnosperms.

Table 2.3 Distribution of lignin in spruce tracheids. [29, 54]

	Morphological Origin	Tissue Volume (%)	Lignin (% of total)	Lignin Conc. (%)
Earlywood	**S**	87	72	23
	ML	9	16	50
	CC	4	12	85
Latewood	**S**	94	82	22
	ML	4	10	60
	CC	2	9	100

The primary wall consists of cellulose, hemicellulose, proteins, and pectic substances embedded in lignin. Although this region of the cell wall contains lignin, it is a very thin layer, ~0.1-0.2 μm thickness, and therefore contains only a minor portion of the total lignin. The cellulose microfibrils are randomly oriented in the outer portion of the primary wall but are nearly perpendicular to the axis of the cell wall in the inner portion.

The majority of the tissue volume is contained in the secondary wall although the relative concentration of lignin is low. Nevertheless, 72-82 % of the lignin is contained in the secondary wall. The secondary wall is comprised of three layers: the thick S_2 (middle) layer, which is 1-5 μm in thickness from early to latewood, and the thin S_1 (0.2-0.3 μm thickness) and S_3 (~0.1 μm thickness) layers.

Within the cell wall, the cellulose microfibrils are oriented helically around the cell wall axis. The microfibril angle in the S_2 layer is 5 ^{o}-10 ^{o}, while in the S_1 and S_3 layers it is 50 ^{o}-70 ^{o} and 50 ^{o}-90 ^{o}, respectively.

2.4. Different Methods of Lignin Isolation

As discussed in **Section 2.3.3**, cellulose is deposited first in each layer of the cell wall, followed by hemicellulose, and finally lignin is deposited. As a result the cellulose is surrounded by a matrix of hemicellulose and lignin, with the latter likely forming some type of chemical bonds. [4] These components form a tight association in the cell wall, making their separation difficult. Further enhancing this difficulty is the fact that the major constituent, cellulose, exists in regions as a highly crystalline material. Due to these crystalline regions and the high molecular weight of the lignin material, efforts to extract lignin from whole wood without alteration of structure have met with little success. As a result it is impossible to completely isolate native lignin as its whole component from wood.

Initially, methods involving acid hydrolysis were performed in an attempt to isolate lignin from wood. It was soon realized that the acid lignin differed from lignin in wood based upon its yield from chemical degradation methods such as nitrobenzene oxidation.

Brauns lignin is extracted with 95 % ethanol from wood meal ground to ~100 mesh and can be isolated in an unaltered form. [55] The yields however are very low, the preparation contains some carbohydrates and may be contaminated with extractives. The lignin extracted therefore cannot be considered representative of lignin in wood.

Nord, et al., attempted to isolate lignin by degrading the carbohydrate material with brown rot fungi. [56, 57] It was determined that the amount of Brauns lignin that could be obtained increased with the fungi treatments. The lignin isolated was identical in property to Brauns lignin and the extrapolation was made that the structure of lignin must be uniform throughout the entire cell wall. However they did not take into that ethanol has a limited solvating power with regards to lignin, and as a result they were isolating only lignin

isolatable with ethanol. This is evidenced by Brauns admission that even several days of ball milling would not fragment the lignin polymer to the point that additional lignin could extracted. [58] Pew proved this point by showing that only 13 % of the total lignin could be isolated by treatment of a spruce with brown rot even after only 6 % of the carbohydrates remain. [59]

2.4.1 Isolation of MWL by the Bjorkman Method

Bjorkman first reported in 1954 on "the isolation of lignin from finely divided wood meal by extraction with neutral solvents". [60] A significant portion of the lignin could be extracted and the yield was based upon the extent of milling.

Based upon the previously reported literature which described the isolation of lignin only by drastic conditions, such as acid or alkaline treatments, Bjorkman hypothesized:

1. Strong chemical bonds exist between lignin and carbohydrates.
2. Lignin has a high molecular weight and forms a three-dimensional network in wood.
3. Physical phenomena and hydrogen bonding are involved in the retention of lignin within wood. [61]

Bjorkman suspected that the third possibility played an important role in this problem and upon this he devised his experimental plan. In reality, it is likely a combination of the three that makes extraction of lignin from wood meal difficult.

2.4.2 Theory on Milling

It has been reported that the degree of polymerization (DP) of cellulose decreases rapidly after only a few hours of milling and that lattice deformation leads rapidly to the formation of amorphous cellulose. [62, Lai, 1971 #199] Mobility of individual portions of the macromolecule allows for lattice deformation, whereas immobility of the macromolecule as a whole leads to degradation. The drop in DP is due to hydrolysis of the glycosidic linkages rather than oxidative degradation of the cellulose molecule. Additionally, cellulose and other high molecular weight materials have DP limits upon where no further degradation can occur. This limit is lower for linear polymers such as cellulose when compared to more three-dimensional polymers such as lignin. When the particle size is sufficiently small that molecular movement is no longer restricted, breakage of bonds will cease. [9]

Materials such as lignin will tend to cake with decreasing particle size if milled dry, therefore it is advisable to utilize wet milling. It is probable that caking limits the minimum achievable particle size in dry milling by agglomeration of smaller particles. Milling reaches a "dynamic equilibrium" where no further division of the original material will occur. Finally, even at this equilibrium point there will always be a "tail" of higher particle size. [9]

2.4.3 Milling Parameters

Bjorkman observed that milled wood would tend to coat the steel balls in the vibratory ball mill even after being thoroughly dried. [9] Therefore he made the decision to use toluene and perform wet milling of the wood. The solvent selection is not critical so long as it is a non-swelling solvent because little or no lignin will be extracted. If the particles are suspended in a solvent such as toluene, however, grinding is promoted and the overall

accumulation of temperature is decreased. Additionally it has been reported that the toluene will adsorb to the surface of wood particles and act as a radical scavenger thereby reducing the dramatic impact of the vibratory ball mill. [10, 63] This may help to reduce the amount of modification occurring in the lignin structure.

In Bjorkman's original proposal for a standard grinding method, he uses a rotary ball mill to grind 12 g of wood for 2-3 days and then 6 g for two days in the vibratory ball mill with yields in the range of 50 %. In fact, he asserts that a two-step milling process seems to produce an increase in yield. [61] However in the manuscript on the effect of milling he uses only a vibratory mill and reports that the highest yield (46 %) was obtained with 1 g milled over the course of two days. [9] An additional 12 days of milling led to only to a 7 % increase in the yield of MWL.

It is evident that the yield obtained will depend on the milling method, the size and efficiency of the mill(s), the amount of wood loaded, and the total milling time. As a result, due to trial and error the milling method and yield can be expected to vary based on operations at different facilities. For example, a yield of 28 % using only a vibratory ball mill was reported after 9 days of milling. [64] Glasser et al., reported only a 9.2 % of MWL after 13 days of rotary ball milling with porcelains balls [65] however Brownell reported yields similar to Bjorkman after 2-3 weeks of rotary ball milling with flint pebbles. [66, 67] Furthermore, new orbital mills are being used with more frequency and these mills can produce a finely milled lignin in a matter hours [68] or even tens of minutes [69]. One author noted that the mill being used was "more violent than the vibratory ball mill used by Bjorkman, and there was a noticeable temperature increase on ball milling". [68]

This calls into question the impact of the milling method on the lignin structure. Therefore in order to quantitatively compare lignins produced by different preparation methods, it is essential to compare lignins with similar yields.

2.4.4 Extraction and Purification of Milled Wood Lignin

The choice of extraction solvent is not as critical as the milling conditions. Methyl cellosolve is the best solvent for extraction of lignin from finely divided wood meal, however, it is not recommended because of the difficulty in completely removing it. A mixture of 1,2-dichloroethane:ethanol dissolves pure lignin well, but is not suitable for extraction purposes. Aqueous dioxane was chosen because it extracts low molecular weight lignin well and it does not extract much carbohydrate.[61]

The dioxane solution containing the dissolved lignin is evaporated under reduced pressure and 50-60 ^{o}C in a heating bath. The concentrated lignin is dispersed in 90 % acetic acid at a concentration of 50 mg/mL and precipitated into deionized water (1 g/ 250 mL H_2O) to remove impurities such as tannins and some LCCs. The lignin is centrifuged, the supernatant discarded and the lignin washed with deionized water. Bjorkman evaporated the remaining water by flowing a rapid air stream over the surface. [61] It is now typical to freeze-dry the lignin after this step but there have been reports that this changes the solubility parameters of lignin. [70]

Either the freeze-dried lignin or the residue from precipitation into water is dissolved in a 2:1 1,2-dichloroethane/ethanol solution. After centrifugation and removal of the undissolved portion, the lignin in solution is precipitated into ether, washed twice with ether and then petroleum ether, and dried in a vacuum dessicator over P_2O_5. [61]

2.4.5 Properties of Lignin Extracted with Dioxane

Table 2.4 lists elemental and functional group analyses as determined by Bjorkman. [71] It was determined that milling in the presence of air resulted in a small increase of carbonyl content and a decrease in *p*-hydroxybenzyl alcohol moieties, which represent the α-hydroxy content. No change in phenolic hydroxyl content was observed. Weight average molecular weight (M_w) was determined to be 11,000 and the density of the MWL determined to be 1.406 g/mL.

Table 2.4 Bjorkman's estimation of the chemical properties of MWL. [71]

	Chemical Formula	Phenolic OH	*p*-hydroxybenzyl alcohol	Total OH	C=O	Arylalkyl Ether	Dialkyl Ether
MWL	$C_9H_{8.83}O_{2.37}(OCH_3)_{0.96}$	0.30	0.05	0.80	0.18	0.70	0.84

2.4.6 Isolation of Lignin (CEL) by Treatment with Cellulolytic Enzymes

Pew was the first to experiment with enzyme digestion of vibratory ball milled wood. [59, 72] He observed that solid wood or Wiley-milled wood ground to pass a 20 mesh was not susceptible to treatment with enzymes. However wood ground for just 10 minutes allowed for enzyme digestion of up to two-thirds of the carbohydrate in two successive three day treatments. An additional 14 treatments did not decrease the carbohydrate appreciably. 5 hours of vibratory ball milling would allow for 95 % of the carbohydrate to be removed and resulted in a lignin containing 12-14 % carbohydrate. 8 hours of vibratory ball milling allowed for only 96 % of the carbohydrate to be removed. Only limited analysis of these lignins were performed because they were not obtained carbohydrate-free.

Chang et al., ball milled spruce in a vibratory ball mill for forty-eight hours in the presence of toluene. [73] The milled wood was extracted with 96 % (v/v) dioxane to obtain MWL (17.4 % yield) and then subjected to treatment with a cellulase mixture. Subsequent 96 % (v/v) dioxane extraction yielded an additional 43.1 % of CEL-96. The insoluble material was then extracted with 50 % (v/v) dioxane yielding 24.9 % of CEL-50 for a total yield of 95 %. MWL and CEL-96 were very similar based on elemental analysis. The 50 % (v/v) dioxane fraction however contained twice as much carbohydrates and was much higher in molecular weight (M_w). (**Table 2.5**)

Table 2.5. Data presented for MWL, CEL-96, and CEL-50. [73]

	M_w	Carbonyl Content per 100 C_9 Units	Phenolic OH per 100 C_9 Units	$KMnO_4$ Oxidation (mol %)	Nitrobenzene Oxidation (wt. %)
MWL	16000	0.11	14.4	11.6	37.3
CEL-96	24000	0.08	13.1	10.1	41.4
CEL-50	35000	0.05	8.9	8.1	38.4

Table 2.5 summarizes the data reported by Chang et al., for MWL, CEL-96, and CEL-50. α-carbonyl content was estimated by UV at 305 nm and decreased from MWL to CEL-96 to CEL-50. Phenolic hydroxyl content followed the same trend as carbonyl content consistent with the changes in M_w.

Permanganate oxidation yields mirrored phenolic hydroxyl content consistent with the method (the method yields monomer products only from C_9 units bearing phenolic hydroxyl units). However, data indicated that MWL may have a slightly higher condensed lignin content based upon permanganate oxidation. A higher monomer yield by nitrobenzene

oxidation for CEL-96 was obtained supporting the theory that MWL is more condensed than CEL-96. Both yields were lower than those for the milled wood, however.

2.4.7 Mechanochemical Reactions and Changes in Lignin Structure During Milling

In order to isolate lignin from wood by solvent extraction, the crystallinity of the cellulose must be interrupted and the DP decreased. Pew isolated lignin by milling 1 and 5 hours and treating with cellulase to achieve comparable yields. [59] The lignin milled only 1 hour was insoluble in the same solvents in which the lignin milled 5 hours was soluble. This proves that adequate depolymerization of the lignin macromolecule is necessary to achieve solubility.

It has been shown that the energy available in the vibratory ball-milling of cellulose is sufficient to rupture not only glycosidic bonds but also covalent bonds. [10-12] Furthermore, most organic substances can be decomposed by processes initiated by mechanical and/or thermal means involving radical processes. [74] It therefore follows that lignin with a rigid structure containing many ether bonds and a highly conjugated system able to stabilize radicals once formed, will likely undergo radical decomposition. In addition it is possible that benzaldehyde-type structures found in MWL may be artifacts from the milling process.

While the existence of free radicals in solid wood is in dispute [12, 74, 75], the fact they are formed a short time after milling has commenced is indisputable. By electron spin resonance spectroscopy (ESR), the concentration of free radicals has been shown to increase 20-fold shortly after commencement of milling [76] with concentration increasing with smaller particle size. [74] All isolated lignin samples will contain free radicals, even after sitting on the shelf for a period of months. [10]

Milling of cellulose by itself results in only a very weak signal by ESR, indicating that either radicals are not formed in the milling of cellulose or more likely they dissipate through secondary reactions rapidly. [77] Lignin or wood meal, on the other hand, exhibit a signal at least 50 times that of cellulose. (**Figure 2.12**) This is not surprising based upon the lignin monomer structure and its ability to stabilize a radical through resonance delocalization. As a result, it is obvious that the free radicals measured originate from the lignin component of the milled wood. [10]

Data indicates that the formation of free radicals increases rapidly during the initial phases of milling, reaches a maximum, and then levels off. (**Figure 2.13**) Presumably the increase of radicals is indicative of ether bond cleavage. The unstable radicals will react leaving the stable radicals which are pronounced after equilibrium is reached. It is possible that the stable radicals are predominately phenoxy radicals since they are able to delocalize the radical throughout the aromatic ring. It is also possible that these radicals are stabilized in structures with limited mobility and hence have little opportunity to be involved in other reactions.

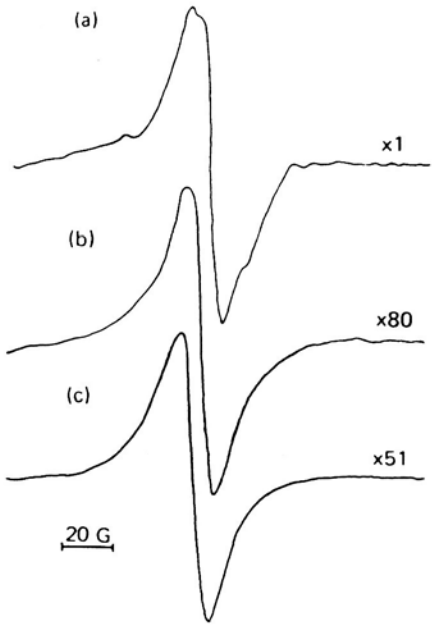

Figure 2.12 ESR spectra of a) cellulose, b) MWL, and c) wood meal, milled with glass beads for three hours in N_2 with glass beads. Multiplication number represents signal intensity. [10]

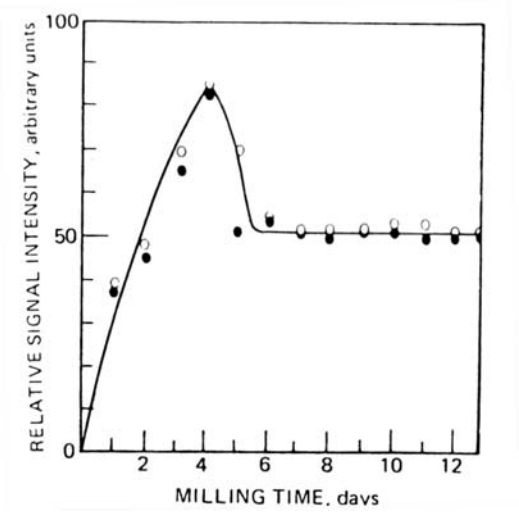

Figure 2.13 Free radicals in wood meal milled with steel balls in CO_2. [10]

Additionally, at day 6 when the free radicals level comes to steady-state may coincide with reaching the "dynamic equilibrium" discussed earlier in **Section 2.4.2**. It should be kept in mind that the rate of formation of radicals is dependent on the mill used, the charge of

wood, etc., so that this is only an example of the accumulation of free radicals which will vary from operation to operation.

2.4.8 Depolymerization of the Lignin Macromolecule by Ether Bond Cleavage

As a result, isolation of lignin involves depolymerization which lowers molecular weight and in turn increases phenolic hydroxyl content. [73] It is evident that the cleavage of β-O-4' bonds (**Figure 2.14**) is the predominant reaction involved in the depolymerization reactions that occur during milling. According to this reaction, the decrease in molecular weight and subsequent formation of a new phenolic hydroxyl group is achieved. Although there is also enough energy present to rupture covalent bonds, depolymerization by this mechanism is probably minimal. While there is probably formation and decay of free radicals occurring throughout the milling process, it is likely that formation of radicals involves β-O-4' cleavage while decay involves processes such as condensation reactions, generation of unsaturated lignin structures, and possibly the formation of *o*- and *p*-quinoid structures.

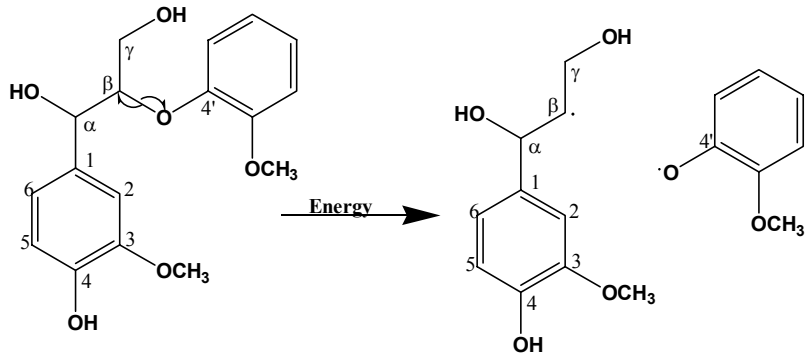

Figure 2.14 Cleavage of β-O-4 interunit linkage in milling of wood.

2.4.9 Formation of Carbonyl and Unsaturated Side Chain Structures

Hon has reported that peroxy radicals will form in toluene even in the absence of oxygen. [10] He states that oxygen will likely be present as a contaminant from one of the components used in the milling. In wood milled in toluene at 77 K these peroxy radicals are readily detected (**Figure 2.15**) but at room temperature they will react very quickly.

Molecular oxygen can react directly with a benzyl radical to form a peroxy radical as shown in **Figure 2.16**. The peroxy radical is unstable at the temperatures involved in ambient ball milling, and hence will decompose to the α-carbonyl structure. The formation of coniferaldehyde is less likely to be involved in this type of process as it would involve an unstable primary alkyl radical intermediate. Therefore it is likely that coniferaldehyde is incorporated into the macromolecule a monomeric precursor in the dehydrogenative polymerization process.

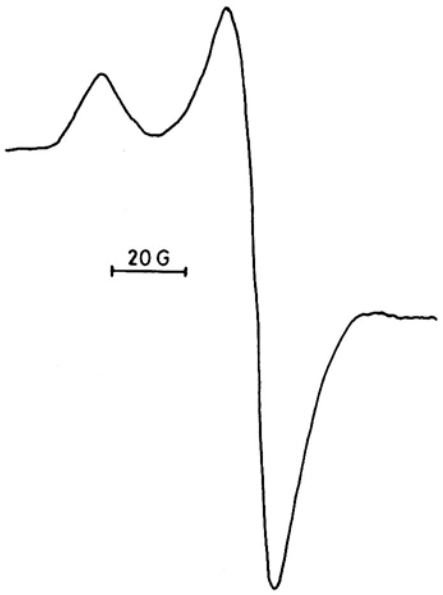

Figure 2.15 ESR of MWL milled in lignin at 77 K. Peak A indicates the presence of peroxy radicals which will decompose readily at room temperature. [10]

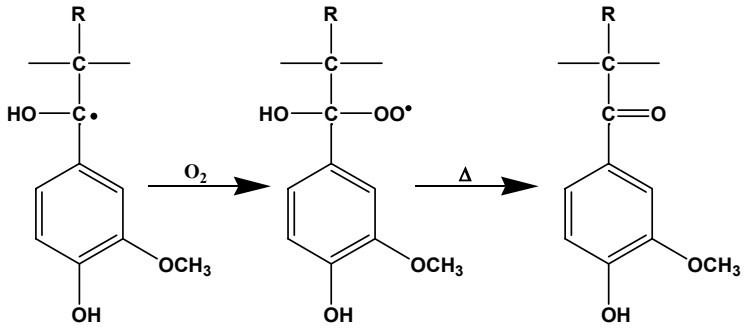

Figure 2.16 Formation of the α-carbonyl structure during milling.

Likewise coniferyl alcohol can be created by a similar process involving the secondary alkyl radical formed from β-aryl ether cleavage. (**Figure 2.17**) Although this is a secondary alkyl radical, it can be somewhat stabilized due to delocalization. Even though β-O-4' cleavage is the predominant reaction occurring in the milling process, the relative proportion of coniferyl alcohol moieties in MWL is rather small. It is likely that delocalization of the secondary radical results in the ultimate stabilization of the radical as the phenoxy radical.

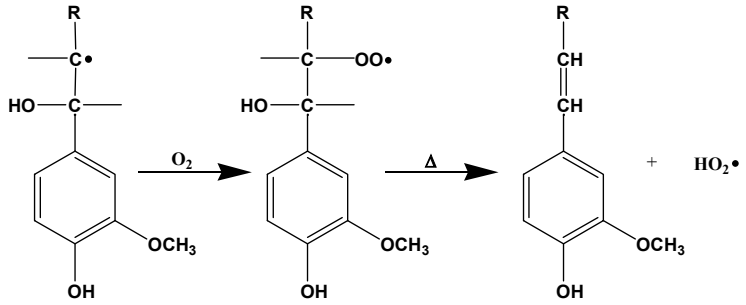

Figure 2.17 Formation of coniferyl alcohol during milling of wood.

2.4.10 Possible Formation of Quinoid Structures During Milling

Hydroxy radicals have been shown to react with lignin aromatic moieties to form *o*- and *p*-quinoid structures.[78] Possible mechanisms for these reactions are shown in **Figure 2.18**. Zhang et al., recently identified a number of quinoid structures present in MWL preparations according to two-dimensional HMQC NMR. [79] Although these moieties are minor components, they may be indicative of structural changes occurring during milling.

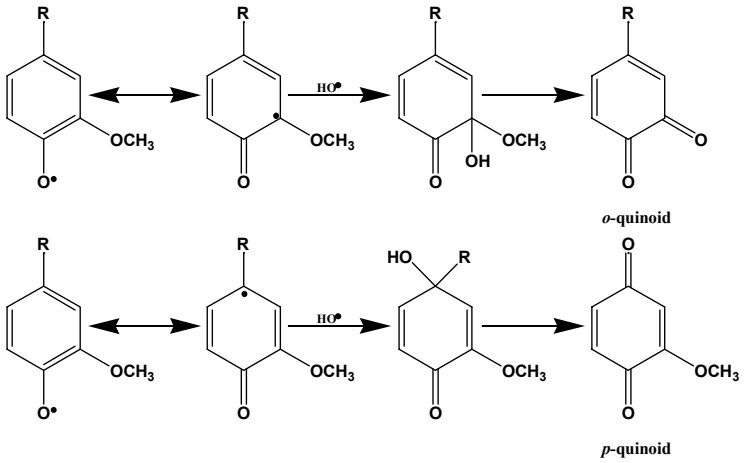

Figure 2.18 Possible mechanism for the formation of *o*- and *p*-quinoid structures during milling.

2.4.11 Condensation Reactions Occurring During Milling

Crosslinking reactions would be most likely to occur as particle size decreases and group achieve greater mobility. This is most likely to coincide with the decrease from the maximum of free radicals in **Figure 2.13** and as milling proceeds. Condensation reactions are believed to most likely follow the mechanism shown in **Figure 2.19**.

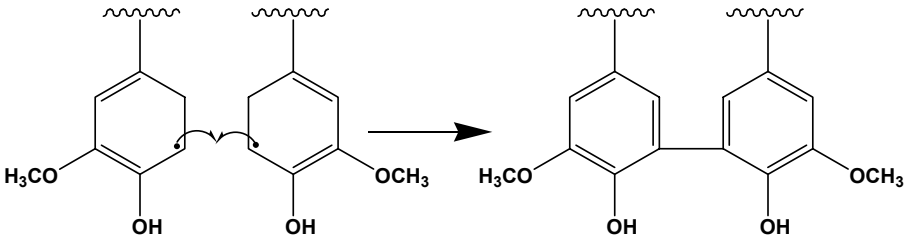

Figure 2.19. Possible mechanism for the formation of a biphenyl linkage during milling.

As mentioned previously, toluene is known to be a radical scavenger and is capable of forming a stable benzyl radical moiety. [10, 63] Toluene will either abstract an electron in a propagation step, dimerize, or react with a radical structure on the lignin polymer to create a toluene-grafted lignin. [80]

Finally, since lignin is a three-dimensional polymer with a rigid structure, it is not likely that any LCC present in the lignin preparation will arise as an artifact of the milling process. All attempts to artificially create these structures by milling hemicellulose or holocellulose and lignin together, have failed. [81]

2.5 Characterization of Lignin by Chemical Degradation Methods

2.5.1 DFRC

DFRC is a relatively new method developed by the Dairy Forage Research Center in Madison, Wisconsin. [82-85] The method involves bromination of the α-position in order to set up the molecule for reductive zinc cleavage of the β-aryl ether. (**Figure 2.20**) Yields of the monomeric product coniferyl alcohol diacetate are in the range of 10-15 mole percent.

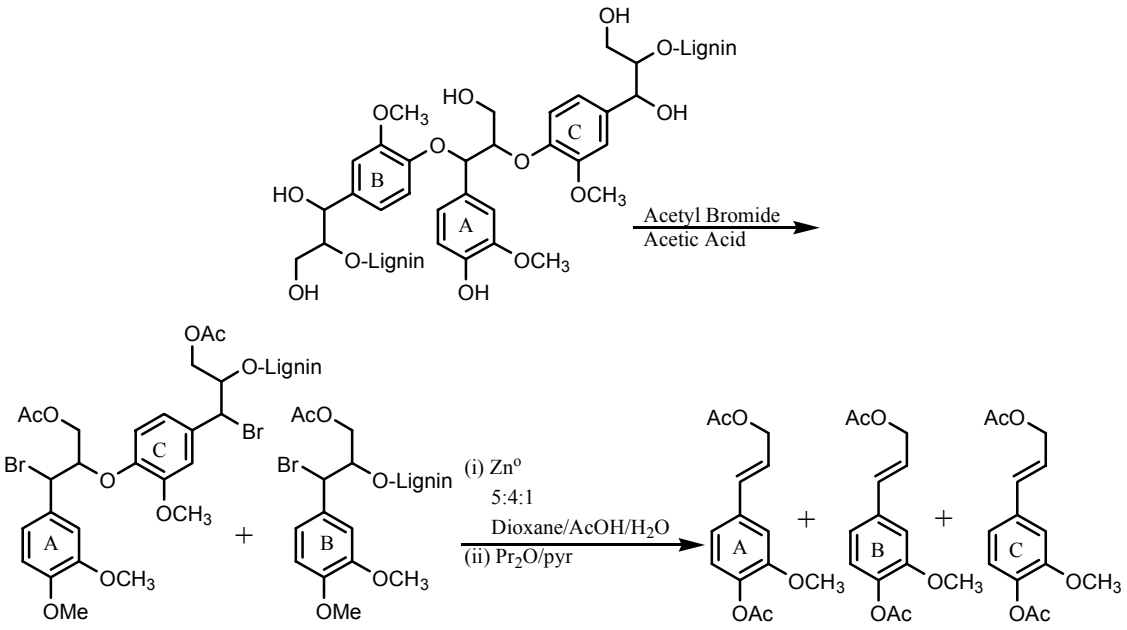

Figure 2.20 Schematic of the standard DFRC reaction. [82-84]

2.5.2 DFRC Procedure

Milled wood (50 mg) and isolated lignin samples (25 mg) are dissolved in 5 mL of acetic acid/acetyl bromide (4:1, v/v) and 0.25 mg of tetracosane as an internal standard was added and stirred for 3 h at 50 °C. The reaction is terminated by removal of the solvent under reduced pressure below 40 °C.

Immediately after the solvent is removed, the lignin is dissolved in 5 mL of a dioxane/acetic acid/water mixture (5:4:1, v/v) and 250 mg of zinc dust is added. The solution is stirred for 30 minutes at room temperature. The products are rinsed into a separatory funnel and the aqueous layer is extracted with CH_2Cl_2.

The organic layer is dried with anhydrous sodium sulfate and removed by evaporation. The residue is dissolved in 2 mL of acetic anhydride/pyridine (1:1, v/v) and stirred for 40 minutes at room temperature. The reaction is stopped by removing the solvent, and the residue is dissolved in dichloromethane (0.5 mL) and analyzed by gas chromatography. The monomeric product of interest from this procedure is coniferyl alcohol diacetate and the quantity obtained can be determined by ratio of the peak area to the internal standard.

2.5.3 Discussion of DFRC Method

Like other degradative methods, DFRC suffers the shortcoming that conclusions must be derived based only upon a yield of a monomeric product. In fact this method relies on release of coniferyl alcohol from either β-O-4' linked endgroups or a monomer linked through β-O-4' linkages at both the β-position and the 4'-positions. However unlike many of the other degradative methods, DFRC performs its cleavage rather selectively and should leave the resultant lignin structure for the most part unmodified. Therefore, with extensive separation through column chromatography, the lignin dimers and in some case even trimers can be analyzed by GC-MS. [86, 87]

Adaptations of this method have been reported in order to gain additional structural information without the exhaustive approach of separation of a large amount of DFRC

degradation products. Ikeda, et al., have reported on a modified DFRC procedure where the lignin is premethylated and the final acetylation step is replaced with a propionation step. (**Figure 2.21**) [88] Argyropoulos, on the other hand, combined the DFRC technique with ^{31}P NMR spectroscopy in order to provide more structural information with only slight modification of the method. [89, 90]

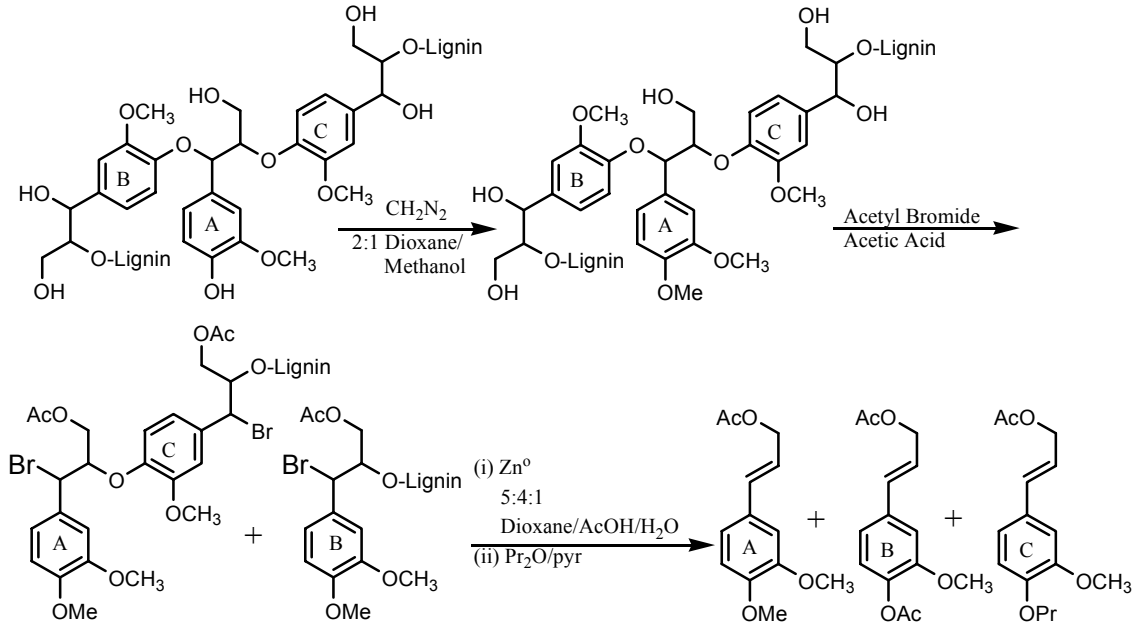

Figure 2.21 Schematic of the modified DFRC reaction. [88, 91]

2.5.4 Acidolysis/Thioacidolysis

These methods both are capable of yielding similar results to that of the DFRC method, namely analysis of the uncondensed β-O-4' structure of the lignin. Acidolysis is performed by heating lignin or wood at 100 ^{o}C in 90 % dioxane with 0.2 M HCl for 2-4 hours. Acidolysis is an interesting method from the standpoint that it yields a number of arylpropanone structures that could provide information about the intact residual lignin. [92]

However the fact that this method utilizes acid for the degradation makes it unlikely that it can produce lignin monomers without structural changes in the intact lignin.

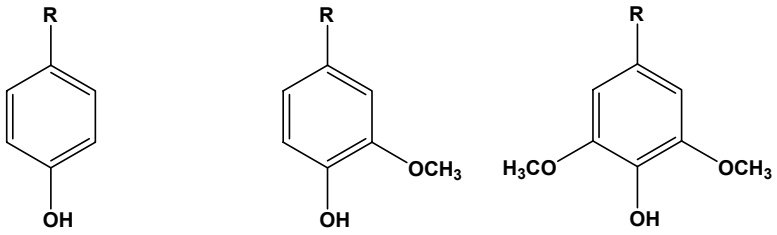

1 **2** **3**

R
a: $-CH_2COCH_2OH$
b: $-CH(OH)COCH_3$
c: $-COCH(OH)CH_3$
d: $-CH_2COCH_3$
e: $-COCOCH_3$
f: $-CH_2CHO$
g: -CHO
h: -COOH
i: -CH=CHCHO
j: -CH=CHCOOH

Figure 2.22 Monomeric phenols detected in lignin acidolysis reaction mixtures.[92]

The primary monomers produced from degradation of guaiacyl (**1**) and syringyl (**2**) units are shown in **Figure 2.22**. These products are derived directly from cleavage of β-aryl ethers which comprise 48-60 % of the interunit linkages in lignin. However the yields of 1a and 2a are only 3-5 %, and **Figure 2.23** shows some of the pathways to other degradation products as analyzed by Lundquist. [93]

It is apparent that these side reactions will minimize the effectiveness of the method for analysis of lignin. While these structures may be assumed to be derived from cleavage of β-O-4' linkages, it may mask the actual presence of a minor structural moiety. In addition to monomers, dimeric products have also been reported. [92] Prominent dimer products reported were a wealth of β-1' structures, phenylcoumarone and stilbene arising from β-5' structural moieties, and structures deriving from β-β'. The fact that β-1' linkage have been

put forth as a major structural unit in lignin according to this technique, indicates the caution which should be observed when analyzing lignin structure based on acidolysis. [94]

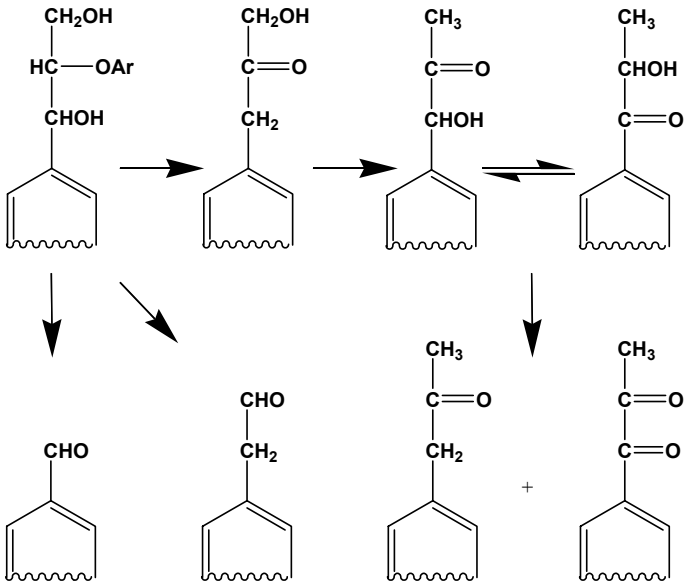

Figure 2.23 Formation of monomeric phenols from β-O-4' structures in lignin during acidolysis. [93]

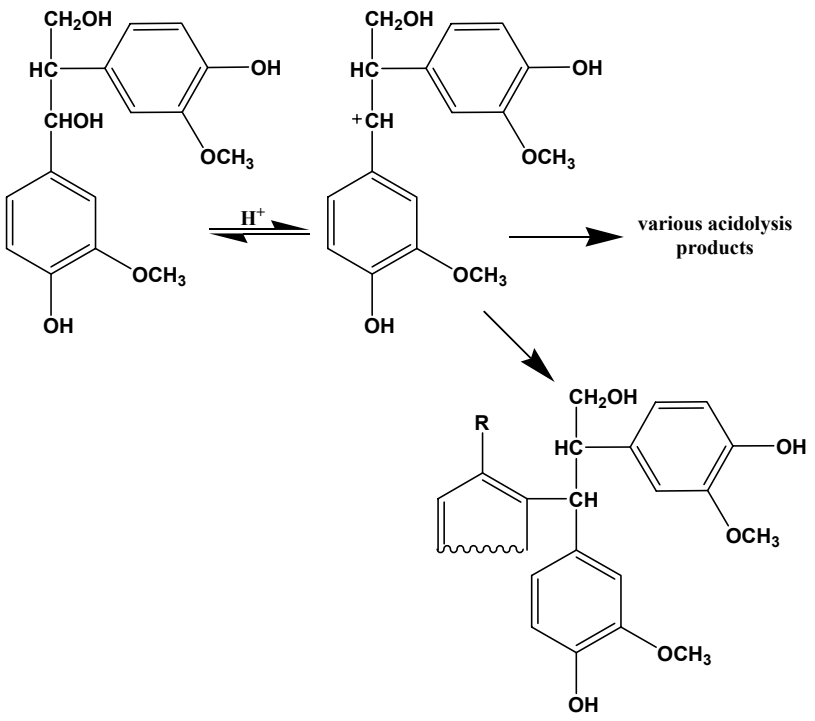

Figure 2.24 Acid-catalyzed condensation reaction occurring during acidolysis reaction. [93]

As a result thioacidolysis was developed to facilitate analysis of lignin structure by decreasing condensation reactions and hydrolysis products and increasing monomer yields. [95] Acidolysis proceeds by an S_N1 mechanism and the condensation reactions occur because of the benzyl cation intermediate formed. (**Figure 2.24**) The thioacidolysis method on the other hand utilizes a nucleophilic ethanethiol which will displace the α-hydroxyl or α-alkoxyl group by an S_Ni mechanism thereby minimizing the formation of the highly reactive benzyl cation. (**Figure 2.25**) In addition, the mineral acid is replaced by the Lewis acid, BF_3 etherate, to assist the displacement of the α-position. [96] The main monomer produced from thioacidolysis is the trithioethyl ether depicted in **Figure 2.25**, thereby simplifying analysis of the product mixture. Yields of the monomeric products are in the range of 20 mol %, much higher than those reported by DFRC. A drawback of this method is that all propane

sidechain carbons are reduced to the thioether minimizing structural information that could be obtained.

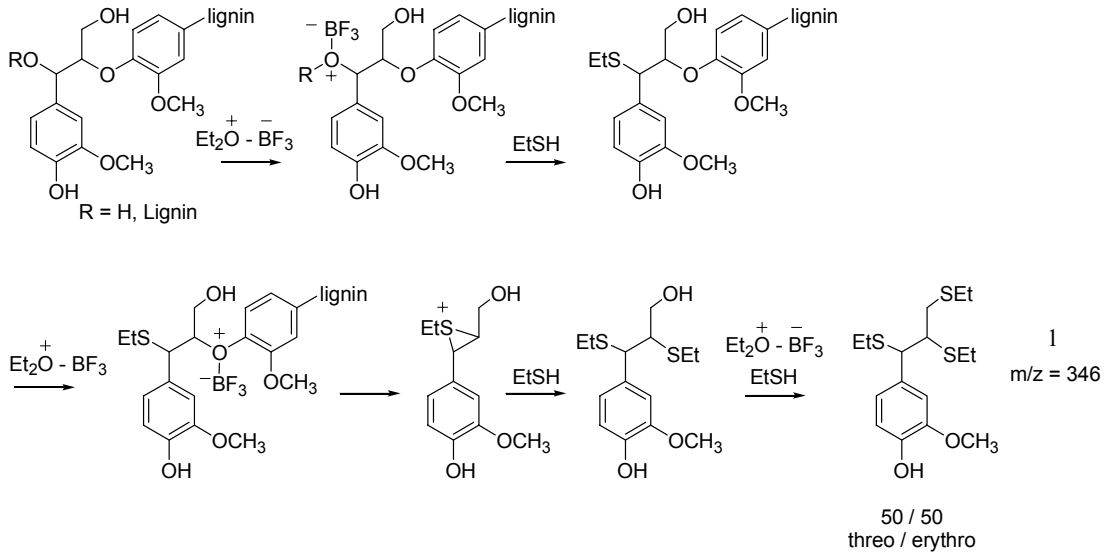

Figure 2.25 Proposed mechanism of the thioacidolysis reaction with lignin. [97]

Nonetheless desulfuration of the trithioethyl ethers by Raney nickel and subsequent trimethylsilane (TMS) derivatization yields dimeric products. [98] This method leads to condensed lignin dimers, which provide very useful qualitative information about the lignin structure. Among the dimers isolated are 5-5', 4-O-5', β-1', β-5', β-6', and β-β' derived structures. These dimers are isolated in the range of 10 mol % leading to a total of 30-40 mol % of the total lignin structure being quantified by thioacidolysis. Recently, ESI-MS was used to analyze the oligomeric fraction from thioacidolysis with some success. [99]

As in the modified DFRC method described above, premethylated lignin can be used to enhance the information obtained using the thioacidolysis technique. (**Figure 2.26**) [100] As a result the monomers obtained from free phenolic endgroups can be differentiated from those derived from consecutive β-O-4' linkages.

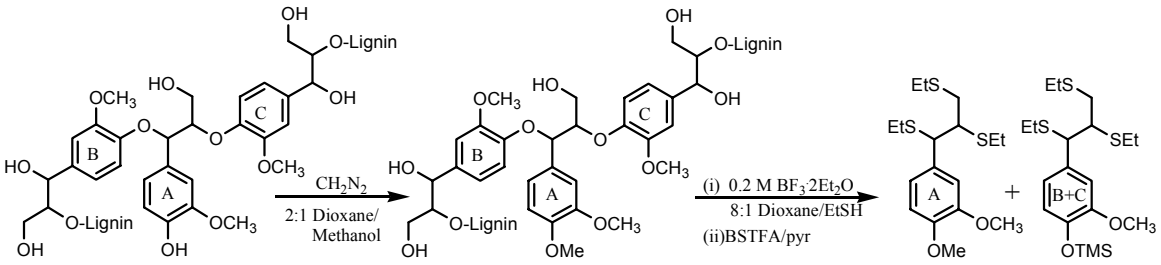

Figure 2.26 Schematic of the modified thioacidolysis reaction. [100]

2.5.5 Nitrobenzene Oxidation

Nitrobenzene oxidation was developed by Freudenberg and coworkers in 1939 to obtain evidence concerning the aromatic nature of lignins. [101] Nitrobenzene oxidation degrades lignin sidechains in uncondensed structures to yield primarily vanillin, syringaldehyde, *p*-hydroxybenzaldehyde from G, S, and H units, respectively. (**Figure 2.27**)

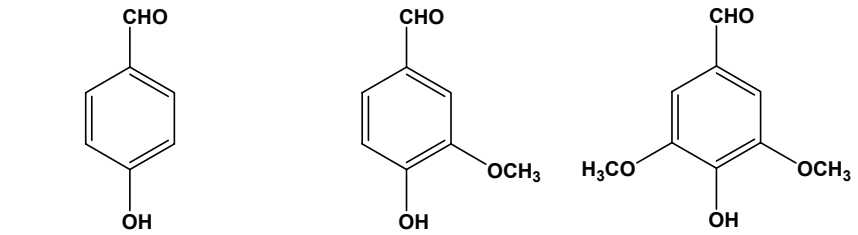

***p*-hydroxybenzaldehyde** **vanillin** **syringaldehyde**

Figure 2.27 Major products from nitrobenzene oxidation.

2.5.6 Nitrobenzene Oxidation Procedure

Leopold optimized the conditions for nitrobenzene oxidation and nowadays it is his method usually used to perform these analyses.[102] 50 mg of a predried isolated lignin or 200 mg of predried lignocellulosic material extracted to remove extractives and Brauns lignin are added to a 10-mL stainless steel bomb along with 7 mL of 2M NaOH and 0.4 mL of

nitrobenzene. The bomb is sealed and placed in a heating mantle. The bomb is heated to 170 ^{o}C and reacted for 2.5 hours with occasional shaking to stir material. The bomb is cooled in an ice water bath and the material is extracted with chloroform to isolate nitrobenzene oxidation products. The aqueous phase is acidified to pH 3-4 by addition of concentrated HCl and extraction with chloroform is once again performed. The chloroform is dried over anhydrous Na_2SO_4 and the solvent is then removed under reduced pressure at 40 ^{o}C. The dried material is diluted tenfold and 1 mL is placed in a GC vial for analysis. Quantification of reaction products are determined by calibration against *m*-meconic acid.

2.5.7 Discussion of the Nitrobenzene Oxidation Method

Nitrobenzene oxidation occurs by a typical alkaline mechanism, in other words, a free phenolic hydroxyl group is required to form the quinone methide and induce degradation. 4-O-alkylated groups will be cleaved to generate free phenolic groups similar to well known alkaline hydrolysis mechanisms.[103] (**Figure 2.28**) Premethylation of lignin results in a decrease in vanillin yield, as would be expected. [104]

Figure 2.29 shows a scheme for the degradation of the β-aryl ether via nitrobenzene oxidation. This mechanism is based on one proposed by Chang for isoeugenol and the complete mechanisms of nitrobenzene oxidation are not fully realized. [105] It has recently been proposed that the reaction proceeds via a one-electron transfer scheme, but this seems unlikely due to the solution chemistry. [106]

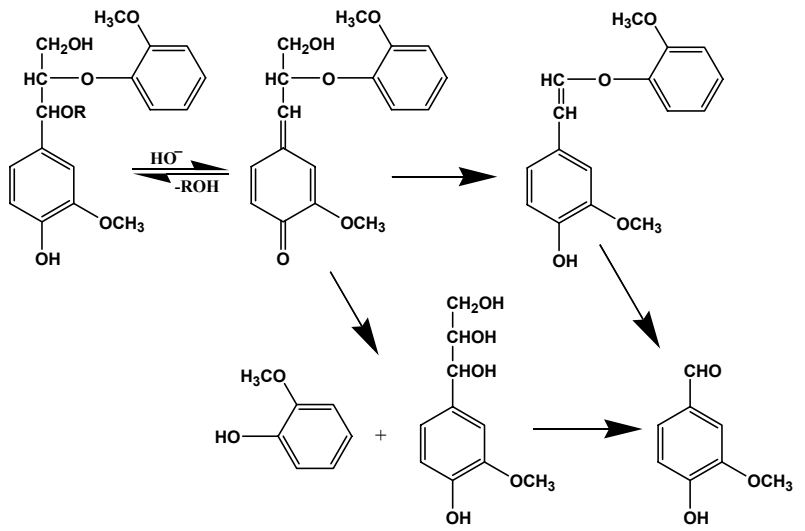

Figure 2.28 Formation of new phenolic hydroxyl group in the nitrobenzene oxidation reaction scheme. [105]

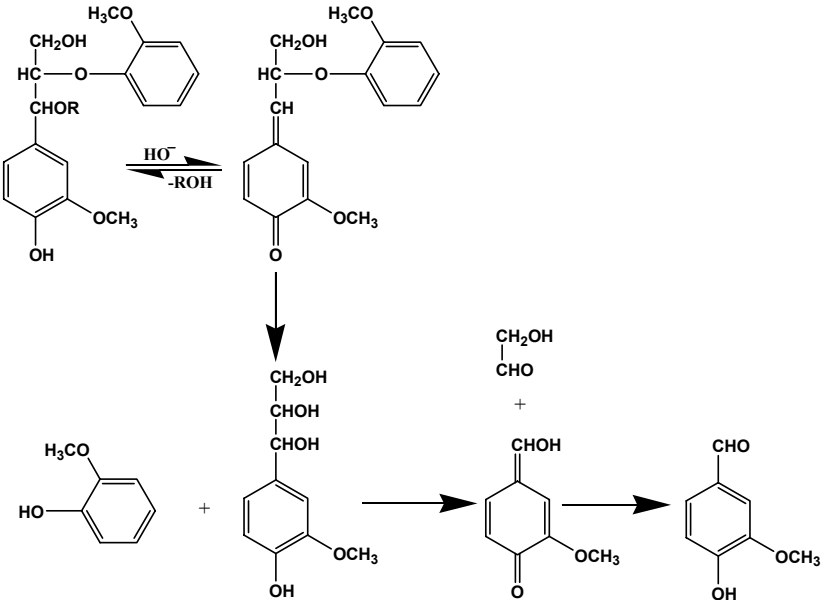

Figure 2.29 Possible mechanism of nitrobenzene oxidation.[105]

β-5' structures can proceed through the vinyl ether intermediate described in **Figure 2.29** to yield one vanillin moiety and a 5-formyl vanillin moiety. (**Figure 2.30**) β-1' structures however proceed through a similar mechanism to yield 2 vanillin monomers.

(**Figure 2.30**) The mechanism for cleavage of the β-β' linkage is unclear and as with these other reactions [107], they are not believed to proceed quantitatively. 5-5' substructures have been shown to yield dehydrodivanillin structures only and no degradation products of 4-O-5' have been reported.

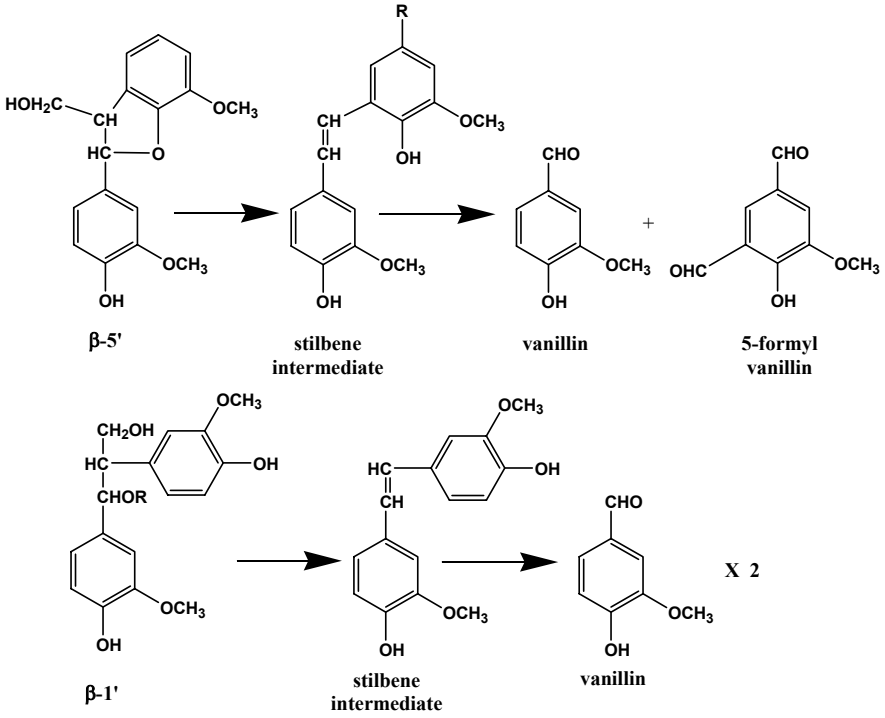

Figure 2.30 Degradation of β-5' and β-1' substructures during nitrobenzene oxidation.[105]

An exception to the rule that nonphenolics will not react in nitrobenzene oxidation is the reaction of structures containing an α-carbonyl and those capable of undergoing reverse aldol reactions. [108] The nonphenolic benzaldehyde such as veratraldehyde, is known to be unstable due to the lack of resonance stabilization and will undergo a Cannizaro reaction to produce veratric acid and methyl veratryl alcohol. (**Figure 2.31**)

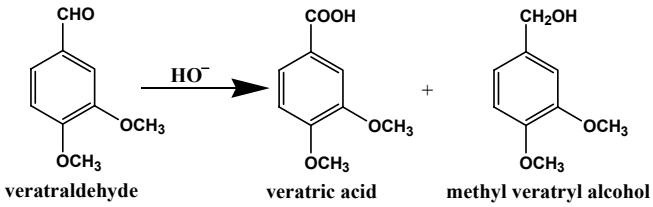

Figure 2.31 Disproportionation of veratraldehyde to form an acid and an alcohol. [105]

Typical yields from nitrobenzene oxidation are in the range of 30-40 %, and it is obvious that these results are not quantitative. In this respect, nitrobenzene oxidation is advantageous when compared to DFRC and thioacidolysis because it will also cleave some sidechain structures and therefore give higher molar yields. However, because the reaction requires free phenolic hydroxyl groups and the reactions are not quantitative, it is difficult to draw any authoritative conclusions from the results.[109]

Nitrobenzene oxidation has been used to determine the S/G ratio in lignins. However, as with any degradative method that considers only a portion of the total lignin structure, nitrobenzene oxidation cannot be considered absolute in the determination of S/G ratio. Furthermore, due to the bias of the analysis, it is likely to overestimate the contribution of syringyl lignin. If one considers that guaiacyl is a more condensed lignin and that a large portion of the condensation is expressed as linkages at the C_5 position on the aromatic ring, then it follows that nitrobenzene oxidation will yield a lower amount of vanillin.

2.5.8 Permanganate Oxidation

Permanganate oxidation was introduced by Freudenberg and coworkers in 1936 [110] and is the probably the most useful lignin degradation method for analysis of condensed linkages. Lignin sidechains are degraded to yield aromatic carboxylic acids that are indicative of the bonding pattern of the lignin moiety from which it was isolated. (**Figure**

2.32) Quantification of these carboxylic acid products will give an estimation of the minimum amount of these structures in the lignin macromolecule.

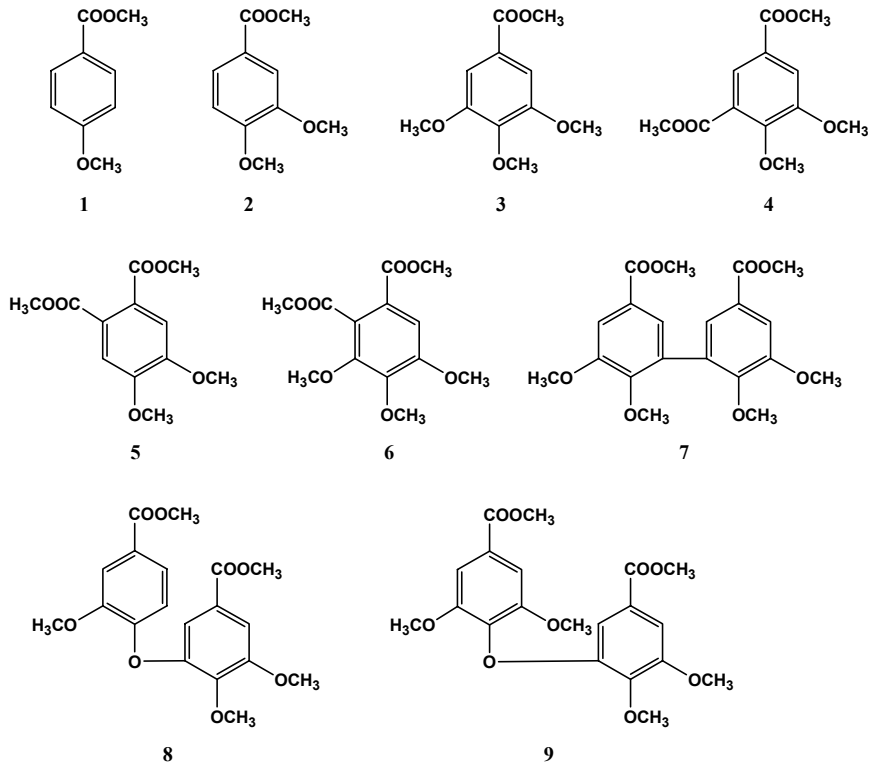

Figure 2.32 Major carboxylic acid methyl esters formed during permanganate oxidation of lignin. [111]

2.5.9 Permanganate Oxidation Procedure

The permanganate oxidation method was altered by addition of a premethylation in order to increase the yield of acids. [112] Although this methodology prescribes methylation by dimethyl sulfate,$(CH_3)_2SO_4$, it has been shown recently that complete methylation of the free phenolic hydroxyl groups can be achieved by diazomethane methylation, the preferred method for our laboratory. [88] **Figure 2.33** illustrates the four-step reaction sequence involved in the permanganate oxidation procedure.

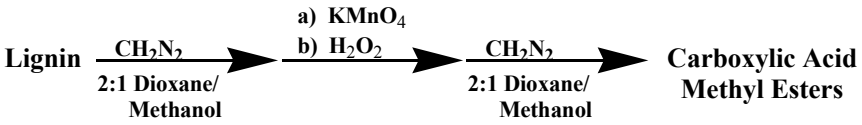

Figure 2.33 The four-step permanganate oxidation reaction sequence. [111]

Therefore 25 mg of material based on Klason lignin content of premethylated lignin or wood are weighed into a 500 mL Erlenmeyer flask and suspended in 40 mL of *t*-butyl alcohol/water mixture (3:1 v/v). 40 mL of 0.5 M NaOH, 100 mL of 0.06 M $NaIO_4$, and 20 mL of 0.03 M $KMnO_4$ are added to the flask which is then placed in a controlled water bath set at 82 ^oC and the reaction is allowed to proceed for 6 hours. The presence of the sodium periodate is intended to keep reoxidizing manganate (V or VI) to permanganate, thereby keeping the levels constant. Periodate may be consumed, however, and the purple color of the solution will fade. For this reason, the reaction should be monitored and solid $NaIO_4$ (1.28 g) and $KMnO_4$ (0.095 g) should be added when necessary.

The reaction is quenched by adding 10 mL of ethyl alcohol and the reaction mixture is filtered to remove solid MnO_2. The authors of the procedure used a bed of silica as the filtering media, however, use of a Whatman paper filter is also acceptable. A small amount of a 1 % (w/v) $NaHCO_3$ solution is added and the aqueous phase is extracted twice with 50 mL portions of ether. The organic phase is extracted with 15 mL of the bicarbonate solution and the aqueous phases are all combined. After the pH is adjusted to 6.5 with 9 M H_2SO_4, the aqueous extracts are evaporated under reduced pressure at less than 50 ^oC until a total volume of 30 mL is achieved.

Larsson and Miksche determined that yields were improved by performing the initial oxidation step under alkaline conditions, but that oxidation was incomplete. [113] As a result they added a second mild oxidation step using alkaline H_2O_2. As a result, 0.25 mL of a 0.3

% (w/v) DTPA solution is added to the above aqueous phase, and 20 mL of the *t*-butyl alcohol:water (3:1 v/v) solution are added. 0.9 g of Na_2CO_3 are added and the oxidation is started by addition of 5 mL of 30 % (v/v) H_2O_2. After 10 minutes at 50 ^oC, the reaction is terminated by the addition of 100 mg MnO_2, and the reaction mixture is allowed to stand for at least 2 hours in order to allow the H_2O_2 to decompose.

The solution is again filtered, the precipitate washed with deionized water, and the aqueous phase acidified to pH 2 with 9 M H_2SO_4. The solution is then extracted 3 times with 1:1 (v/v) acetone/dichloromethane and the combined organic extracts are combined, dried over anhydrous Na_2SO_4, and concentrated under reduced pressure.

The reaction products are then dissolved in 5 mL methanol and 15 mL ether and 2 mL of diazomethane are added. The mixture is allowed to mix for 1 hour at room temperature, and if the solution is not yellow, then more diazomethane is added. This is repeated until the color persists, and the solution is allowed to mix overnight. The solvent is then evaporated under reduced pressure and the products dissolved in 1 mL CH_2Cl_2 for GC analysis. Quantification is performed by calibration against pyromellitic acid tetramethyl ester. [111]

2.5.10 Discussion of the Permanganate Oxidation Method

Similar to nitrobenzene oxidation, permanganate oxidation only produces monomeric products from lignin moieties containing a phenolic hydroxyl group. Premethylation will protect the lignin from being overoxidized, as reports indicate the presence of succinic acid in the product mixture of lignin containing free phenolic hydroxyl groups.

Model compound experiments indicate that sidechains are efficiently degraded by permanganate oxidation. The major products in **Figure 2.32**, are the monocarboxylic acid

products, **1-3**, resulting from the degradation of the sidechain of uncondensed moieties. If both groups contain free phenolic hydroxyl groups, a maximum of 2 acid groups can be created by degradation of β-O-4', β-β', and β-1' linkages, and one from β-5' and α-6' linkages. Product **4** can result from the other lignin monomer in the β-5' linkage and from the cleavage of 5-5' biphenyl groups. Product **7** obviously indicates that a 5-5' bond has not been degraded. Products **5** and **6** derive from linkages involving the C_6 position on the aromatic ring. Finally **9** and **10** derive from 4-O-5' linkages. **Table 2.6** lists the relative composition of carboxylic acid moieties obtained for a spruce wood and MWL. Erickson, et al., estimated a theoretical yield of condensed linkages based upon the actual yield of products **4-9** to be 36 %. If the material used is MWL, then the yields are fairly quantitative based upon estimations by ^{13}C NMR spectroscopy. [114] However, in order to make this estimation, one has to ignore the heterogeneity of the lignin in the cell walls. In any case this may indicate that the phenolic hydroxyl groups can be estimated based upon the yield of acids from permanganate oxidation. [115, 116]

Table 2.6 Relative frequency of carboxylic acid methyl esters from permanganate oxidation of spruce wood and MWL. [111]

	Relative Frequency of Individual Carboxylic Acid Methyl Esters (mol %)					
	1	**2**	**4**	**5**	**7**	**8**
Spruce Wood	6	67	10	8	6	3
Spruce MWL	4	54	12	8	15	7

It has been suggested that the yield can be increased by selectively cleaving the β-aryl ether linkages with alkali and cupric oxide prior to permanganate oxidation. However, this may induce changes in the lignin structure making the analysis pointless. [117] It has also

been suggested to essentially perform kraft pulping on the sample prior to analysis. [118] However, it is well known that not all β-O-4' linkages are cleaved during kraft pulping, and once again structural changes may introduced.

Finally, useful information can be obtained on lignins having undergone structural changes due to bleaching. Specifically, the oxidation and substitution of the aromatic ring as well as the phenolic hydroxyl content may be determined. [111]

2.6 NMR Spectroscopy of Lignin

NMR spectroscopy is indispensable for structural characterization of organic and biological molecules. Unlike degradative methods, the main advantage of NMR spectroscopy is that it is able to examine the entire polymer rather than make assumptions based upon monomeric products. One-dimensional solution-state NMR experiments such as quantitative ^{13}C NMR and ^{13}C DEPT can be implemented to estimate the interunit linkages in lignin. [119] Two-dimensional techniques can be utilized in the search for new structural features in the lignin polymer. [14, 16, 17, 38] Still other techniques are being used in the attempt to map the linkages in the lignin macromolecule. [120-124] Attempts to make the two-dimensional techniques into a method for quantitative analysis of lignins have recently been reported. [125, 126] In this section, a brief review of the theory of NMR will be presented, followed by a survey of applications of the techniques to lignin structural elucidation.

2.6.1 Introduction to Nuclear Magnetic Spectroscopy[127]

Almost all organic compounds contain hydrogen and for the purpose of NMR hydrogen has angular momentum properties resembling the classical concept of a spinning particle. The spinning nucleus is positively charged and when spinning creates a magnetic field possessing a magnetic moment, μ. (**Figure 2.34**) The magnetic moment is a vector and it will be exploited by the NMR experiment.

When the atomic number and mass are even, the nucleus is nonmagnetic and has a spin quantum number (**I**) of 0. ^{12}C and ^{16}O are common nonmagnetic nuclei. Spinning nuclei

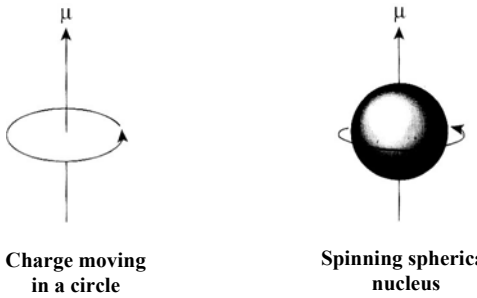

Figure 2.34 Magnetic field generated by positively charged spinning particle. [127]

can be spherical or quadrupolar in nature. Those being spherical have a spin of ½, and include ^{1}H, ^{13}C, ^{15}N, ^{19}F, ^{29}Si, and ^{31}P. All of these nuclei have been used in the attempt study lignin. Quadrupolar nuclei have a spin of 1 or more increasing in increments of ½ and include ^{2}H, ^{11}B, ^{14}N, ^{17}O, ^{33}S, and ^{35}Cl.

The magnitude of μ is defined by the equation,

$$\mu = \gamma(h/2\pi)I \quad (1)$$

where,
γ = gyromagnetic ratio
h = Planck's constant

and is proportional to the magnitude of γ.

In the absence of a magnetic field, all nuclei of the same isotope have the same energy. However, when a magnetic field, B_0 is applied along the *z*-axis, the nuclei begin to precess about the *z*-axis. (**Figure 2.35**) In the case of a spherical nuclei, spins of I_z= + ½ and - ½ because of precession with and against B_0 will occur, with a slight preference for + ½. The population preference is defined by Boltzmann's law:

$$\mathbf{n(+½)/\ n(-½) = \exp(\Delta E/kT)} \quad (2)$$

where,
n = the population of each spin state
ΔE = the energy difference between the two spin states
k = Boltzmann's constant
T = absolute temperature (^oK)

Figure 2.36 shows the energy difference between the two spin states.

μ precesses about the magnetic field B_0 with an angular frequency, ω_0, called the Larmour frequency. ω_0 and B_0 are proportional with their relationship defined by the gyromagnetic ratio:

$$\omega_0 = \gamma B_0 \quad (3)$$

Therefore the energy difference, **ΔE**, between the two states is defined by the Larmour frequency:

$$\Delta E = (h/2\pi)\omega_0 = (h/2\pi)\gamma B_0 \quad (4)$$

As a result, the energy differences between the two state increases proportionally with magnetic field.

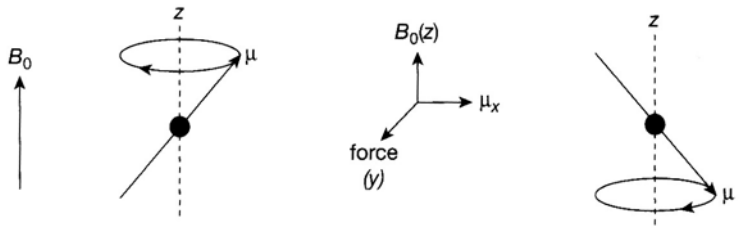

Figure 2.35 Precession of spins around the *z*-axis. [127]

In an NMR experiment, a second magnetic field, $\mathbf{B_1}$, equivalent to the Larmour frequency is applied along the *x*-axis, the spin states of the nuclei will flip. When the state flips from +½ to -½, absorption of energy will occur and in the opposite case emission will

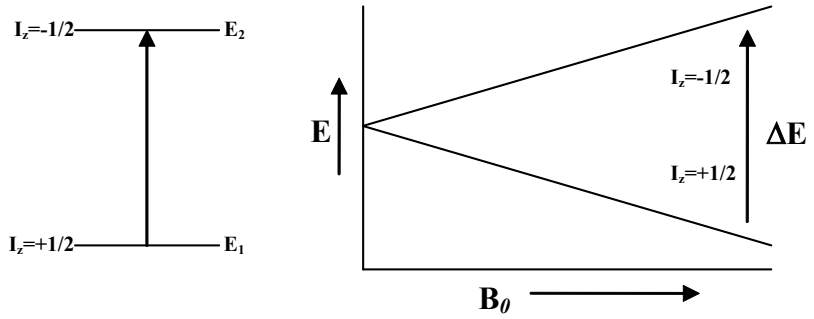

Figure 2.36 Energy differences between spin states. [127]

occur. Since there is an initial excess in +½ spins, net absorption occurs, and this is called the resonance. Absorption may be detected electronically and plotted versus frequency to get the typical NMR spectrum. Resonance frequency ($\mathbf{v_0}$) is highly dependent upon the structural environment of the nuclei and becomes the basis of the NMR experiment.

The net absorption is dependent on gyromagnetic ratios (γ) and as a result will vary between nuclei. ^{1}H has a very large γ, and will have a large energy difference. Other nuclei including ^{13}C have much smaller γ and will have a smaller difference in energy. This will become important in experiments described later in which transfers of magnetization will be employed.

The electron clouds surrounding the nuclei also have charge, motion, and hence a magnetic moment. Therefore the magnetic field generated by the electrons will have an effect on B_0 and hence impact the environment of each individual nucleus. The term for this

effect on B_0 is called the shielding, σ. The actual field experienced by the individual nucleus is therefore equivalent to $B_0(1-\sigma)$. Therefore the resonance frequency can be expressed as:

$$\nu_0 = \gamma B_0(1-\sigma)/2\pi \quad (5)$$

Electron-withdrawing groups will decrease shielding, increase resonance frequency, and shift the signal downfield. Electron-donating groups will have the opposite effect.

In order to make the chemical shift uniform in different magnetic fields, the common practice is to plot the spectrum with ppm on the *x*-axis instead of Hz. The value of ppm is determined by dividing the resonance frequency of the nuclei by the resonance frequency of a known reference TMS (tetramethylsilane). Therefore the chemical shift, δ, is expressed as:

$$\delta = (\nu_i - \nu_{TMS})/\nu_{TMS} \quad (6)$$

2.6.2 The Basic NMR Experiment

When only B_0 is applied, the spins will traverse around the *z*-axis and the net magnetization, **M**, will equal zero. As mentioned previously, B_1 is applied to equal the Larmour frequency and perpendicular to the *z*-axis. Application of this magnetic field will force the net **M** into the *x*-*y* axis, also known as the rotating frame. Typically B_1 is applied for the length of time required to transfer all magnetization from the *z*-axis to the *y*-axis. This is known as a 90^o pulse and the time length required is referred to as the pulse width, which is typically in the range of 5-10 μs.

When the B_1 field is removed, the magnetization will begin to decay and will return to the *z*-axis. This occurs by two mechanisms: spin-lattice and spin-spin relaxation. Spin-lattice relaxation occurs as energy is transferred to the local environment and is usually a first-order process with a time constant T_1. Spin-spin relaxation involves energy transfer

between spins allowing them to return to their Boltzmann distribution. The reduction in the *y*-magnetization can be measured with time and is also a first-order process with a time constant T_2 known as the free induction decay (FID). Multiple resonating nuclei will complicate the FID but fortunately the data can be unraveled with a computer program known as Fourier transform (FT).

2.6.3 ^{1}H NMR

^{1}H NMR spectroscopy was first applied to lignin in 1960's comparing the chemical shifts of model compounds to those of the lignin polymer. [128, 129] Valuable information may be obtained from the ^{1}H NMR spectrum and **Table 2.7** lists the general chemical shifts identifiable in acetylated spruce lignin. Ludwig compiled a comprehensive collection of lignin model compound chemical shifts from literature reports. [130]

^{1}H spectra are most commonly collected using acetylated lignins as information concerning the phenolic and aliphatic hydroxyl groups can be obtained. Acetylated lignins are typically dissolved in $CDCl_3$, although other solvents such as DMSO-d_6 may be used. With modern spectrometers low concentration samples may be used, however the standard method usually calls for 50 mg to be dissolved in 0.75 mL of solvent. Spectra are acquired using a pulse delay long enough to ensure that all spins have returned to the z-axis, typically 5 s is used for lignins. The number of scans required is only 16-64, making the total experimental time for ^{1}H NMR very short. Integration can made by estimating in a number of ways: ratio to the methoxyl peak at δ_H 3.81; ratio to the integration of the entire spectrum[131]; the use of an internal standard [132, 133]; or ratio to the aromatic protons. [134]

Table 2.7 ^{1}H NMR chemical shifts for sidechain chemical shifts of common lignin interunit linkages. [16, 17, 124, 133-141]

	Chemical Shift, ppm		
	H_α	H_β	H_γ
β-O-4'	6.0-6.1	4.9-5.0	4.1-4.3/4.2-4.4
β-5'	5.5-5.6	3.5-3.8	4.4
β-β'	4.6-4.7	~3.1	3.8-3.9/4.2-4.3
Dibenzodioxocin	4.9	4.1-4.2	4.0-4.1/4.5
α-C=O in β-O-4	--	5.4-5.5	4.4-4.5
Ar-CH=CH-CH_2OAc	~6.60	~6.2-6.3	4.7-4.8
Ar-CH=CH-CHO	7.6	6.6	9.7
Ar-CHO	9.9	--	--
β-1'	6.0-6.2	3.5	4.2-4.4
Ar-CH_2-CH_2-CH_2OAc	2.5-2.7	1.8-2.0	~4.0
Spirodienone	~5.2	3.1-3.3	4.0-4.2
Ar-CO-CH_2-CH_2OAc	--	3.2-3.3	4.3-4.4
Ar-CH(OAc)-CH_2-CH_2OAc	5.8	2.1-2.2	4.1
Aliphatic OAc	~2.0	--	--
Aromatic OAc	2.2-2.3	--	--

2.6.4 ^{13}C NMR Spectroscopy

Since the development of broadband decoupling and Fourier transform, ^{13}C NMR has become routine for researchers in the arena of structural characterization. Broadband decoupling allowed for better resolution by preventing signals from being split into mutliplets by protons. ^{13}C NMR does not suffer homonuclear splitting as does ^{1}H NMR because of the low natural abundance of the ^{13}C isotope, which is 1.1% compared to 99.99% for ^{1}H. Fourier transform allowed for collection and analysis of large amounts of data in a short period of time, improving the signal to noise ratio. [142]

^{13}C NMR is advantageous compared to proton NMR because it allows for direct analysis of the carbon backbone, including the quaternary carbons. Quaternary carbons are almost exclusively aromatic carbons in lignin, therefore ^{13}C NMR can estimate the degree of condensation in lignin. ^{13}C NMR also has the advantage over ^{1}H NMR of being able to

disperse the signals over a range of ~200 ppm as opposed to ~12 ppm allowing for better separation of signals.[142]

^{13}C NMR spectroscopy is a reliable method to investigate the structure of the carbon skeleton in lignin. Unlike chemical methods NMR provides a more comprehensive view of the entire lignin macromolecule. ^{13}C NMR can be used to estimate the abundance of each interunit linkage and can be considered to be quantitative provided adequate experimental conditions are utilized if the pulse delay between acquisitions is sufficiently long to ensure that all carbons have returned to their initial Boltzmann distribution. The pulse delay required to achieve these conditions is generally considered to be 5 times the longest rate of relaxation. [119]

There have been several reports on quantification of lignin structure using ^{13}C NMR, although only Chen and Robert have attempted to make detailed quantification of interunit linkages. [138, 143] Despite these attempts there still exists quite a bit of overlap in the ^{13}C NMR spectrum making estimation of structural formations difficult. Recently, there have been reports of the use of a combination the acetylated and nonacetylated spectra to estimate interunit linkages has been performed. [114, 144] Signals that may overlap in the nonacetylated spectrum may separate in the acetylated spectrum due to the alteration of its chemical environment. Capanema, et al., utilized not only these ^{13}C spectra but also the ^{1}H spectrum to make quantitative estimations. **Tables 2.8** and **2.9** list the chemical shifts of important carbons in the nonacetylated and acetylated ^{13}C NMR spectra.

Table 2.8 ^{13}C NMR chemical shifts for the sidechain carbons of the major interunit linkages in nonacetylated softwood lignin. [16, 79, 119, 138, 141, 143, 145-149]

	Chemical Shift, ppm			
	C_α	C_β	C_γ	Other
β-O-4'	71.0-72.0	83.5-83.7/ 84.0-84.4	59.8-60.0	
β-5'	~87.0	53.4	~63.0	
β-β'	~86.0	53.8	~71.0	
Dibenzodioxocin	85.0-86.5	85.0-86.5	60.0	
α-C=O in β-O-4	--	85.2	62.0	
Ar-CH=CH-CH_2OH	127.5	126.5	61.5	
Ar-CH=CH-CHO	153.0	129-130	194-195	
Ar-CHO	191-193	--	--	
β-1'	72.0-75.8	54.7-56.5	62.2-64.5	
Ar-CH_2-CH_2-CH_2OH	33-34	31-32	64.0	
Spirodienone	--*	--*	--*	180.7 (C=O)
Ar-CO-CH_2-CH_2OH	198	42	57.1	
Ar-CH(OH)-CH_2-CH_2OH	71.4	42.9	56.4	
Methoxyl	56.3	--	--	

* Nonacetylated chemical shifts not reported in literature.

Table 2.9 ^{13}C NMR chemical shifts for the side chain carbons of the major interunit linkages in acetylated softwood lignin. [14, 16, 17, 79, 119, 140, 141, 147, 149-155]

	Chemical Shift, ppm			
	C_α	C_β	C_γ	Other
β-O-4'	73.5-75.4	79.3-80.6	62.8-63.5	
β-5'	88.1-88.6	50-51.5	65.0-66.1	
β-β'	85.1-86.1	55.0	71.8-72.5	
Dibenzodioxocin	84.2-84.9	82.5-83.4	64.5	
α-C=O in β-O-4	194-195	79.7-81.6	63.3-64.3	
Ar-CH=CH-CH_2OAc	133.5-134.8	123.2-123.7	64.8-65.6	
Ar-CH=CH-CHO	151.8	128.8-132	193.4	
Ar-CHO	191	--	--	
β-1'	74.8-76.0	50-51.2	64.0-64.9	
Ar-CH_2-CH_2-CH_2OAc	32.2	30.2	63.8	
Spirodienone	83-84	57-58	62-63	180.7 (C=O)
Ar-CO-CH_2-CH_2OAc	198	37-38	60-61	
Ar-CH(OAc)-CH_2-CH_2OAc	72.5-73.0	35.3	60.6-61.0	
Methoxyl	N/A	N/A	N/A	56.3
Primary OAc (γ-hydroxyl)	N/A	N/A	N/A	171.5
Secondary OAc (α-hydroxyl)	N/A	N/A	N/A	170.8
Phenolic OAc	N/A	N/A	N/A	169.6

2.6.5 Quantitative ^{13}C NMR Experiments

Quantitative ^{13}C NMR experiments involve a 90^{o} pulse using an inverse gated decoupling (IGD) sequence to remove carbon/proton coupling while also suppressing the Nuclear Overhauser Effect (NOE). In this experiment, broadband decoupling is only used during the acquisition period and is gated off during the recovery period. [119]

2.6.6 ^{13}C DEPT (Distortionless Enhancement by Polarization Transfer)

DEPT involves a more complicated pulse sequence designed to generate –CH, $-CH_2$, and $-CH_3$ subspectra. The DEPT experiment involves three different ^{1}H pulses along the *y*-axis ($\theta_1=\pi/4$; $\theta_2=\pi/2$; $\theta_3=3\pi/4$) and separates the signals onto different subspectra. (**Figure 2.37**) The DEPT experiment has been used on many occasions for structural characterization of lignin, [156, 157] however, it suffers from the drawback that it is not completely quantitative. It is useful for some elucidation of peak overlap in the ^{13}C quantitative NMR spectrum. It is also possible that with sufficient recovery delays, DEPT may be considered quantitative, however this would require much longer experiments. [119]

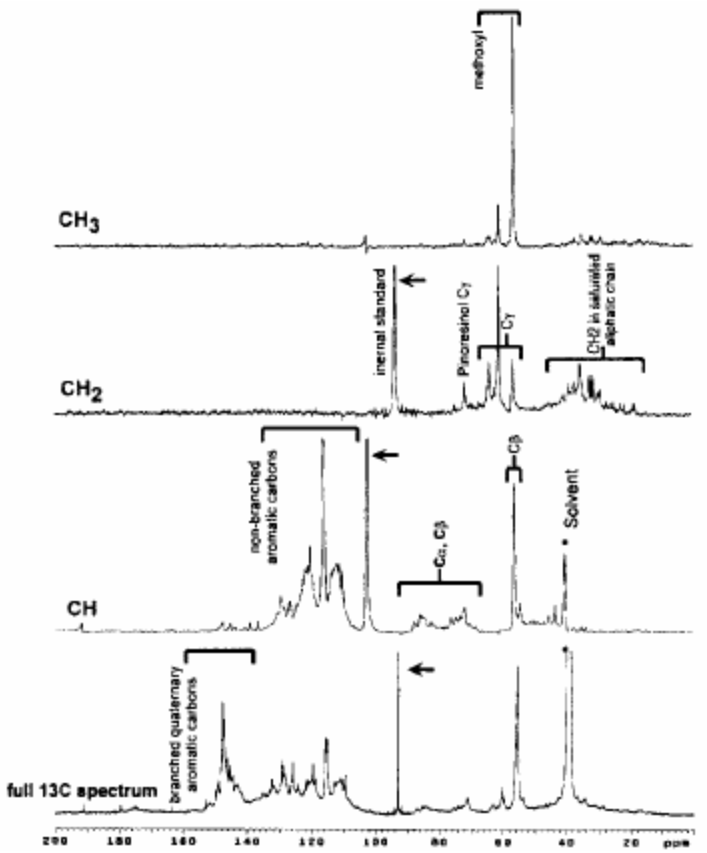

Figure 2.37 Quantitatively edited ^{13}C spectra using the DEPT pulse sequence. [157]

2.6.7 Two-dimensional homonuclear correlation experiments

2.6.7.1 ^{1}H-^{1}H COSY (COrrelation SpectroscopY)

In the single pulse experiments, a 90^{o} pulse along the *x*-axis moves the *z*-axis magnetization into the rotating frame, *x*-*y* axis. COSY involves a second 90^{o} pulse that transfers the y-axis magnetization to the negative and as a result only the *x*-axis magnetization is seen in the rotating frame. COSY utilizes a series of t_1 periods with different values and frequency from Fourier transform of the FID will yield a plot of frequency (v_1) versus t_1 along the diagonal. A plot with v_2 and v_1 on the *x*- and *y*-axes, respectively, yields the COSY spectrum. [127] Correlation between two coupled protons can therefore be mapped out on the two-dimensional plot.

2.6.7.2 TOCSY (TOtal Correlation SpectroscopY

In the COSY experiment, connectivity must be mapped from proton to proton correlation. TOCSY is a variant of the COSY experiment in which proton spin-locking is applied during the second 90° pulse. As a result, all spins within a spin system become closely coupled allowing magnetization to be transferred among all protons. As a result, the spin system can be directly mapped out.

TOCSY have been reported numerous times in analysis of lignins and have been shown to be useful in identification of minor structures as well as elucidation of new structural moieties. [38, 94, 158-161]

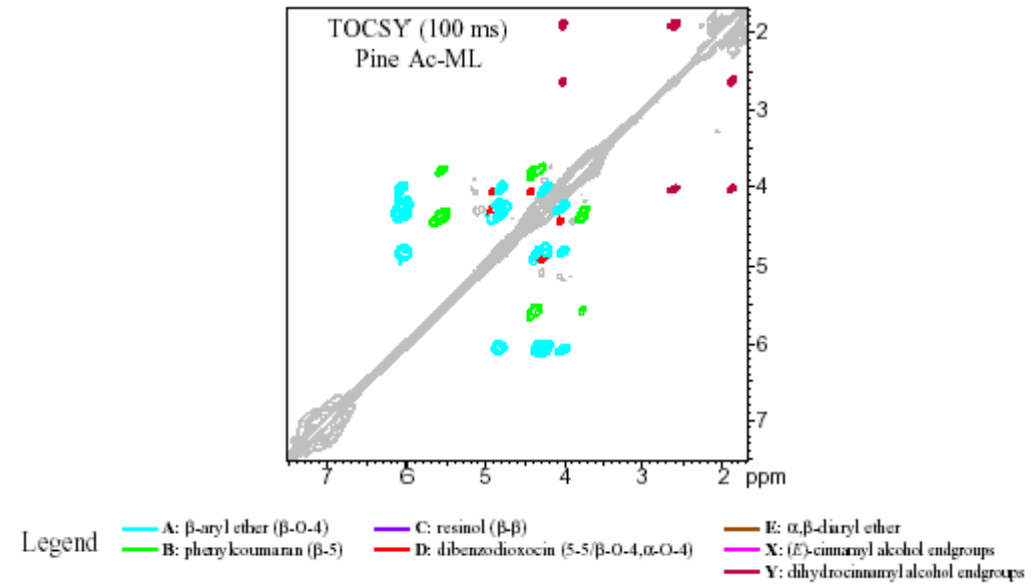

Figure 2.38 TOCSY spectrum of an acetylated *Pinus taeda* milled wood lignin. [149]

2.6.7.3 ^{13}C-^{13}C INADEQUATE

The INADEQUATE experiment shows the correlation between adjacent ^{13}C carbons. Because the natural abundance of the ^{13}C is so low, this is a low sensitivity experiment, however this can be enhanced by ^{13}C enrichment. [121] The INADEQUATE experiment

also suffers from the fact that since carbon-carbon connectivities are being mapped, ether bonds will interrupt mapping.

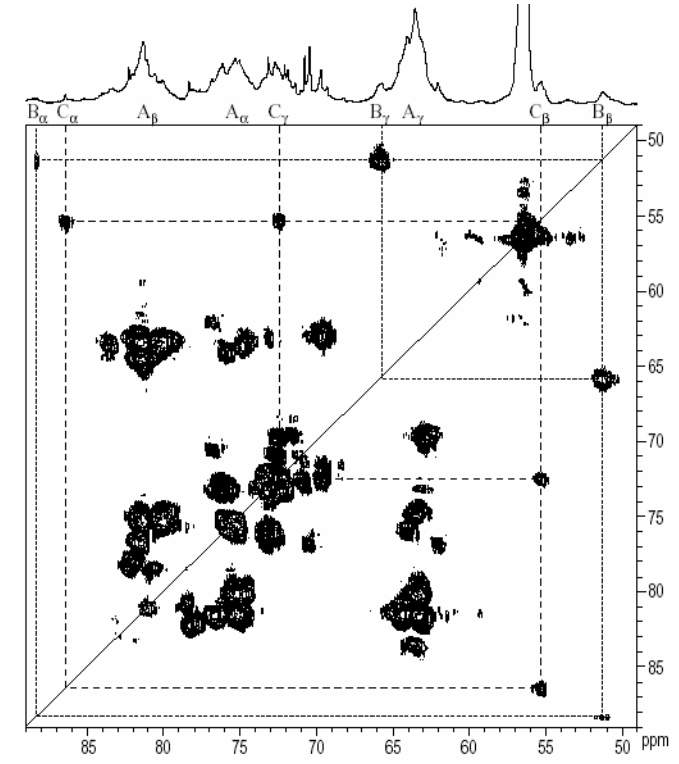

Figure 2.39 Partial INADEQUATE spectrum showing just the sidechain region, from a ^{13}C-enriched ryegrass isolated lignin that contained substantial polysaccharide components. [149]

2.6.8 Two-dimensional heteronuclear correlation experiments

2.6.8.1 HMQC (Heteronuclear Multiple Quantum Coherence)

HMQC is one of the most useful NMR techniques available for analysis of lignin structure. With the HMQC technique, one is able to detect the correlation between primarily attached pairs of protons and carbons. The spectra therefore consists of ^{1}H and ^{13}C axes allowing the signals to be spread out into two dimensions. As mentioned previously signals will be heavily overlapped in the ^{13}C NMR spectrum and structural elucidation utilizing the HMQC analysis is helpful.

Another advantage of the HMQC experiment is the enhanced resolution gained from inverse detection, which means that the ^{13}C signals are acquired from the proton dimension rather than the carbon dimension. This is achieved by quantum coherence, when multiple spin systems, in this case ^{1}H and ^{13}C, precess around the same axis. [162] Ralph, et al., have demonstrated how good the resolution is for this experiment by demonstrating the qualitative advantages of this method after only 4 minutes of acquisition. [149] The major disadvantage is that this experiment does not detect quaternary carbons because it is a proton-carbon correlation. Therefore, no information about lignin condensation can be ascertained. On the other hand, this experiment is more useful for elucidation of side chain structures and therefore this drawback is minimized.

The use of HMQC has been well documented in the literature in lignin structural analysis. [149, 159, 163-165] As with other NMR experiments, assignment of major structural moieties can begin with assignments from model compound data found in the literature. Identification of new structures such as dibenzodioxocin[14], isochroman[15, 149], and spirodienone[16] have been identified by using this technique.

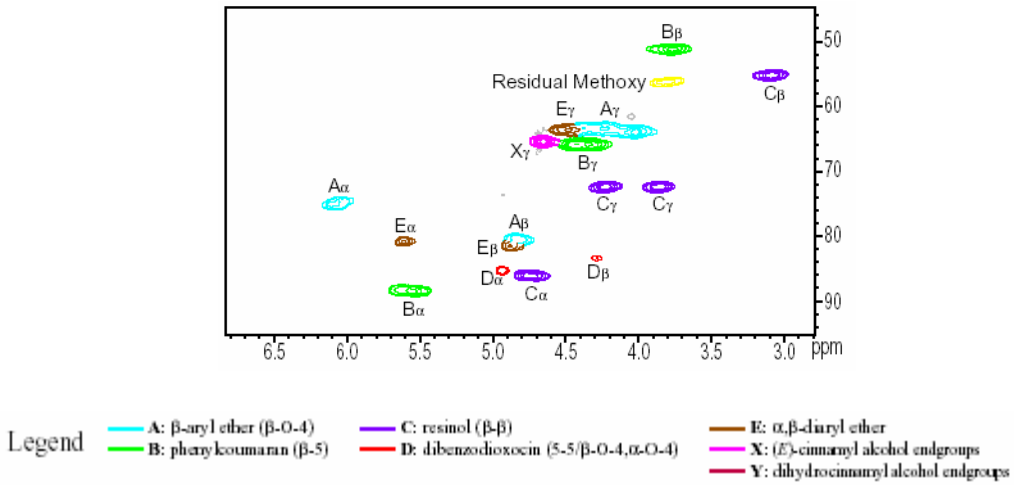

Figure 2.40 HMQC NMR spectrum of a "methoxy-less" coniferyl alcohol synthetic lignin. [149]

2.6.8.2 HMBC

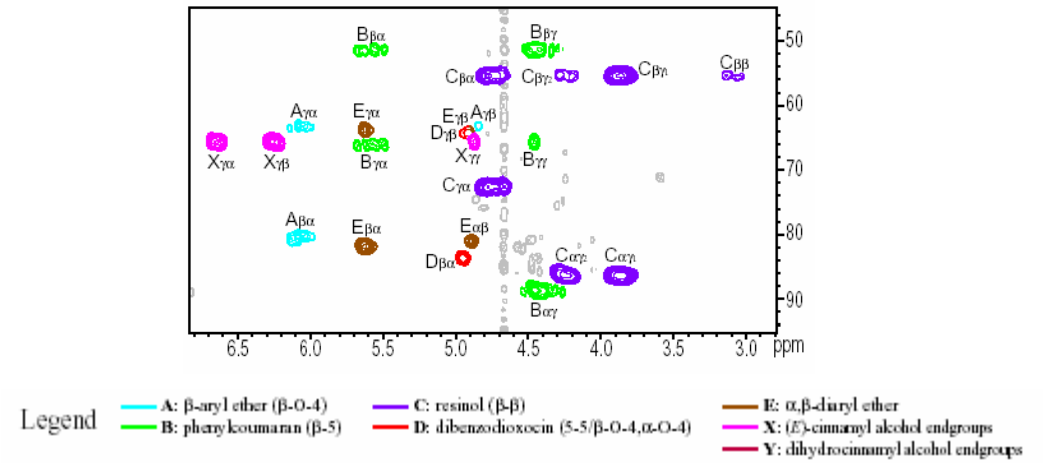

Figure 2.41 HMBC NMR spectrum of a "methoxy-less" coniferyl alcohol synthetic lignin. [149]

HMBC is in the same class as HMQC but is useful for long range correlations, typically two to three bond ^{13}C-^{1}H correlations. HMBC is particularly useful in the quest to confirm structural moieties. A couple of examples have been the confirmation of the incorporation of ferulate esters into ryegrass lignin. [166, 167]

2.7 Solid-State NMR

Under conditions similar to solution-state, solid-state NMR spectra are broad and poorly resolved. Both solution and solid-state NMR experience *J*-coupling, which is through bond spin-spin interactions. Solid-state NMR also suffers from dipole-dipole coupling (*D*-coupling) because of rigid chemical structure and chemical shift anisotropy (CSA). In solution-state dipoles are constantly reoriented due to tumbling in solution and the dipole interactions are averaged out. While the *J*-coupling is typically on the order of 10 Hz, *D*-coupling is on the order of several hundred to a few thousand Hz making it the dominant interaction in solid-state NMR. *D*-coupling can be eliminated by irradiation with a strong B_2 field and thus high-powered decoupling is typically used to reduce linewidths.

Chemical shift anisotropy depends upon orientation of the molecule surrounding the nuclei in relation to the B_0 magnetic field. To eliminate this anisotropy the axis of spinning is set at a 54.7^o to the magnetic field to mimic the effects of tumbling. [168] This is the so-called magic angle spinning (MAS), and is the angle between the edge of a cube and the adjacent diagonal through the cube. This allows for the averaging of all orientations similar to tumbling in solution. Magic angle spinning must be at a rate higher than the *D*-coupling, and typically spinning speed are from 2-20 kHz.

2.7.1 Cross Polarization/Magic Angle Spinning (CP/MAS)

Sensitivity can also be a problem in the solid-state NMR due to the low natural abundance of ^{13}C. As a result, cross polarization (CP) is commonly used to enhance the carbon signal. A 90^o ^1H pulse on the *x*-axis brings the protons to the *y*-axis and then a second 90^o pulse on the *y*-axis induces spin-locking of the protons. During this time, a 90^o ^{13}C

pulse, brings the ^{13}C magnetization onto the *y*-axis. In this way magnetization from the much more abundant protons is transferred to the less abundant carbons, enhancing their resolution. [169]

CP/MAS was first used by Schaefer and Stejskal to analyze wood in 1976 [168] and later Bartuska, et al., introduced spectra with higher resolution. [170] Since that time, many researchers have investigated solid wood and isolated lignins by CP/MAS. While the peaks are broad relative to those in solution-state NMR, assignment of particular carbons can still be made, however information regarding interunit linkages is still lacking.

Nonetheless, researchers have been able to ascertain some structural information regarding lignin. Lignin content in wood has been estimated by the ratio of the integration of the region from 159-141 ppm, assigned to C_3 and C_4 in lignin, to the integration of the entire spectrum. From this an estimation based upon C_9 units can be performed. [171] This is not valid for hardwoods, however, as the syringyl C_4 will lie at ~135 ppm. Haw integrated over the entire aromatic region and this works for a softwood, but hardwoods contain an overlap from carbohydrates at ~108 ppm. [172] A method to estimate the syringyl/gauaicyl ratio has been proposed. [173]

2.7.2 Interrupted Decoupling (Dipolar Dephasing)

In this experiment the high-powered decoupler used to eliminate the carbon-proton interaction is gated off for a period of time prior to acquisition. As a result, spin-lattice relaxation can occur and the magnetization of the carbon is allowed to decompose. However, because this process occurs much more quickly if there is a directly attached proton, only the

protonated carbon signals will decay and as result a spectrum containing quaternary carbons, of which the vast majority are located on the aromatic ring, can be obtained.

Condensed lignin structures are generally substituted at the C_5 or C_6 positions in kraft lignin and will shift the resonance of the substituted carbon to 126 ppm. C_1 will center around 133 ppm. As a result, integration of the chemical shift ranges 164-141 ppm (Region A) and 141-100 ppm (Region B) will provide an estimate of the etherified and nonetherified aromatic protons, respectively. Integration of the regions can result in determination of the A/B ratio and will give an indication of the degree of condensation in the lignin. This method for determining the degree of condensation in lignin has been reported numerous times in the literature. [172-178] Peak fitting of these spectra can also result in an estimation of the free phenolic and etherified β-O-4' content of the lignin. [23, 169]

Although CP/MAS is a widely used to technique in lignin analysis, it suffers from three drawbacks:

1. It is not quantitative because of inefficiency of polarization transfer to the unprotonated carbons.
2. Spinning sidebands will reduce the centerbands of peaks reducing intensity.
3. Baseline distortion due to deadtime associated with each pulse.

The following experiments serve to address these problems.

2.7.3 Direct Polarization (DP/MAS) or Bloch Decay Experiment

To avoid the inefficiencies of cross polarization, direct irradiation with a 90^{o} ^{13}C pulse on the *x*-axis can be employed. [25, 176] In this experiment, care must be taken so that the relaxation time is sufficiently long to allow all spins to return to their *z*-axis

magnetization. Typically this value should be 5 times the longest relaxation delay and can result in very lengthy experiments. In lignins a relaxation delay of 2-4 s is usually sufficient. [169, 176, 178]

2.7.4 CP/TOSS (TOtal Sideband Suppression)

The TOSS pulse sequence is applied prior to the start of signal detection to remove spinning sidebands. [179] CP/TOSS is not completely quantitative because the suppressed sidebands are not fully added back to the center peak. Aromatic and carbonyl carbons are particularly underestimated as their large chemical shift anisotropy lead to large sidebands.

This problem can be corrected by employing a correction factor based upon the DP/MAS spectrum and using high spinning speeds. Therefore, large amounts of similar samples can be analyzed by employing the correction factor Mao, et al., have shown that this can be a reliable technique and have termed this experiment CP/T_1-TOSS. [23]

2.7.5 Efficient CH-group selection

This is a new spectral editing technique that can selectively filter methylene and quaternary carbons and reduces methyl carbon signals. The authors consider this method to be "essentially…a solid-state, slow-magic-angle-spinning version of the distortionless enhancement by polarization transfer (DEPT) experiment". [26]

The benefit of this experiment is indeed that a DEPT-like separation of the –CH_3, -CH_2, and -CH carbons into subspectra. Part of the drawback of solid-state NMR spectroscopy of lignins has been the relative lack of information obtained. We have

discussed above that the degree of condensation, free phenolic hydroxyls, and etherified β-O-4' moieties can estimated by the interrupted decoupling technique.

The efficient –CH group selection experiment can aid in the estimation of sidechain structures. Although resolution is still not equivalent to the solution-state experiment, integration and deductive reasoning can lead to valuable conclusions. Specifically, of the region 55-50 ppm will yield the relative amount of condensed side chain structure, i.e., β-β', β-5', and β-1'. Integration of the region from 90-60 ppm will yield primarily etherified side chain structure and secondary hydroxyl groups. The ultimate goal of developing this technique is an in-depth evaluation of the unaltered lignin structure in Wiley-wood meal.

2.7.6 HETeronuclear CORrelation Experiment (HETCOR)

The HETCOR is a two-dimensional experiment that can be applied to the solid-state. HETCOR yields results somewhat similar to the HMQC solution-state experiment as it displays ^{1}H-^{13}C correlations in a two-dimensional spectrum. However, depending on spin diffusion time different correlations can be observed. Specifically, shorter spin diffusion time results in a spectrum similar to HMQC, longer spin diffusion time will give longer range correlations. Nonprotonated carbons can even be observed with longer spin diffusion times, however this yields a much more complex spectrum. [180] Mao et. al., have shown that the spectrum can be simplified by including a dipolar dephasing step in the sequence. [24]

Liitia, et al., have attempted to use HETCOR in the analysis of residual and milled wood lignins. [181] However, their resolution was very poor, limiting the information that could be obtained. A high resolution spectrum using Mao's pulse sequence will allow us to detect some of the actual linkages in Wiley wood meal. [24] Some interesting questions can

possibly be answered. For instance, are coniferyl alcohol and coniferaldehyde incorporated during biosynthesis or are they an artifact of the milling process as has been indicated as being possible?

3. Methods and Materials

3.1 Isolation of Milled Wood Lignin (MWL) and other isolatable lignins

All samples were produced from loblolly pine (*Pinus taeda* L.) sapwood that was ground to pass a 20-mesh screen in a Wiley mill. Following successive Soxhlet extractions with ethanol/benzene (1:2, v/v) and ethanol each for 24 h, the resulting **Wiley Wood** was air-dried and stored in a desiccator under vacuum over P_2O_5. This dried Wiley wood is the sample referred to in the DFRC, thioacidolysis, and solid-state NMR studies. All lignins produced from various isolation methods were produced from the bulk Wiley-milled wood.

3.1.1 Isolation of lignin via the Bjorkman isolation procedure

According to the standard MWL isolation procedure[61], Wiley wood (100g) was ground in a 1-gallon porcelain jar under a nitrogen atmosphere using glass ballson a rotary mill for a period of 1 week. The rotary-milled wood was removed and dried in a vacuum dessicator over P_2O_5. A portion of this material was saved as the sample **Rotary Glass 1 Week Wood**.

10 g of the rotary-milled wood was then placed in a vibratory ball mill (Siebtechnik GMBH, 433 Mulheim 011380, Germany) with stainless steel balls and ground for 48 h under a nitrogen atmosphere in the presence and absence of toluene. These samples are referred to **Vibratory Wood** and **Vibratory (Dry) Wood**, respectively.

3.1.2 Milled Wood Lignin Isolation

MWL, CEL (celluloytic enzyme lignin), and REL (residual enzyme lignin) were isolated according to the methods of Bjorkman[61] and Chang[73]. (**Figure 3.1**) 25 g of

either Vibratory wood or Vibratory (dry) wood was weighed into a 500 mL centrifuge bottle and 250 mL of dioxane/water (96:4, v/v) were added and the solution was stirred at room temperature for 24 h under a nitrogen atmosphere. The solution was centrifuged and the supernatant was collected. The remaining solid material was once again dispersed in the 96 % dioxane solution and the above procedure repeated. The final solid material was washed twice with deionized water and freeze-dried. The supernatant from centrifugation was concentrated to a volume of about 100 mL. The concentrated dioxane solution was added dropwise to deionized water in a freeze-dry flask with stirring to induce precipitation. This sample was freeze-dried and the resulting crude MWL stored in a desiccator under vacuum over P_2O_5.

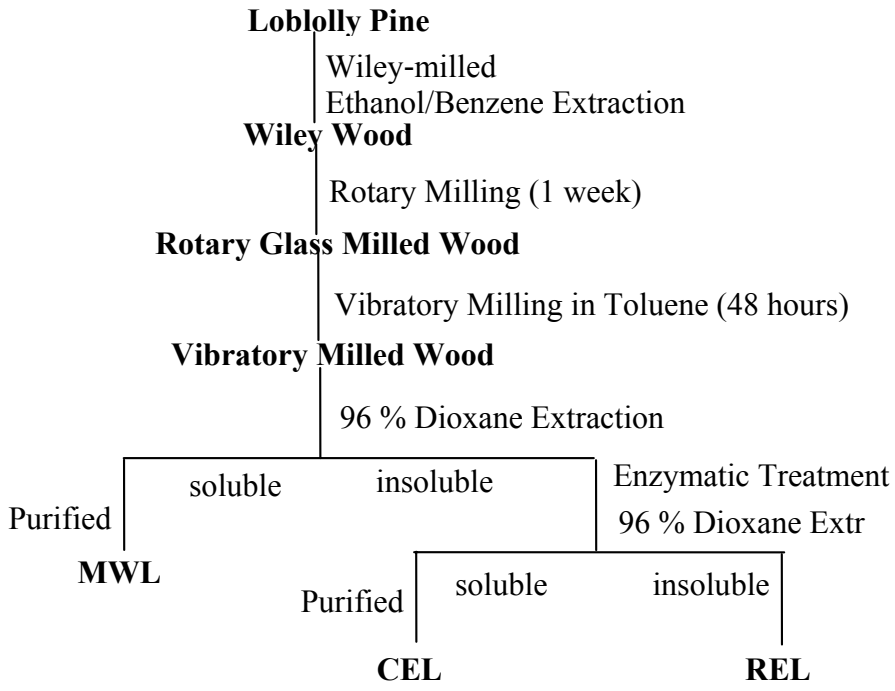

Figure 3.1 Bjorkman MWL isolation procedure.

The crude MWL was dissolved in 20 mL of 90 % acetic acid (9:1, v/v) and precipitated into water (400 mL). The precipitated lignin was filtered, dried, and dissolved in 10 mL of 1,2-dichloroethane/ethanol (2:1, v/v), precipitated into 200 mL of ether, and then washed with petroleum ether. This final lignin material was air-dried, ground to further facilitate evaporation of ether, and finally stored in a desiccator under vacuum over P_2O_5. These samples are labelled **Vibratory MWL** and **Vibratory (Dry) MWL**.

3.1.3 Preparation of Cellulolytic Enzyme Lignin (CEL) and Residual Enzyme Lignin (REL)

CEL was isolated from the freeze-dried insoluble materials from the MWL isolation procedure discussed above. This residue was suspended in 250 mL of an acetate buffer (4.1 g of sodium acetate and 2 mL of glacial acetic acid in a 1-L volumetric flask filled to the mark with deionized water, pH 4.8). [73] 10 mL of an industrial cellulase enzyme solution (Dyadic SuperAce, Dyadic International Inc., Jupiter, FL) was added, and the reaction slurry was incubated for 24 h at 55 °C. The mixture was centrifuged for 10 min. at 500 rpm and the supernatant removed and discarded. The insoluble material was again dispersed in the acetate buffer and the enzyme treatment repeated twice. The solution was centrifuged and the enzyme-treated residue was washed twice with deionized water and freeze-dried.

At this point, the enzyme-treated residue was extracted twice with 96 % dioxane, analogous to the MWL isolation procedure described above. The concentrated dioxane-soluble material was again precipitated and freeze-dried. The purification of the freeze-dried material was performed identically to the procedure described above for MWL. This

cellulolytic enzyme lignin was stored in a desiccator under vacuum over P_2O_5 and labeled **Vibratory CEL** and **Vibratory (Dry) CEL**.

The insoluble material from the dioxane extractions was washed thoroughly with water and freeze-dried. This residual enzyme lignin was stored in a desiccator under vacuum over P_2O_5 and labelled **Vibratory REL** and **Vibratory (Dry) REL**.

3.1.4 MWL Isolation Procedures Involving only Rotary-milling of Wood

Brownell reported that milling of wood could be performed using only the conventional rotary ballmill provided that milling was prolonged to a period of weeks.[66, 182] This procedure is advantageous from the standpoint that a large portion of milled wood can be prepared in one simple step. The vibratory ball mill can handle only 10 g at a time, so the 100 g of rotary-milled wood must be handled numerous times to achieve a full sample of finely milled wood. In addition it is possible that the rigorous action imposed upon the wood in the vibratory ball mill can be minimized by performing a longer, more gentle milling. This approach may minimize to some extent the structural changes occurring during milling.

Different rotary-milled wood samples were created by varying the milling time and by using different types of balls to perform the milling. Specifically, 100 g of Wiley wood was ground in a 1-gallon porcelain jar under a nitrogen atmosphere using either glass, porcelain, or Teflon balls. The wood samples were then milled for periods of 1, 2, 4, and 6 weeks. (**Figure 3.2**) These milled wood samples were labelled according to their milling history, i.e., **Rotary Glass 6 Week Wood**. MWL, CEL, and REL were then isolated as described previously for the Bjorkman and Chang isolation procedures. [61, 73] All samples were

stored in a desiccator under vacuum over P_2O_5 and labelled accordingly, i.e., **Rotary Glass 6 Week MWL**.

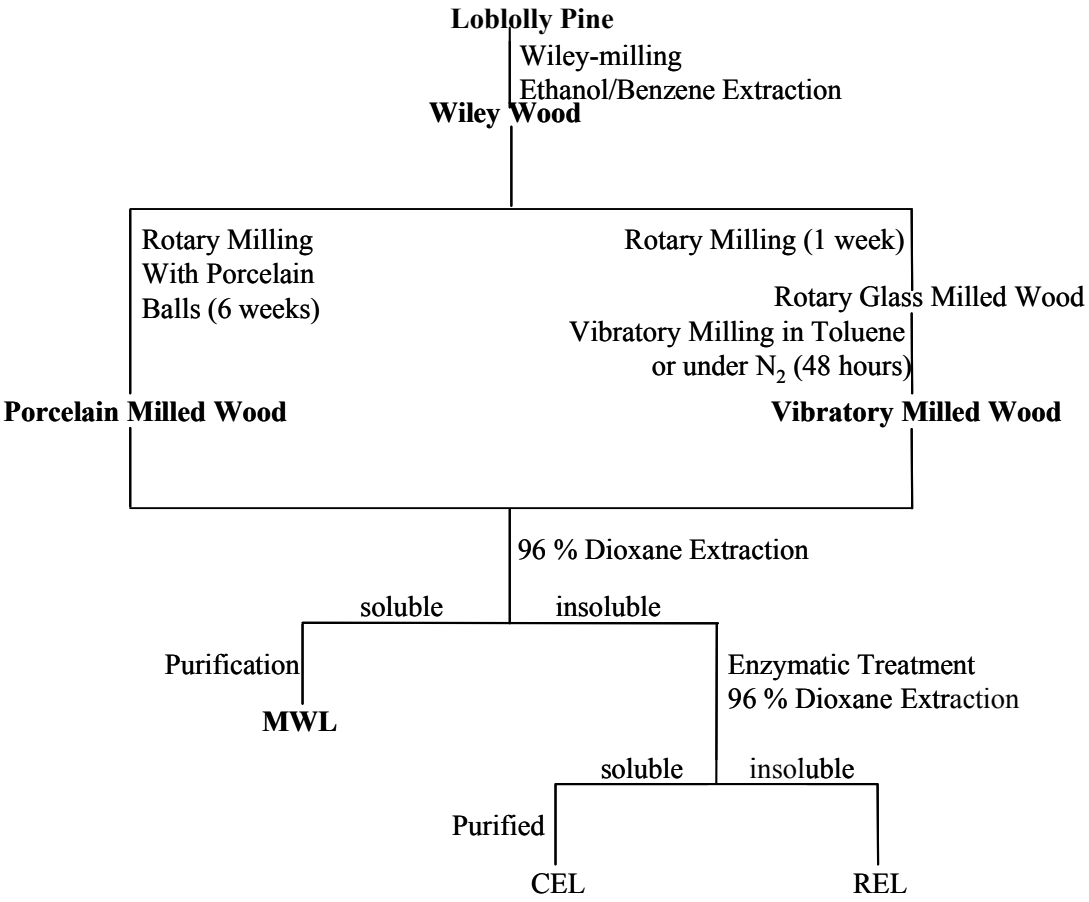

Figure 3.2 Various milling techniques employed in MWL isolation.

3.2 Derivatization Followed by Reductive Cleavage (DFRC)

3.2.1 Standard DFRC Procedure

The standard DFRC procedure was recently developed by Lu and Ralph. [82-85](**Figure 2.20**) Milled wood (50 mg) and isolated lignin samples (25 mg) are dissolved in 5 mL of acetic acid/acetyl bromide (4:1, v/v) and 0.25 mg of tetracosane as an internal standard is added and stirred for 3 h at 50 °C. The reaction is terminated by removal of the solvent using a vacuum manifold at 20 mTorr. Immediately after the solvent is removed, the lignin was dissolved in 5 mL of a dioxane/acetic acid/water mixture(5:4:1, v/v) and 250 mg of zinc dust was added. The solution is stirred for 30 minutes at room temperature. The zinc dust is removed by filtration through a folded piece of filter paper in a small glass funnel, and the solution is extracted two times with 20 mL of CH_2Cl_2. The organic layer is dried with anhydrous sodium sulfate and removed by evaporation. The residue is dissolved in 2 mL of acetic anhydride/pyridine (1:1, v/v) and stirred for 40 minutes at room temperature. The reaction is stopped by removing the solvent, and the residue is dissolved in dichloromethane (0.5 mL) and analyzed by gas chromatography. The monomeric product of interest from this procedure is coniferyl alcohol diacetate and the quantity obtained can be determined by ratio of the peak area to the internal standard.

3.2.2 Modified DFRC Method

The DFRC method can be modified by two simple modifications to obtain a much larger amount of structural information: The wood and lignin samples must be premethylated prior to the DFRC analysis, and the acetylation step is replaced by a

propionation step by simply changing derivatizing agents. (**Figure 2.21**) Otherwise, the DFRC methods are identical in procedure. (**Section 4**)

Milled wood (50 mg) and isolated lignin samples (25 mg) are dissolved in 5 mL of acetic acid/acetyl bromide (4:1, v/v) and 0.25 mg of tetracosane as an internal standard is added and stirred for 3 h at 50 °C. The reaction was terminated by removal of the solvent using a vacuum manifold at 20 mTorr. Immediately after the solvent was removed, the lignin was dissolved in 5 mL of a dioxane/acetic acid/water mixture (5:4:1, v/v) and 250 mg of zinc dust was added. The solution was stirred for 30 minutes at room temperature. The zinc dust was removed by filtration through a folded piece of filter paper in a small glass funnel, and the solution was extracted two times with 20 mL of CH_2Cl_2. The organic layer was dried with anhydrous sodium sulfate and removed by evaporation. The residue was dissolved in 2 mL of propionic anhydride/pyridine (1:1, v/v) and stirred for 40 minutes at room temperature. The reaction was stopped by removing the solvent, and the residue was dissolved in dichloromethane (0.5 mL) and analyzed by gas chromatography. Three monomeric products of interest are obtained, each representing the cleavage of a different type of structural unit in the lignin structure. More thorough discussion of these products will be addressed in **Section 4**.

3.2.3 Methylation

All methylations were performed using a diazomethane ether solution produced from *N*-methyl-*N*-nitroso-*p*-toluenesulfonamide. 1 g of the insoluble lignin preparations (Wiley wood, milled wood, and REL), the samples were suspended in 20 mL of dioxane/methanol (2:1, v/v) followed by the addition of 5 mL of the diazomethane ether solution and stirred for

3 hours at room temperature. The ether phase was removed by evaporation, and 2 mL of fresh diazomethane were added. This procedure was repeated 6 times. After the final methylation, the solution was removed by evaporation, and the residue was washed with 100 mL of ether and dried.

1 g of the soluble lignin preparations (MWL or CEL) were dissolved in 20 mL dioxane/methanol (2:1, v/v) and reacted for 1 h with 5 mL of diazomethane. Methylation with diazomethane was repeated 3 times and then the samples were concentrated, dissolved in 5 mL of dioxane/methanol (2:1, v/v), precipitated into 100 mL of ether, and collected by filtration.

The completeness of methylation was determined using the $\Delta\varepsilon$ method [183] by the absence of a bathochromic shift in the UV difference spectra. Additionally, ^{1}H NMR analysis of acetylated methylated lignin showed no phenolic acetate group. [139]

3.3 Nitrobenzene Oxidation

Leopold optimized the conditions for nitrobenzene oxidation which is the method usually used to perform these analyses.[102] 50 mg of a predried isolated lignin or 200 mg of pre-dried, pre-extracted lignocellulosic material is added to a 10-mL stainless steel bomb along with 7 mL of 2M NaOH and 0.4 mL of nitrobenzene. The bomb is sealed and placed in a heating mantle, heated to 170 ^{o}C, and reacted for 2.5 hours with occasional shaking to stir material. The bomb is cooled in an ice water bath and the material is extracted with chloroform to isolate nitrobenzene oxidation products. The aqueous phase is acidified to pH 3-4 by addition of conc. HCl and extraction with chloroform is performed. The chloroform is dried over anhydrous Na_2SO_4 and the solvent is then removed under reduced pressure at 40

^{o}C. The dried material is diluted tenfold and 1 mL is placed in a GC vial for analysis. Quantification of reaction products are determined by calibration against *m*-meconic acid.

3.4 Thioacidolysis

The thioacidolysis solution is generally prepared immediately prior to use and will keep for only a day or two before the stock solution needs to be replaced. 1,4-dioxane is distilled over $NaBH_4$ in order to remove peroxides and 20 mL are added to a 100 mL volumetric flask. Boron trifluoride etherate ($BF_3{\cdot}Et_2O$) can be used directly if it is purchased in a sure seal bottle. Otherwise a clear solution indicates that it is fresh, a black solution must be redistilled. As a result it is preferrable to use a newly purchased product with a sure seal. 2.5 mL of $BF_3{\cdot}Et_2O$ and 10 mL ethanethiol (CH_3CH_2SH) are added to the 100 mL flask containing the dioxane and the flask is filled to the mark with dioxane. [96, 184]

Thioacidolysis can be performed on milled wood and isolated lignins to achieve a single monomeric product, similar to the standard DFRC method. Like the modified DFRC method,a premethylated lignin sample can provide additional structural information. This will be discussed in more detail in **Section 5**. [100]

As a result, 10 mg of either the methylated or unmethylated material were added to a 20 mL tube with a Teflon cap, and 10 mL of the thioacidolysis solution were added by pipette to the tube. The solution was generously blanketed with Ar and the cap replaced tightly on the tube. The tube is then placed in an oil bath and heated to 100 ^{o}C for 4 hours with occasional shaking.

The reaction is quenched by placing the tube in an ice water bath. The solution mixture is washed into a 250 mL separatory funnel with about 15 mL of deionized water and

1 mL of the internal standard in CH_2Cl_2 (0.25 mg/mL) is added. The pH of the aqueous phase is adjusted to pH 3-4 using 0.4 N $NaHCO_3$. The aqueous phase is extracted three times with about 50 mL of CH_2Cl_2. The combined organic phases are dried over anhydrous Na_2SO_4 and evaporated under reduced pressure at 40 ^oC. The dried extracts are then redissolved in 0.5 mL CH_2Cl_2 and an aliquot of this solution is silylated for GC analysis. Specifically, 10 μL of this solution is added to a GC vial along with 50 μL of N,O bis (trimethylsilyl) trifluoroacetamide (BSTFA) and 5 μL of pyridine. Silylation is complete within a couple of hours and the silylated compounds are stable for at least 24 hours.

3.5 Gel Permeation Chromatography

GPC analyses were performed on a Waters HPLC system at ambient conditions using two μ-Styragel columns (HR-1 and 5E) connected in series. For the soluble lignins discussed in **Sections 4** and **5**, THF was the eluent, and for the rest of the samples, DMF with 0.1 N LiCl, added to eliminate lignin association, was the eluent. The fractions were monitored using refractive index (Waters refractometer model 410) and UV absorbance at 280 nm (Waters UV spectrometer model 484). All lignins were dissolved at a concentration of 1 mg/mL, and the flow rate was 0.5 mL/min, 120 μL of this solution were then injected into the HPLC. Molecular weight determinations were made using polystyrene as a calibration standard.

3.6 ^{1}H NMR Analysis

^{1}H NMR analyses were performed using a GE 300 MHz instrument. 10 mg of samples were dissolved in 0.6 mL of $CDCl_3$ containing 0.1 % TMS (tetramethylsilane) and placed in a 5-mm NMR tube.

3.7 ^{1}H-^{13}C Two-Dimensional Correlation NMR (HMQC) Spectroscopy

HMQC spectra were recorded on an Avance 500 MHz spectrometer (Bruker, Billerica, MA) using a narrow-bore magnet (Oxford, U.K.). 40 mg of dry lignin or dried material after DFRC or thioacidolysis degradation were accurately weighed and dissolved in 0.75 mL of either $CDCl_3$ or DMSO-d_6. The chloroform-d crosspeak at δ_C/δ_H 77.23/7.265 and the DMSO-d_6 crosspeak at δ_C/δ_H 39.5/2.50 were used as internal references. The system was controlled by the SGI INDY host workstation, and the data were processed with XWIN NMR. The instrument was equipped with three frequency channels with waveform memory and amplitude shaping, three channel gradient control units (GRASP III), and one variable temperature unit, as well as one unit for precooling and temperature stabilization. All measurements have been carried out with a 5 mm i.d. ^{1}H/BB (109Ag-31P) triple-axis gradient ID500-5EB probe (Nalorac Cryogenic Corp., Martinez, CA). The operational frequency for ^{1}H nucleus was 500.128 MHz and and for the ^{13}C nucleus was 125.032 MHz. Conditions for analysis included a 90° pulse width of 10 μs and a 1.5 s pulse delay (d_1).

3.8 Quantitative ^{13}C NMR Spectroscopy

Quantitative ^{13}C NMR spectroscopy was performed on the same instrument as described above for the HMQC experiment using a ^{13}C NMR GE probe. The operational frequency for the ^{1}H nucleus was 500.128 MHz and for the ^{13}C nucleus was 125.032 MHz. Samples were accurately weighed to 70 mg and dissolved in 0.25 mL of $CDCl_3$ and carefully pipetted into a 5 mm Shigemi tube. Acquisition was facilitated by the addition of 10 μL of a 0.25 mg/mL chromium acetoacetonate solution, a commonly used relaxant, to decrease acquisition time. Conditions for analysis included a 90^{o} pulse width of 10 μs,an acquisition delay of 1.4 μs, and a 1.7 μs pulse delay (d_1).

3.9 Elemental Analysis

Elemental analyses (C, H, N, and Br) were performed by Complete Analysis Laboratories, Inc., Parsippany, NJ. O was calculated separately by difference.

3.10 Methoxyl Analysis

Methoxyl analyses were performed according to the modified Zeisel method. [185]

3.11 Carbohydrate content

Filtrates were analyzed by high performance anion-exchange chromatography (HPAEC) on an ion exchange CarboPac PA-1 column using a Dionex DX-500 system equipped with a pulsed amperometric detector with a gold electrode (Dionex, Sunnyvale, CA) and a Spectra AS 3500 autoinjector (Spectra-Physics, Mountain View, CA). Prior to injection, samples were filtered through 0.45 μm HV filters (Millipore, Bedford, MA) and a volume of 20 μL

was loaded. Samples were eluted with water at a flow rate of 1 mL/min, with a post-column addition of 0.5 mL/min 250 mM NaOH prior to detection. [186]

3.12 Dissolution of Lignin Isolated from Porc 6 Wood, Porc 6 MWL, and Porc 6 REL Preparations in DMSO/N-methylimidazole (NMI)

Wood chemistry has been limited from the standpoint that wood and lignin preparations of high molecular weights are insoluble, particularly in NMR solvents. Specifically, REL and milled wood samples have not been analyzed by solution-state NMR because of the insolubility of these samples. Recently however, there has been a report that finely milled wood has been dissolved using a novel solvent system, DMSO/N-methylimidazole (NMI). [21, 22] In order to study these lignins, therefore, this protocol was employed.

In order to make a direct comparison between the MWL,the REL, and milled wood portions, all samples were dissolved in the DMSO/NMI solution. Each sample was first subjected to enzymatic hydrolysis to remove carbohydrate material for NMR analysis. The MWL portions analyzed were treated only once to assure that carbohydrate overlap would not occur in the quantitative ^{13}C NMR spectrum. (**Section 6**) The milled wood and REL have much lower lignin contents, 27 % and 42 %, respectively, and therefore were treated five times to remove carbohydrates.

Lignin samples dried over P_2O_5 were carefully weighed to 100 mg and placed in a 20 mL scintillation vial. In the case of the MWL samples, the Ralph protocol was identically repeated. [21, 22] 2 mL of DMSO and 1 mL of N-methylimidazole (NMI) were added to the vial and the solution was stirred for 3 hours at room temperature even though the MWL went

almost immediately into solution. The solution was yellowish-orange in color. After three hours, 0.5 mL of acetic anhydride was added and the mixture allowed to mix for an additional 1.5 hours. The color of the solution turned completely dark brown almost immediately after addition of the acetic anhydride.

For the wood and REL, the Ralph protocol was followed, however because these samples were more difficult to dissolve, longer reaction times were used. The initial DMSO/N-methylimidazole step was allowed to mix for 8 hours, and the acetylation step was allowed to proceed overnight. Prior to addition of the acetic anhydride, the solution was light brown in color and it appeared that little of the lignin was actually dissolved. After acetylation the lignin gradually went into solution. It is interesting to note that the REL samples were the most difficult to dissolve, even more so than the milled wood. This fact could be attributable to the higher concentration of high molecular weight material in the REL.

At this point all samples were treated identically. Because the **Rotary Porcelain 6 Week Wood** and **REL** contain considerable amounts of ash from milling with porcelain balls, each sample was filtered through a No. 2 Whatman filter. In each case, only light colored ash material was left on the filter pad, indicating that the lignin was in solution. The lignin was then precipitated into two liters of deionized water and centrifuged at 5000 rpm for 10 minutes. The supernatant was decanted and the precipitated lignin material combined and washed twice with deionized water. All supernatants were collected and filtered through a Whatman 0.45 μm nylon membrane filter.

The collected lignin was washed twice with deionized water so that the filtrate ran clear and then dried in a vacuum oven at 40 ^{o}C, 30 in. Hg overnight. The lignin was

dissolved once again in $CHCl_3$ and filtered through a No. 2 Whatman paper filter to remove the remaining ash in the solution. Again, dark material indicative of lignin was not present on the filter. The $CHCl_3$ was removed by passing a stream of Ar over the surface of the solution. The final lignin material was crushed, placed in a drying pistol, and dried for a minimum of 24 hours prior to analysis by NMR. Typical yields were in the range of 110 mg and any loss in yield can be attributed to the excessive handling of the samples.

3.13 CP/MAS Solid-State NMR Spectroscopy

A Chemagnetics CMX-200 spectrometer operating at a frequency of 200 MHz for proton and for 50 MHz for carbon was used to obtain all spectra. Samples were placed in a 7.5 mm zirconia magic angle-spinning (MAS) rotor. A standard cross polarization (CP) pulse sequence was utilized with ^{13}C chemical shifts referenced to hexamethylbenzene (HMB). Conditions were optimized and used as follows: the spinning speed was 5 kHz, the contact time was 2 ms, the pulse width was 6.5 μs, the pulse delay was 3 s, and 10,000 scans were performed per sample at a temperature of 25 ^{o}C.

Conditions identical to the CP/MAS experiment described above were followed in the dipolar dephasing experiment. However, in this experiment the high-powered decoupler used to eliminate the carbon-proton interaction is gated off for a period of time prior to acquisition. As a result, spin-lattice relaxation can occur and the magnetization of the carbon is allowed to decompose. However, because this process occurs much more quickly if there is a directly attached proton, only the protonated carbon signals will decay and as result a spectrum containing only quaternary carbons is obtained. In the case of isolated lignins in particular, the overwhelming majority of quaternary carbons are located on the aromatic ring.

4. Studies on the Effect of Ball Milling on Lignin Structure Using Modified DFRC Method

T Ikeda; KM Holtman; JF Kadla; H-m Chang; H Jameel. *J. Agri. Food Chem.*, 50(1), 129-135 (2001).

4.1 Modified DFRC Method

In the original DFRC method, three steps are involved as shown in **Figure 2.20**. The first step involves acetylation of all free hydroxyl groups, including both phenolic and aliphatic hydroxyl groups, and bromination of the α-position in both α-hydroxyl and α-ether structures. In the second step, the β-O-4' structures are reductively cleaved with zinc followed by acetylation of the newly released phenolic hydroxyl groups with acetic anhydride. Thus, a single monomeric product, coniferyl alcohol diacetate, is produced from the trilignol as shown in **Figure 2.20** (Units A, B, and C). Both the *cis* and *trans* isomers of the diacetate are formed and quantitatively determined by GC.

In our modified DFRC method, a new step is added to first methylate the free-phenolic hydroxyl groups in the original lignin. This is followed by the same acetyl bromide treatment and zinc reduction steps as in the original DFRC procedure. In the final step, propionic anhydride, instead of acetic anhydride, is used to esterify the newly generated phenolic hydroxyl groups. Thus, the modified DFRC method, as shown in **Figure 2.21**, allows the quantitative determination of three different monomeric units, the uncondensed phenolic β-O-4' (Unit A), the uncondensed α-O-4' (Unit B), and the uncondensed etherified β-O-4' (Unit C) structures in lignin.

In this study with loblolly pine, DFRC monomeric products derived from both guaiacylpropane and *p*-hydroxyphenylpropane moieties were found, whereas no syringylpropane structures were observed. The yield of monomers from guaiacylpropane

structures accounted for over 95% of the total monomer yield, therefore only the yields from guaiacylpropane structures were reported.

4.2 Effect of MWL Isolation on Lignin Structure

A typical procedure used in the isolation of MWL is to first Wiley mill the wood and then subject it to vibratory milling in toluene for 48 hours. [71] The resulting wood meal is then extracted to yield MWL. The progressive mechanical treatments facilitate the disruption of the wood structure to enable the lignin to be removed by extraction. We first analyzed the various steps in the MWL isolation procedure to determine whether MWL is representative of lignin in its native state. **Wiley Wood**, **Rotary Glass 1 Week Wood**, vibratory wood milled in toluene (**Vibratory Wood**), vibratory wood milled under a N_2 atmosphere (**Vibratory (Dry) Wood**)and MWL that was isolated from vibratory wood (**Vibratory MWL** and **Vibratory (Dry) MWL**) were analyzed using the original and our modified DFRC methods. The results are given in **Table 4.1**. Good agreement was obtained for the total yield of monomeric products detected from each sample by the original and modified DFRC methods. Furthermore, the values obtained for **Vibratory (Dry) MWL** (11.7 mol % modified, 12.2 mol % original) were very close to the results reported by Lu and Ralph [84] for loblolly pine MWL (11.8 mol %). These results clearly indicate the efficacy of the modified DFRC method.

Comparing DFRC results between the **Rotary Glass 1 Week Wood** and the original **Wiley Wood** shows little change in the amount of the three different monomeric units. There was a slight increase (3.4 mol %) in the phenolic β-O-4' structures (Unit A, **Table 4.1**) and a slight decrease (6.4 mol %) in the etherified β-O-4' structures (Unit C, **Table 4.1**). Thus, rotary

ball milling appears to have minimal effect on the structure of lignin. The **Vibratory (Dry) Wood**, which was produced from the **Rotary Glass 1 Week Wood** by grinding in a vibratory ball mill, without toluene, for 48 hours showed a dramatic decrease in the DFRC monomeric products. The total yield of monomeric products decreased by one-third. However, in the toluene vibratory ball milled wood, no decrease in monomer yield was observed. As the monomeric products originate exclusively from the uncondensed units in lignin, the results suggest that vibratory ball milling under nitrogen atmosphere (dry ball milling) may cause some condensation reactions in lignin. In fact, the α-aryl ether content increased somewhat as a result of dry vibratory milling (Unit B, **Table 4.1**). In addition, the total yield of DFRC monomeric products decreased by over 30 %. This is not surprising in view of the report by Hon and Glasser that ball milling of lignocellulosics results in mechanical depolymerization involving free radicals. [187] In contrast, the vibratory milling in the presence of toluene showed almost no difference in monomeric linkages or yield as compared to the original **Wiley Wood**.

Table 4.1 Unit Composition and Total Molar Yields for the standard and modified DFRC methods.

	Unit Composition [a], mol %			Total Yield [b], mol %	
	Unit A	Unit B	Unit C	Modified Method	Standard Method
Wiley Wood	21.6	6.8	71.6	13.2	13.8
Rotary Glass 1 Week Wood	25.0	9.7	65.3	13.6	14.1
Vibratory (Dry) Wood	23.9	12.5	63.6	9.2	8.5
Vibratory (Dry) MWL	40.9	10.0	49.1	11.7	12.2
Vibratory Wood	26.7	7.8	65.5	14.8	[c]
Vibratory MWL	41.3	7.7	51.0	14.5	[c]

[a] Units A, B, and C are based upon monomeric products discussed above.
[b] Based upon a C_9 unit molecular weight of 182 g/mol.
[c] Samples not analyzed due to consistency of above results.

MWL was isolated from the vibratory wood in a yield of 22.8 wt % (dry milling) and 18.0 wt % (toluene milling) based on the Klason lignin content of the original wood. As shown in **Table 4.1**, total monomeric DFRC products of the yield of the **Vibratory (Dry) MWL** (11.7 mol %) was lower than that of the **Wiley Wood** (13.2 mol %) and the **Rotary Glass 1 Week Wood** (13.6 mol %), but was higher than that of the **Vibratory (Dry) Wood** (9.2 mol %). In contrast, the total monomeric DFRC products of the **Vibratory MWL** (14.5 mol %) were the same. The distribution of the three monomeric products was quite different between the **Vibratory MWL** and **Vibratory (Dry) MWL** and their corresponding vibratory wood. The vibratory MWLs had higher phenolic β-O-4' (40.9 mol % and 41.3 mol %) and lower etherified β-O-4' (49.9 mol % and 51.0 mol %) structures than the vibratory wood (23.9 mol % and 26.7 mol %, and 63.6 mol % and 67.0 mol %, respectively) consistent with the recent findings of Onnerud and Gellerstedt using thioacidolysis. [188] It appears that structural changes occur during vibratory ball milling, whether under dry conditions or in the presence of toluene, resulting in depolymerization of the lignin. In addition to this is the selective extraction of specific lignin structures in the isolation of the corresponding MWL. Thus, **Vibratory MWL** and **Vibratory (Dry) MWL** may represent the lower molecularweight and less-condensed fraction and may not be representative of the total lignin, representing instead that of the secondary wall lignin as presented by Whiting and Goring[68] and Terashima et al.[189]. Furthermore, based on these results, it is clear that dry vibratory ball milling is not as good a method as vibratory ball milling in toluene.

4.3 Effect of Ball Milling on Lignin Structure

Rotary ball milling, 1 week, has minimal impact on the yield and structure of the lignin units detectable by DFRC. However, to isolate MWL in appreciable yields, more extensive milling, namely vibratory milling, is required. To minimize the effect of structural changes associated with vibratory milling, and to increase MWL yields, longer rotary ball milling stages were investigated. Milling times were increased to 4 weeks (**Rotary Glass 4 Week Wood**) and 6 weeks (**Rotary Glass 6 Week Wood**). In addition, rotary ball milling with porcelain balls and Teflon balls (which have higher densities than glass balls) were performed at 4 weeks (**Rotary Porcelain 4 Week Wood**), and 6 weeks (**Rotary Porcelain 6Week Wood** and **Teflon 6 Week Wood**). All rotary ball milling was dry milling under a nitrogen atmosphere. MWL, CEL, and REL were isolated from the various ball milled woods, and subjected to modified DFRC analysis. Included for comparison are the results obtained from the classical Bjorkman method.

The yields of MWL and CEL are given in **Table 4.2**. As expected, yields increased with increasing milling time. Ball milling with porcelain balls gave higher MWL and CEL yields than milling with glass balls. The higher density of the porcelain balls inflicts a larger mechanical impact on the wood meals, enabling more lignin to be extracted in the subsequent aqueous dioxane extraction stage. Ball milling with Teflon balls, also of higher density than glass balls, gave much lower MWL and CEL yields than milling with glass balls. In this case, the low surface energy of the Teflon balls does not enable enough friction and mechanical action to be imposed on the wood meal, limiting the effective milling. To obtain MWL and CEL yields comparable to those produced from 1 week rotary ball milling

followed by 48 hours vibratory milling (conventional Bjorkman MWL isolation), 6 weeks of ball milling with porcelain balls is required.

Modified DFRC analysis of the various milled samples is shown in **Table 4.3**. Regardless of the milling time, the monomeric product yield of each milled wood preparation was 12-15 mol %. These yields are in good agreement with that of the **Wiley Wood** (13.2 mol %, **Table 4.1**). Unit A (phenolic β-O-4') composition of all the milled wood was higher than that of the **Wiley Wood** (**Table 4.1**), whereas Unit C (etherified β-O-4') compositions were lower. This can be explained by depolymerization of the lignin macromolecule during milling, where etherified β-O-4' linkages are cleaved producing new phenolic β-O-4' lignin structures.

Table 4.2 Yields of MWL and CEL from various milling methods.

		Yield [a], %	Klason Lignin (%)
Rotary Glass 4 Week	**MWL**	3.7	87.3
	CEL	5.3	68.3
Rotary Porcelain 4 Week	**MWL**	11.1	87.1
	CEL	7.9	64.2
Rotary Glass 6 Week	**MWL**	13.1	83.2
	CEL	7.6	87.5
Rotary Porcelain 6 Week	**MWL**	18.1	87.7
	CEL	12.3	84.4
Rotary Teflon 6 Week	**MWL**	0.9	71.8
	CEL	1.0	66.5
Vibratory	**MWL**	18.0	91.1
	CEL	11.0	84.7
Vibratory (Dry)	**MWL**	22.8	87.7

[a] **Based on ash-free Klason lignin content.**

Table 4.3 Unit composition and total molar yields from the modified DFRC method for preparations of the various milling methods.

		Unit Composition[a], mol %			Total Yield[b], mol %
		Unit A	Unit B	Unit C	
Rotary Glass 4 Week	**Wood**	25.7	7.6	66.7	13.1
	MWL	38.2	3.8	58.0	14.2
	CEL	34.4	5.8	59.8	14.4
	REL	27.7	5.1	67.2	11.6
Rotary Porcelain 4 Week	**Wood**	33.6	6.7	59.7	15.8
	MWL	37.8	4.7	57.5	14.2
	CEL	32.5	6.2	61.3	14.8
	REL	27.8	4.1	68.1	9.2
Rotary Glass 6 Week	**Wood**	26.6	5.5	67.9	13.2
	MWL	46.1	4.8	49.1	16.3
	CEL	39.0	6.3	54.7	15.1
	REL	23.7	5.0	71.3	10.8
Rotary Porcelain 6 Week	**Wood**	30.5	6.8	62.7	12.5
	MWL	44.0	4.7	51.3	15.5
	CEL	42.3	5.4	52.3	14.4
	REL	24.5	5.8	69.7	12.4
Vibratory	**Wood**	26.7	7.8	65.5	14.8
	MWL	41.3	7.7	51.0	14.5
	CEL	36.6	6.5	56.9	14.5
	REL	25.2	5.3	69.5	12.9

[a] **Units A, B, and C are based upon monomeric products discussed above.**
[b] **Based upon a C_9 unit molecular weight of 182 g/mol.**

In the MWL and CEL preparations, Unit A compositions were much higher than the respective milled woods and **Wiley Wood**, whereas Unit C compositions were lower. As was observed with the MWL isolation results shown in **Table 4.1**, phenolic rich lignin structures are more easily and preferentially isolated in the extraction procedure utilized for both MWL and CEL isolation. This selective fractionation explains the much lower Unit A composition, and higher Unit C composition for the REL preparation. More significantly, the results obtained indicate that the fraction of lignin linked to carbohydrates (CEL) is structurally the same as the lignin free of carbohydrate linkages (MWL). Thus, MWL and

CEL may be combined to further increase the yields of isolated lignin. Together, the aqueous dioxane soluble fraction (CEL) and the insoluble fraction (REL) for the **Rotary Porcelain 6 Week Wood**, when added together and averaged, have Unit A, B, and C values (33.4 mol %, 5.6 mol %, and 61 mol %) very close to those obtained for the milled wood (30.5 mol %, 6.8 mol %, and 62.7 mol %). Furthermore, the total monomeric yield from DFRC analysis of MWL, CEL, and Wiley milled wood are practically identical, indicating that both MWL and CEL are representative, structurally, of the majority of lignin in wood, with the exception of higher phenolic hydroxyl content and presumably lower molecular weight. Further evidence for the similarity between MWL, CEL, and the lignin in Wiley milled wood can be seen from the nitrobenzene oxidation data, **Table 4.4**. Finally, in all cases, Unit B compositions of MWL, CEL, and REL were lower than that of the wood. Thus, cleavage of α-O-4' bonds occurs during the respective isolation procedures.

Table 4.4 Comparison of the total molar yields from the modified DFRC method and nitrobenzene oxidation.

	Modified DFRC Total Yield[a] (mol %)	Nitrobenzene Oxidation Vanillin Yield[a] (mol %)
Wiley Wood	13.2	28.7
Vibratory Wood	14.8	28.9
Vibratory MWL	14.5	31.8
Vibratory CEL	14.5	32.3
Vibratory REL	12.9	25.9

[a] **Based upon a C_9 unit molecular weight of 182 g/mol.**

Comparison of the modified DFRC results for the **Vibratory Wood** and the **Rotary Porcelain 6 Week Wood** showed only slight changes in the lignin structure versus the **Rotary Glass 1 Week Wood**. However, the porcelain marble rotary milling took 6 weeks, whereas the vibratory milling was completed in 9 days (1 week rotary ball milling and 2 days

vibratory ball milling). Therefore, the preferred milling process is 1 week rotary ball milling followed by 2 days vibratory ball milling in toluene. Nevertheless, if a vibratory ball mill is not available, satisfactory wood meal can be obtained by prolonging the ball milling time and using porcelain balls.

4.4 DFRC Analyses and the Significance of the Results Obtained

A distinct advantage of the DFRC method for lignin structure analysis is its relatively simple protocol and applicability to all types of woody tissues. [82, 83, 190] Through a simple protocol modification, outlined above, identification of the various aryl ether structures can be obtained. However, only ~14 mol % of the total lignin is analyzed by DFRC using GC. Although this number is in good agreement with values reported by Lu and Ralph, it does seem low, particularly when compared to yields reported for thioacidolysis. [184] DFRC and thioacidolysis selectively degrade β-O-4' interunit linkages, therefore these methods should yield comparable results. However, our DFRC results, as well as those in the literature, are 5-10 mol % lower than those reported from thioacidolysis. [184] Furthermore, even repeated applications of DFRC to our various lignin samples did not increase monomer yields. Therefore, further research into increasing monomer yields from DFRC, and understanding the differences between DFRC and thioacidolysis is needed, and is presently underway in our laboratory.

DFRC results using this new modified method show that MWL and CEL have a much higher phenolic unit content, ~50% more phenolic β-O-4' units and ~25% less etherified β-O-4' units, than that of the initial milled wood. It appears that phenolic-rich lignin structures are preferentially isolated in the aqueous dioxane extraction step, as DFRC

results of the vibratory milled wood are consistent with that of the original wood. MWL and CEL are structurally identical, and indicate that the portion of lignin linked to carbohydrates and that not linked to carbohydrates are structurally the same. Vibratory ball milling under nitrogen atmosphere (dry milling) appears to cause substantial changes in lignin structure. Rotary ball milling with glass balls and porcelain balls, and vibratory ball milling in toluene, caused no significant structural changes. However, extensive milling times were required for the dry ball milling (greater than 6 weeks) to obtain MWL and CEL yields comparable to rotary ball milling for 1 week followed by vibratory ball milling in toluene for 48 h (9 days total).

5. Elucidation of Lignin Structure through Degradative Methods: Comparison of Modified DFRC and Thioacidolysis.

KM Holtman; JF Kadla; H-m Chang; H Jameel. *J. Agri. Food Chem.*, 51(12), 3535-3540 (2003).

5.1 Comparison of Monomer Yields from Thioacidolysis and DFRC Treatment of Milled Wood and MWL

Recently, we demonstrated that the DFRC method could be modified to provide additional structural information through the determination of three different structural monomeric products originating in lignin. (**Section 4**) In this protocol, the free phenolic hydroxyl groups in lignin are methylated by diazomethane followed by the same acetyl bromide treatment and zinc reduction steps as in the original DFRC procedure. In the final step, propionic anhydride, instead of acetic anhydride, is used to esterify the newly generated phenolic hydroxyl groups. Thus, the modified DFRC method allows the quantitative determination of three different monomeric units in lignin; the uncondensed phenolic β–O–4' (Unit A), the uncondensed α–O–4' (Unit B) and the uncondensed etherified β–O–4' (Unit C) structures (**Figure 2.21**).

While DFRC is a flexible method due to its three distinctly separate steps, thioacidolysis does not have this utility. Thioacidolysis follows a pathway similar to kraft pulping in which the thiol group displaces the α-hydroxy or α-ether group and the β-aryl ether to form an episulfide-type intermediate (**Figure 5.1**). Because these reactions all proceed during the single thioacidolysis step, such derivatizations as in the modified DFRC method cannot be performed. Therefore, thioacidolysis can only differentiate between phenolic hydroxyl groups (Unit A) and aryl ethers, which will be referred to as Units B+C.

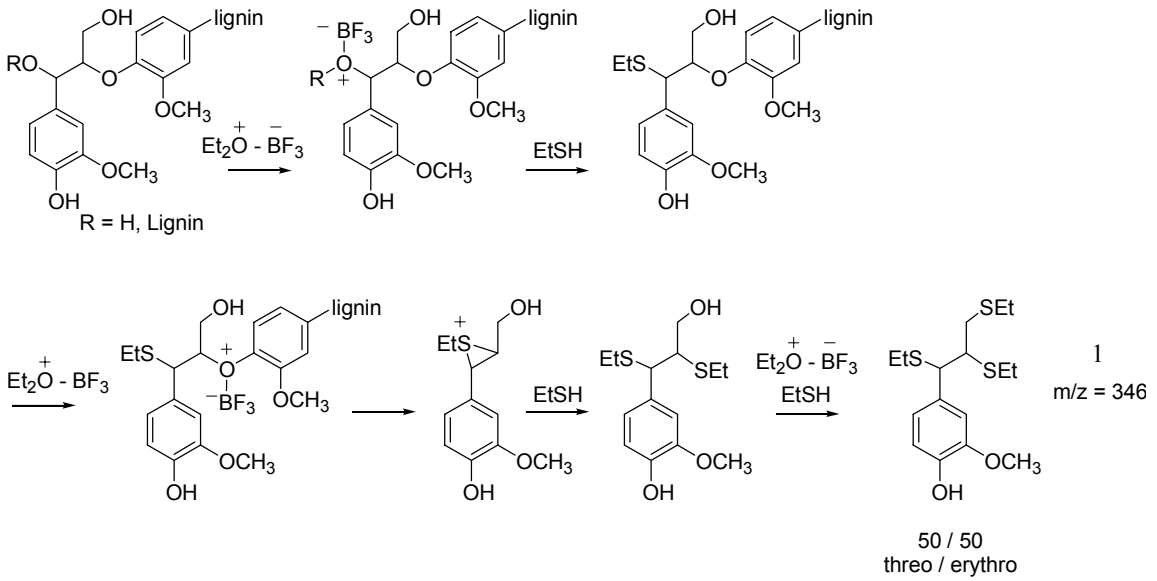

Figure 5.1 Proposed mechanism of lignin thioacidolysis. [97]

The mechanism by which thioacidolysis and DFRC degrade various lignin structures has been thoroughly investigated using specific lignin model compounds.[85, 97] In both thioacidolysis and DFRC the predominant β-aryl ether structures in lignins are selectively degraded as depicted in **Figures 5.1** and **Figure 5.2**.

Each method releases monomeric products from an uncondensed portion of the lignin (i.e., a monomer linked by a β-O-4' linkage through both the β- and the 4-positions) or a β-O-4' linked monomer end group. Therefore, it is expected that the yield of monomeric degradation products detected would be comparable. However, **Table 5.1** shows that the modified thioacidolysis gives much higher monomer yields than the modified DFRC; 21.8 mol % vs 14.8 mol %, respectively for the vibratory milled wood; and 18.1 mol % vs 14.5 mol % respectively for the MWL. These results are in good agreement with literature values and clearly indicate that the DFRC method is inefficient at cleaving β-aryl ether linkages. [82-84, 191, 192]

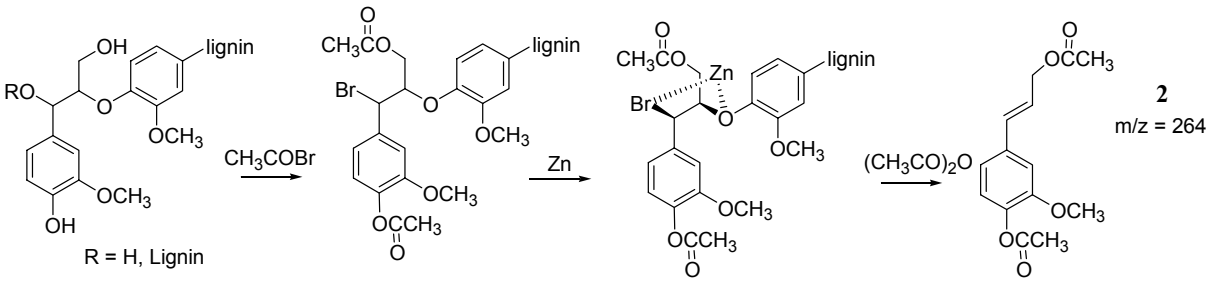

Figure 5.2 Proposed mechanism of DFRC degradation of lignin. [193]

Table 5.1 Total yields and unit composition (mol %) data for modified DFRC and thioacidolysis analysis of Vibratory Wood and MWL.

	Modified DFRC				Modified Thioacidolysis		
	Unit Composition, mol %			Total Yield (mol %)	Unit Composition, mol %		Total Yield (mol %)
	Unit A	Unit B	Unit C		Unit A	Units B+C	
Milled Wood	26.7	7.8	65.5	14.8	21.8	78.2	21.8
MWL	41.3	7.7	51.0	14.5	33.4	66.6	18.1

According to the reaction mechanism proposed for DFRC degradation of β-O-4' linkages (**Figure 5.2**), a *cis* orientation of the bromine and β-O-4' ether oxygen is required. The inability to obtain such geometry would preclude the reductive cleavage of the β-O-4' ether linkage and the α-brominated structure would persist. In fact Iiyama and Wallis [194] reported a 9 % bromine content in the acetyl bromide dissolution of wood pulp (*Pinus radiata*). Likewise, Ralph et al showed that cinnamyl model compounds on DFRC treatment gave rise to brominated arylpropanes. [195] Bromine analysis of the DFRC degraded lignin revealed a 3 mol % bromine content.

Another possible explanation for the ineffective cleavage of β-O-4' linkages by the DFRC method may be due to hydrolysis of the α-bromide on etherified phenylpropanoid

units prior to reductive cleavage. [196] Prolonged exposure of the lignin to AcBr, or the presence of water can facilitate the elimination of the α-bromo group, and the replacement with an α-OAc group.

Comparison of the yields of phenolic hydroxyl groups (Unit A) obtained from the modified DFRC and thioacidolysis reveals that the Unit A composition from the DFRC method is higher than from thioacidolysis for both the vibratory milled wood and the MWL. The percent increase for both samples is essentially the same, i.e., 18 % for the milled wood and 19 % for the MWL. This percent increase may be explained by the fact that there are β-O-4' linkages remaining in the DFRC degradation product. These linkages are likely of the etherified β-O-4' type (Unit C), rather than end groups (Unit A). Therefore, complete cleavage would result in a higher relative Unit C composition and a lower relative Unit A composition.

5.2 Effect of Thioacidolysis and DFRC on the Molecular Weight Distribution of Lignin

Figure 5.3 shows the GPC chromatograms of the MWL before and after thioacidolysis and DFRC treatment. Comparison of the chromatographs of the two treatments reveals substantial differences. Thioacidolysis has much more completely degraded the lignin than DFRC. As can be seen in **Figure 5.3**, thioacidolysis degraded the lignin polymer to a significant extent and it no longer has any resemblance to the initial MWL molecular weight profile. The GPC chromatogram shows the presence of three sharp peaks, which calibrated against polystyrene standards are below an average relative molecular mass of 700 Da. The first peak is centered near 650 Da and is probably comprised of dimeric material. The second is centered near 350 Da and probably represents **1** (*m/z*

346), the uncondensed monomer released from aryl ether cleavage. The final peak is centered near 250 Da and represents other monomeric material. This observation implies that thioacidolysis caused significant depolymerization of the lignin and that a significant number, if not all of the β-O-4' interunit linkages have been cleaved. Again, as with the DFRC protocol, incomplete cleavage could occur in lignin thioacidolysis if the method is not carefully optimized. [193]

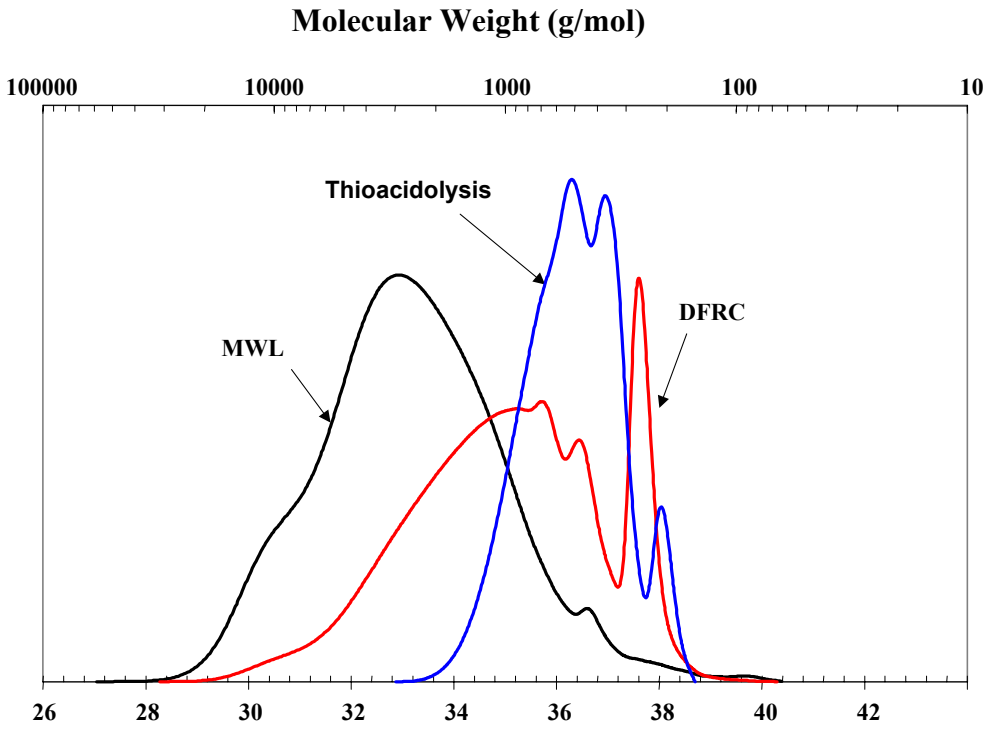

Figure 5.3 GPC chromatographs of MWL before and after thioacidolysis and DFRC treatment.

By comparison, the DFRC treated MWL exhibits a GPC trace that maintains much of the characteristics of the original MWL curve (**Figure 5.3**). Like the thioacidolysis treated MWL, the DFRC treated MWL has two peaks that are representative of low relative molecular weight moieties, monomers and dimers. However, a large amount of high relative

molecular weight highly polydispersed material similar to the initial MWL is still present. Probably due to incomplete β-aryl ether cleavage, these findings are consistent with and support the lower monomer yields detected by GC analyses from DFRC degradation relative to thioacidolysis. In addition, the lower relative incidence of monomers from etherified β-O-4' linkages (Unit C) verify that the decrease in yield is attributable to internally located moieties that remain uncleaved, and result in the observed higher degree of polymerization. It should be noted that the relative intensities of the monomeric peaks by no means imply concentration. The UV absorbance will be dependent on the compound structure, with compounds having double bonds (**2**) having stronger absorbance than those without (**1**) or the higher relative molecular weight fractions.

5.3 ^{1}H-^{13}C HMQC NMR Analysis of Thioacidolysis and DFRC Degraded Lignins

To minimize the number of structural differences in the analyzed lignins and ease the interpretation of the NMR spectroscopic data, the standard DFRC protocol was used. **Figure 5.4** shows the HMQC spectra for the MWL, DFRC and thioacidolysis degraded lignins.

The aliphatic oxygenated region of the HMQC spectra of the DFRC treated MWL (**Figure 5.4B**) exhibits cross signals of δ_C/δ_H 80.0/4.63 ppm and δ_C/δ_H 73.9/6.0 ppm corresponding to C_β/H_β and C_α/H_α respectively for β-O-4, **3**, structures. The intensity is

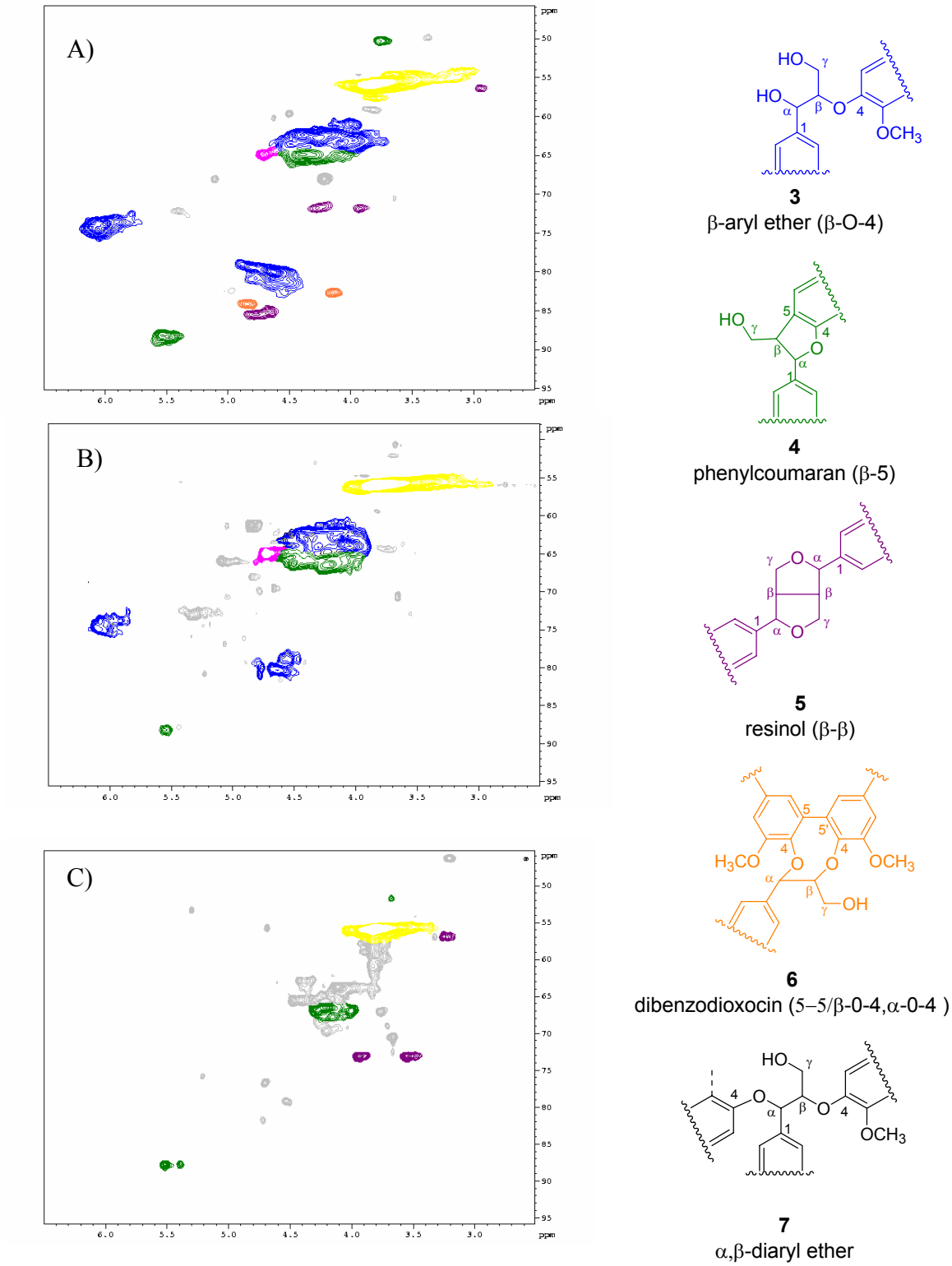

Figure 5.4 Expansion of the oxygenated aliphatic region of the ^{1}H-^{13}C HMQC Spectrum of the A) original MWL, B) acetylated DFRC degraded MWL, and C) acetylated thioacidolysis degraded MWL.

substantially lower than the corresponding signal in the spectrum of the original MWL (**Figure 5.4A**). By comparison, these signals are not observed in the HMQC spectra of the thioacidolysis lignin (**Figure 5.4B**). This is consistent with the results obtained from GC and GPC analyses, and confirms that complete β-aryl ether cleavage occurs as a result of thioacidolysis, but is incomplete in the DFRC procedure. In thioacidolysis the lignin macromolecule undergoes a series of thiethylation reactions (**Figure 5.1**). Under the acidic reaction conditions used the lignin becomes completely solublized. This facilitates better accessibility of the reagents to the lignin and as a result more complete lignin degradation. Since DFRC fully solubilizes the lignin, it is not clear however, as to why the DFRC method does not completely cleave all the β-*O*-4 linkages. This may be due to accessibility issues, inefficiency in the chemistry of the method, or the existence of lignin units that are less susceptible to cleavage by DFRC.

One possibility for the observed difference is that dibenzodioxocin structures, **6**, which contain both α-aryl and β-aryl ether linkages through the phenolic groups of a biphenyl (5-5′) condensed lignin structure are some how stable to DFRC. [89] The DFRC mechanism (**Figure 5.2**) proceeds through a 5-membered Zn-coordination step, depending on the stereochemistry, erythro versus threo, the lignin macromolecular structure about this region may be too rigid to allow this coordination. Thus, the bromination and resulting α-aryl ether cleavage step may occur, but the β-aryl ether reductive cleavage will be prevented, leaving the unreacted β-O-4' linkage intact. **Figure 5.4A** clearly shows the existence of **6** in the original MWL, however the cross signals δ_C/δ_H 84.5/4.84 ppm and δ_C/δ_H 82.6/4.13 ppm corresponding to C_α/H_α and C_β/H_β respectively are absent in the DFRC degraded material (**Figure 5.4B**). Although during DFRC degradation, α-bromination will result in ring-

opening (cleavage of the α-O-4' linkage), the typical β-O-4' linked structure (δ_C/δ_H 80.0/4.63 ppm and δ_C/δ_H 73.9/6.0 ppm corresponding to C_β/H_β and C_α/H_α respectively) and the ability to differentiate the dibenzodioxocin structure will be lost. In fact, it has been shown that rearrangement reactions seen in model compound studies under DFRC conditions, do not occur in MWL as a result of steric factors which imposed rotational restrictions within the lignin macromolecule. [90]

In addition to 5-5' linkages, lignins contain other inter-unit carbon-carbon bonds: β-5', β-β', β-1', etc. Of these subunits, the β-5' (**4**) and β-β' (**5**) structures contain α-aryl ether linkages that one would expect to be cleaved during DFRC (**Figure 5.2**). The cleavage of these bonds would not release a monomeric unit detectable by GC, but incomplete cleavage would be detectable using the HMQC correlation signals. Lignin moieties such as **5** show cross signals δ_C/δ_H 85.4/4.78 ppm / δ_C/δ_H 85.1/4.67 ppm for the respective C_α/H_α and δ_C/δ_H 71.8/4.27 ppm / δ_C/δ_H 71.9/3.93 ppm for the respective C_γ/H_γ correlations. The HMQC spectrum of the DFRC degradation products clearly indicates that these ether linkages have been cleaved.

The HMQC spectra for **4** has cross signals δ_C/δ_H 88.2/5.50 ppm and δ_C/δ_H 50.4/3.77 ppm for the C_α/H_α and C_β/H_β correlations, respectively. [141] While the intensity of these correlations are clearly reduced in the DFRC reacted MWL (**Figure 5.4B**) relative to the original MWL (**Figure 5.4A**), it is apparent that β-5' structures still remain in the DFRC degradation products. However, it is unclear as to whether this is the result of incomplete bromination or displacement of the bromide ion via an intramolecular etherification reaction.

Thioacidolysis of milled wood and MWL produced 7 mol % and 3.5mol %, respectively, higher monomer yields than DFRC. GPC analysis revealed the thioacidolysis

treated lignins were degraded to a lower average molecular weight than by DFRC. In fact, the DFRC treated MWL retained much of the characteristics of the original lignin. Two-dimensional ^{1}H-^{13}C HMQC NMR spectroscopy showed the presence of β-O-4' linkages in the DFRC treated lignin. No β-O-4' interunit linkages were detected in the thioacidolysis treated lignin (**Figure 5.4C**). In addition, the DFRC treated MWL had a ~3 mol % bromine content. Contrary to results reported for lignin model compounds, these findings indicate that the DFRC method does not completely or efficiently degrade the lignin polymer. The presence of elemental bromine within the lignin, combined with the existence of β-O-4' interunit linkages and the high average relative molecular weight, suggests the DFRC treatment of the lignin may be affected by the rigid 3-dimensional structure of the lignin macromolecule. Restricted rotational mobility of certain C_9 units precludes the formation of the necessary geometry to enable reductive cleavage of all of the β-O-4' interunit linkages.

6. A solution-state NMR study of the similarities between MWL and CEL

KM Holtman and JF Kadla. Submitted for peer review to the *J. Agri. Food Chem.*, Sept. 23, 2003.

6.1 Elemental Composition

Table 6.1 contains information regarding the elemental and chemical compositions of the MWL and CEL. As can be seen the Klason lignin content is much lower for the CEL as compared to the MWL (85 % vs. 91 %). The elemental analyses are corrected to represent only the contributions from lignin and result in chemical compositions of $C_9H_{9.23}O_{3.33}$ for MWL and $C_9H_{9.97}O_{3.34}$ for CEL. With the oxygen contents being equivalent, an increased hydrogen content for CEL may be indicative of a lower degree of condensation or a lower carbonyl content. It is noteworthy that the nitrogen content of the CEL is similar to that of MWL (below detection limit) showing that contamination by enzyme should not be a problem in this analysis.

Table 6.1 Elemental and functional group analysis of MWL and CEL.

	Elemental Composition (%)*				Functional Group / C_6			
	C	**H**	**O**	**N**	**OCH_3**	**Phenolic OH**	**Aliphatic OH**	**C=O**
MWL	63.2	5.4	31.2	< 0.2	0.96	0.17	0.98	0.12
CEL	62.8	5.8	31.1	< 0.2	0.94	0.19	1.02	0.08

*** Elemental analysis based on Klason lignin content.**

Laboratory data indicates that CEL and MWL have similar methoxyl contents, 0.94 and 0.96 per aromatic ring, respectively. (**Table 6.1**) This is expected as both MWL and

CEL are derived primarily from the secondary wall, and in softwood the primary precursor is guaiacyl-based. As a result the expected methoxyl content would be close to one, in agreement with reported literature values. [109]

The phenolic and aliphatic hydroxyl and carbonyl contents were estimated using quantitative ^{13}C NMR. The hydroxyl contents were similar with those for CEL being slightly higher for both phenolic, 0.19 versus 0.17, and for aliphatic, 1.02 versus 0.98, per aromatic ring. The carbonyl content is slightly higher in the MWL than CEL, 0.12 for the MWL and 0.08 for the CEL (**Table 6.1**). The presence of a larger amount of oxidized moieties in the MWL somewhat explains the higher hydrogen content in the CEL. This suggests that either the milling leads to more side chain oxidation in the MWL or that more end group material is isolated in the MWL portion.

6.2 Chemical Degradation Analysis of Lignins

As reported previously, similar total yields in DFRC degradation products and vanillin from nitrobenzene oxidation were obtained for both MWL and CEL, leading to the conclusion that they may be similar in structure. (**Section 4**) Thioacidolysis has been shown to completely cleave β-O-4' bonds and result in consistently higher total molar yields than DFRC even though both methods cleave aryl ether bonds. (Section 5) While DFRC does not reveal a difference between the two lignins, total molar yields for thioacidolysis are 2.2 % higher for CEL than MWL, 20.3 % versus 18.1%, respectively (**Table 6.2**). The higher monomeric yield from thioacidolysis may indicate that the CEL has a larger amount of β-O-4' substructures than MWL, and may have a lower degree of condensation.

Similar results were obtained from nitrobenzene analysis of the two lignin

preparations. **Table 6.2** shows that the vanillin yields were slightly higher for CEL than MWL, 32.3 % versus 31.8 %. Although these values are quite a bit higher than those obtained from thioacidolysis, this is expected based on the fact that nitrobenzene oxidation cleaves sidechain linkages other than β-O-4', e.g., pinoresinol (β-β') is also degraded to yield vanillin. Nitrobenzene oxidation however is not quantitative.

Table 6.2 Monomer yields from chemical degradation methods.

	DFRC (mol %)	Thioacidolysis (mol %)	Nitrobenzene Oxidation (mol %)
MWL	14.5	18.1	31.8
CEL	14.5	20.3	32.3

6.3 Structural Analysis of Lignins via NMR Techniques

^{13}C NMR spectroscopy is a reliable method to investigate the structure of the carbon skeleton in lignin. Unlike chemical methods NMR provides a more comprehensive view of the entire lignin macromolecule. ^{13}C NMR can be used to estimate the abundance of each interunit linkage and can be considered to be quantitative provided adequate experimental conditions are utilized. Specifically, the pulse delay between acquisitions must be sufficiently long to ensure that all carbons have returned to their initial Boltzmann distributions. The pulse delay required to achieve these conditions is generally considered to be 5 times the longest rate of relaxation. [143] Despite this, ^{13}C NMR suffers the drawback that signals are often overlapped, making the estimation of linkages difficult. As a result, a two-dimensional NMR technique such as HMQC can be considered useful for elucidation of overlapping signals. While HMQC is almost entirely qualitative, its advantage involves a

^{1}H-^{13}C correlation that stretches the signals onto an *x*-*y* axis. Detailed assessment of the HMQC spectrum reveals which signals overlap at what point in the carbon spectrum enabling more accurate quantification using ^{13}C NMR.

The quantitative ^{13}C NMR spectra for MWL and the oxygenated aliphatic region for the acetylated MWL are shown in **Figure 6.1**. **Table 6.3** lists the corresponding peak assignments identified for the lignin preparations. [138, 143] The ^{13}C NMR spectra can be broken into structural unit regions and integrated to obtain structural information. **Table 6.4** lists the various spectral regions identified in the quantitative ^{13}C spectra with results reported as the number of moieties per aromatic ring. Integration was performed by setting a value of 6.12 for the aromatic region (160-100 ppm) representing all aromatic carbons plus a contribution of 0.12 per 100 aromatic units from the sidechain carbons of coniferyl alcohol and coniferyl aldehyde. [143]

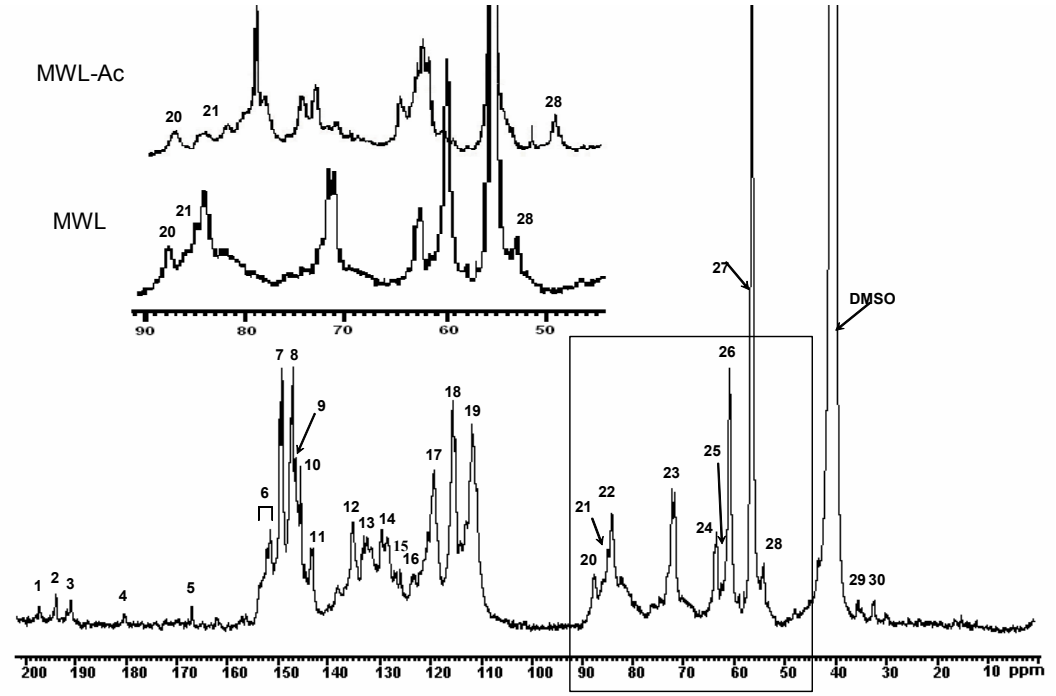

Figure 6.1 Quantitative ^{13}C NMR spectra of MWL. Included is an expansion of the oxygenated aliphatic region of the MWL and acetylated MWL (MWL-Ac).

Table 6.3 Assignment of the quantitative ^{13}C NMR spectra.

Peak Number	δ (ppm)	Assignment	Peak Number	δ (ppm)	Assignment
1	198	C=O in (**IV**)	**16**	124.5-122	C_1 and C_6 in α-C=O units
2	194	C=O in (**III**)	**17**	122-117	C_6 in G units
3	191	C=O in (**I**)	**18**	117-113	C_5 in G units
4	181	C=O in (**XIV**)	**19**	113-108	C_2 in G units
5	168	C=O in **–OAc**	**20**	87	C_α in (**V**)
6	155-151	$C_3/C_{3'}$ in etherified (**V**) C_α in (**III**) C_5 in ring B of (**XI**)	**21**	86.5-85	C_α in (**VIII**) C_α and C_β in (**IX**)
7	151-148.5	C_3 in etherified G units	**22**	85-82	C_β (*e*,*t*) in (**X**)
8	148.5-146.8	C_4 in etherified G units C_3 in nonetherified (**X**)	**23**	74-71	C_α (*e*,*t*) in (**X**) C_γ in (**VIII**)
9	146.2	C_4 in nonetherified G units C_4 in ring B of (**V**)	**24**	64-62	C_γ in (**III**), (**V**), and (**XII**)
10	145.2	$C_4/C_{4'}$ in etherified (**VI**)	**25**	61.5	C_γ in (**VII**)
11	143.5	C_3 in ring B of (**V**) $C_4/C_{4'}$ in nonetherified (**VI**)	**26**	61-59	C_γ in (**IX**) and (**X**)
12	137-134	C_1 in etherified G units	**27**	56	**-OCH_3**
13	134-130	C_1 in nonetherified G units $C_5/C_{5'}$ in etherified (**VI**)	**28**	54-52	C_β in (**V**), (**VIII**), and (**XII**)
14	130-127	C_β in (**II**) C_α and C_β in (**VII**)	**29**	34.5	C_α in (**XIII**)
15	127-124.5	$C_5/C_{5'}$ in nonetherified (**VI**)	**30**	31.5	C_β in (**XIII**)

Table 6.4 Quantification of the spectral regions of the ^{13}C NMR spectra.

Spectral Region	Chemical Shift Range (ppm)	Number of Moieties per Aromatic Ring	
		MWL	CEL
Methoxyl Content	57-54	0.96	1.17*
Aromatic Methine Carbons	125-103	2.57	2.64
Aromatic Carbon-Carbon Structures	141-125	1.53	1.42
Oxygenated Aromatic Carbons	160-141	2.02	2.06
Carbon from Carbonyl Type Structures	195-190	0.12	0.08
Degree of Condensation	125-103	0.43	0.36

*** Overestimated due to overlap with unknown contaminant.**

Integration of the MWL methoxyl peak at 57-54 ppm yields a methoxyl group content of 0.96 methoxyl groups per aromatic ring (**Table 6.4**), identical to the result obtained via chemical analysis (**Table 6.1**). Surprisingly, NMR analysis of the CEL spectra determined the methoxyl content to be 1.17 methoxyl groups per aromatic ring. This is clearly higher than the 0.94 obtained via chemical analysis (**Table 6.1**). However, the HMQC spectrum reveals the presence of an overlapping impurity revealed by a correlation at δ_C/δ_H 55.0/5.8 in the CEL spectrum. (**Figure 6.2B**)

Analysis of the carbonyl region (200-190 ppm) of the ^{13}C NMR spectra reveals differences between the two lignin preparations. Integration indicates a total of 0.12 and 0.08 carbonyl (-C=O) groups per aromatic ring for MWL and CEL, respectively (**Table 6.4**). The peak at 191 ppm, representing vanillin (**I**) is higher in the MWL (0.04 per aromatic ring) than the CEL (0.02 per aromatic ring), whereas the integration of the peak at 194

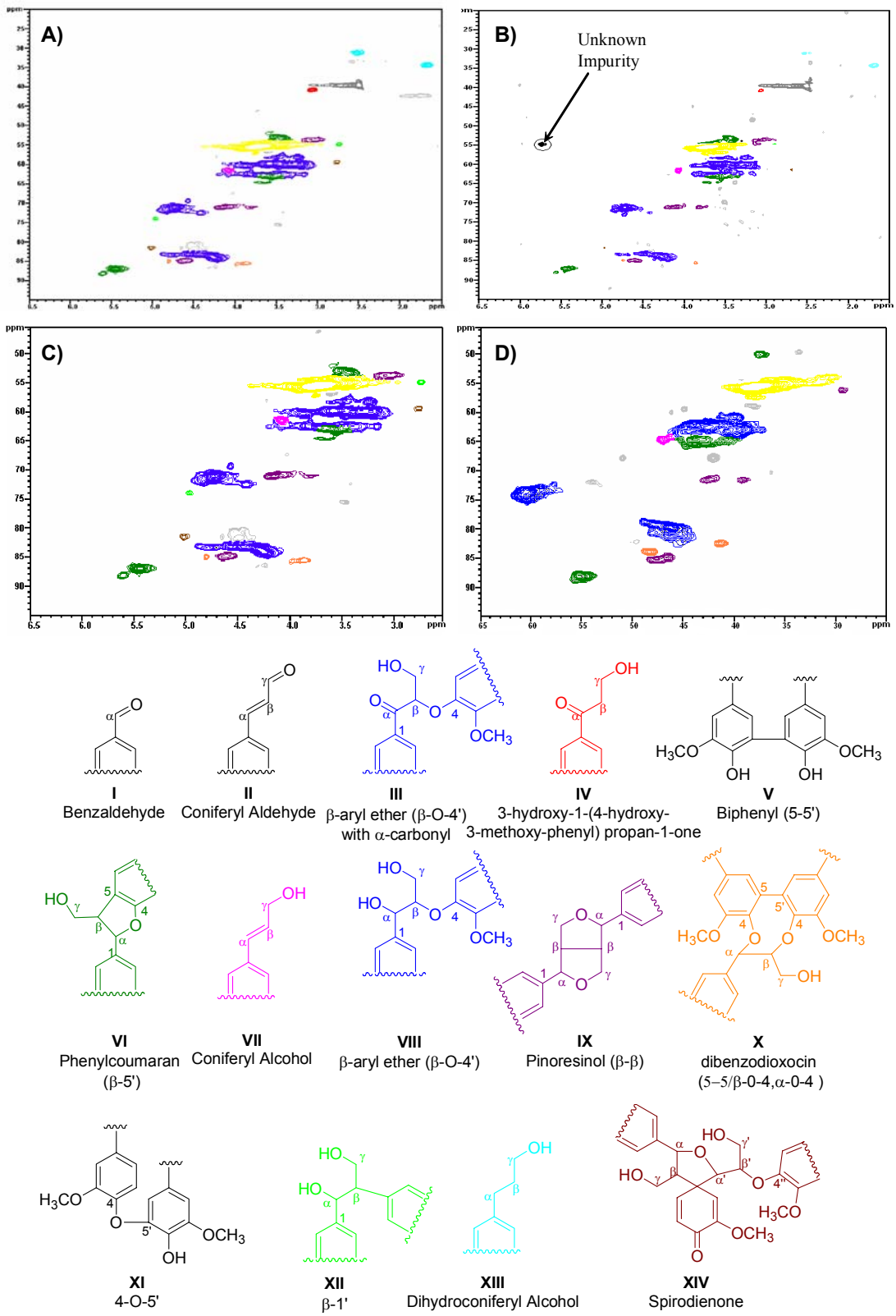

Figure 6.2 **^{1}H-^{13}C HMQC spectra of the oxygenated aliphatic region of A) MWL; and B)CEL; included are the magnified regions of C) MWL and D) acetylated MWL.**

ppm representing coniferyl aldehyde (**II**) and α-carbonyl type β-O-4' substructures (**III**) are identical in value (0.04 per aromatic ring). Additionally, the peak at 198 ppm, reported to be an Ar-CO-CH_2-CH_2OH (**IV**) group [79] contributes 0.03 units per aromatic ring in the MWL and 0.01 units in CEL.

The presence of α-carbonyl type structures indicates oxidation probably occurs during the milling process. The presence of benzaldehyde structures such as vanillin further suggests that the milling process leads to not only sidechain oxidation, but also degradation. [59] While the content of these moieties in the lignin is relatively low, there does appear to be some structural modification occurring. There is a slightly higher degree of oxidation in the MWL as compared to the CEL. This is likely due to the accumulation of these groups in low molecular weight lignin isolated as MWL.

Analysis of the aromatic region of the ^{13}C NMR spectra also reveals differences between the MWL and CEL. The aromatic region can be divided into oxygenated aromatic carbons (160-141 ppm), condensed aromatic carbons (141-125 ppm), and protonated aromatic carbons (125-103 ppm). The latter two regions can provide an estimation of the degree of condensation, e.g. C-C linkages in the lignin macromolecule. The condensed aromatic region (141-125 ppm) contains the C_1 sidechain position and the C_5 position from condensed aromatic ring linkages such as phenylcoumaran (β-5'), **V**, or biphenyl (5-5'), **VI**, substructures. However, calculation of the degree of condensation by integration of this region results in some ambiguity as this region is overlapped by the vinylic carbons in coniferyl alcohol (**VII**) and the β-carbon in coniferaldehyde (**I**). Therefore, it may be more precise to use the protonated aromatic region (125-103 ppm) to determine the degree of condensation.

The protonated aromatic region (125-103 ppm) consists of the methine carbons: C_2, C_6, and any protonated C_5 carbons and is not expected to contain any overlapping signals. Softwood lignin consists of guaiacyl-based phenylpropanoid units that contain amethoxyl group and a phenolic hydroxyl at C_3 and C_4, respectively. Therefore, a completely uncondensed softwood lignin will contain three protonated aromatic carbons per aromatic ring. Three minus the integration of this region (125-103 ppm) yields the degree of condensation. Integration values obtained for the MWL and CEL indicate a degree of condensation of 0.43 and 0.36, respectively, per aromatic ring. (**Table 6.4**)

The oxygenated aliphatic region can also provide more detailed structural information about the quantities of interunit linkages in the lignin preparations. The HMQC NMR spectrum is used to determine the unobstructed chemical shifts for important interunit linkages in lignin, e.g. β-O-4', β–β', β-5'. **Figure 6.2** shows the oxygenated aliphatic region (δ_C/δ_H 95-45/6.5-2.5) for MWL and CEL in the two-dimensional HMQC spectra. Qualitatively, the apparent intensity for each signal representing a lignin structural feature in this region appears to be lower in the CEL spectrum than in the MWL, consistent with the 6 % higher carbohydrate content in the CEL than MWL.

The α-carbon of the β-5' substructure exhibits a correlation at δ_C/δ_H 88.1/5.5 in the HMQC spectrum of acetylated MWL. (**Figure 6.2C**) The signal in the two-dimensional spectrum is unobstructed in the carbon spectrum allowing for integration to determine the quantity of these moieties. [197] As a result, quantitation of the β-5' substructures leads to the estimations of other substructures, as seen below. The ^{13}C spectra yield values for β-5'of 0.09 per aromatic ring for MWL and 0.07 for CEL (**Table 6.5**). These values are in agreement with literature values previously reported for MWL. [198]

Table 6.5 Estimation of interunit linkages in MWL and CEL via quantitative ^{13}C NMR.

Spectral Region	Chemical Shift Range (ppm)	Number of Moieties per Aromatic Ring	
		MWL	CEL
Ar-CHO (I)	191	0.04	0.02
Ar-CH=CH-CHO (II) + α-C=O in β-O-4 (III)	194	0.04	0.04
Ar-CO-CH_2-CH_2OH (IV)	198	0.03	0.01
β-5' (V)	Ac(90-86)[a]	0.09	0.07
5-5' (VI)	145-141[b]	0.16	0.12
Ar-CH=CH-CH_2OH (VII)	62	0.04	0.05
β-O-4' (VIII)	61.5-57.5[c]	0.41	0.47
β-β' (IX)	54.3-52.0[d]	0.02	0.04
Dibenzodioxocin (X)	Ac(86-83)[e]	0.08	0.07
β-1' (XII)	Ac(51-48)[f]	<0.01	0.01
Ar-CH_2-CH_2-CH_2OH (XIII)	31	0.03	0.02
Spirodienone (XIV)	181	0.01	0.01

[a] **β-5' (V) was directly integrated from 90-86 ppm in the acetylated ^{13}C spectrum. (inset Figure 6.1)**
[b] **5-5' was determined by integration of 145-141 ppm of the nonacetylated spectrum minus the value of (V).**
[c] **β-O-4' (VIII) calculated from region of 61.5-57.5 in the nonacetylated spectrum minus the values for (III), (IV), (X), (XII), and (XIII).**
[d] **β-β' (IX) calculated from integration of the region 54.3-52 in the nonacetylated spectrum minus the value of (V).**
[e] **Dibenzodioxocin was calculated by integration of 86-83 ppm in the acetylated ^{13}C spectrum minus the value of (IX).**
[f] **β-1' (XII) was calculated by integration of 51-48 ppm of the acetylated ^{13}C spectrum minus the value of (V).**

In the nonacetylated ^{13}C spectra, the β-carbons of the β-5' and the β-β' (**VIII**) substructures overlap at 54-52 ppm and the amount of β-β' substructures per aromatic ring is

0.02 for MWL and 0.04 for CEL. (**Table 6.5**) The value for MWL is in agreement with literature data, but the value is somewhat high for CEL. [198, 199]

From the acetylated HMQC spectra, the signal for the α-carbon of dibenzodioxocin (**IX**) at δ_C/δ_H 84.5/4.84 is overlapped by only the α-carbon in the β-β' substructure in the acetylated ^{13}C spectra. [14] Therefore, integration of the region from 86-83 ppm yields values of 0.08 dibenzodioxocin substructures per aromatic ring in MWL but only 0.07 in CEL. [197] The values for dibenzodioxocin are slightly higher than those previously reported in the literature. [200] (**Table 6.5**)

From the HMQC spectra, the γ-carbon for the β-O-4' (**X**) side chain is centered at δ_C/δ_H 59.8/3.0-3.85, is relatively unobstructed and can be integrated from ~61.5-57.5 in the ^{13}C spectra. This region is overlapped by the γ-carbon from the dibenzodioxocin substructure, which contains a β-O-4' linkage, as well as the γ-carbons from substructures **III**, **IV**, **XII**, and **XIII**. Therefore the amount of β-O-4' linkages is 0.41 for MWL and 0.47 CEL, both within agreement of literature values. [51, 52, 198] The difference in β-O-4' content between the two lignin preparations is consistent with previously reported data on the amount of free phenolic content versus etherified β-O-4' content as obtained by the modified DFRC method. (**Section 4**) It can be surmised that CEL is released by degradation of the associated carbohydrate material rather than the degradation of ether bonds within the lignin structure.

The spectral region of 145.5-141 ppm represents etherified and nonetherified C_4 carbons of biphenyl (5-5') groups and C_3 carbons of phenylcoumaran (β-5') substructures. Integration of this region results in values of 0.40 and 0.30 for MWL and CEL. The degree of condensation as determined by integration of the aromatic methine region (125-103 ppm)

was previously determined to be 0.43 and 0.36 for MWL and CEL, respectively. (**Table 6.4**) Based upon these values, either the total amount of 5-5' and β-5' subunits are either slightly underestimated or other structural moieties such as 4-O-5' (**XI**) are contributing to condensation in the lignin polymer. Based upon the above integrations, MWL and CEL contain 0.16 and 0.12 5-5' substructures per aromatic ring, respectively. These values agree with those reported in the literature. [199, 201, 202]

The apparent increase in condensed linkages in the MWL versus CEL can be either attributed to condensation reactions occurring during milling or morphological origin. Widespread condensation probably does not occur due to the rigidity of the solid lignin matrix, however, condensation may still occur in structures of close proximity. It is likely that at least some of the difference in condensed lignin content between the MWL and CEL results from morphological origin. It has been reported that the initial release of lignin during milling occurs primarily from regions of high lignin content, presumably the cell corners and middle lamella. [13] These regions are known to contain a higher degree of condensation than the lignin contained in the secondary wall. Since CEL is produced by degradation of carbohydrates, it should be derived primarily from the secondary wall.

Correlations for other minor structural units identified by HMQC include coniferyl alcohol, β-1 (**XII**), dihydroconiferyl alcohol (**XIII**), and spirodienone (**XIV**). As discussed earlier, the γ-carbon of coniferyl alcohol exhibits a crosspeak at δ_C/δ_H 62.0/4.1 and integration of the peak in the ^{13}C spectra reveals that a maximum of 0.04 and 0.05 units of coniferyl alcohol per aromatic ring. This value may be inflated however, due to overlap with the peak for the γ-carbon of the β-O-4' substructure.

The correlation for the β-carbon on the sidechain of the β-1' substructure exhibits a

crosspeak at δ_C/δ_H 49.9/3.4 in the acetylated HMQC spectra. In the ^{13}C spectra, the peak at 50 ppm is overlapped by that of the β-carbon in the phenylcoumaran (β-5') substructure. Integration of this region and subsequent subtraction of the contribution from the β-5' carbon yields values of <0.01 β-1 moiety per aromatic ring in MWL and as much as 0.02 in CEL.

The α- and β-carbons of dihydroconiferyl alcohol have chemical shifts of 35 and 31 ppm. While there is a slight overlap of the α-carbon, the β-carbon can be integrated to yield a value indicating that MWL contains a maximum of 0.03 dihydroconiferyl alcohol moieties per aromatic ring, while CEL contains a maximum of 0.02.

Spirodienone is a newly discovered structural unit in lignin and has a characteristic chemical shift of 181 ppm in the ^{13}C spectrum representing the β-carbon. [16] Integration indicates that these structures are present at values of 0.01 and <0.01 in MWL and CEL, respectively.

6.4 Molecular Weight Distributions

The gel permeation chromatograms of the acetylated MWL and CEL preparations are shown in **Figure 6.3**. Comparison of the two lignin preparations reveals similar molecular weight distributions, with CEL having a slightly higher M_w. This is expected based upon β-O-4' content, however similar molecular weight ranges are expected because the isolation of these portions is more dependent upon the solvent system than the material being extracted.

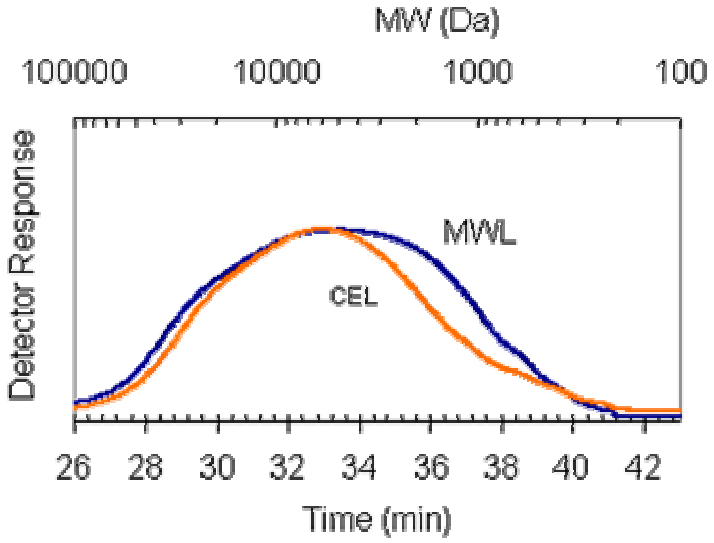

Figure 6.3 GPC chromatographs of MWL and CEL.

6.5 Carbohydrate Analysis

The monosaccharide compositions of MWL and CEL are listed in **Table 6.6**. The MWL and CEL have similar amounts of D-xylose, D-glucose and L-arabinose, but differ in the amounts of D-galactose and D-mannose. The MWL has a substantially higher amount of D-galactose than CEL, while the CEL is richer in D-mannose. Interestingly, it has been reported that polysaccharides rich in L-arabinose and D-galactose are deposited in the middle lamella during the early stages of biosynthesis. [18] Although the majority of the lignin in CEL and MWL originates from the secondary wall, this may indicate that there is more lignin derived from the middle lamella in MWL than in CEL. Finally, the abundance of glucose, ~42% of the monosaccharides determined, indicates that some cellulose remains in both preparations.

Table 6.6 Monosaccharide composition of MWL and CEL.

	Carbohydrate Composition (% Monosaccharide Composition)				
	Xylose	**Arabinose**	**Glucose**	**Mannose**	**Galactose**
MWL	18.8	7.2	41.5	18.8	13.1
CEL	18.5	6.5	42.5	22.6	6.5

7. An NMR comparison of the whole lignin from milled wood, MWL, and REL dissolved by the DMSO/NMI procedure

KM Holtman, JL White, H-m Chang, and JF Kadla, under preparation for submission to *Biomacromolecules*.

7.1 Comparison of lignin preparations by degradative techniques

It was previously shown by DFRC that the different MWL preparations consistently had a higher total molar yield than the **Wiley Wood** from which they were isolated. (**Section 4**) Additionally, it was shown that the CEL isolated after removal of carbohydrates was structurally similar to the MWL, supporting the data presented in the modified DFRC study. (**Section 6**) It was suggested based upon the DFRC data, however, that the insoluble REL must have a more condensed structure because less DFRC monomers were released. This conclusion was based upon the assumption that the DFRC reaction procedure was efficient. However the DFRC method does not completely degrade β-aryl ethers in MWL, resulting in a lower than expected yield of DFRC monomers. (**Section 5**)

Thioacidolysis on the other hand completely degrades all β-aryl ethers in MWL and contrary to the DFRC data, the modified thioacidolysis actually showed a higher yield of monomers from the **Rotary Porcelain 6 Week REL** (25.5 mol %) than the **Rotary Porcelain 6 Week MWL** (18.1 mol %). (**Table 7.1**) The **Wiley Wood** and **Rotary Porcelain 6 Week Wood** were 23.6 and 21.8 mol %, respectively. Yields and the Unit A content indicative of etherified end groups based on the thioacidolysis results for the **Rotary Porcelain 6 Week REL** were similar to those of the **Wiley Wood**. This suggests that the **Rotary Porcelain 6 Week REL** is actually more similar to the native lignin than is the **Rotary Porcelain 6 Week MWL**. It could also suggest that both the **Wiley Wood** and **Rotary Porcelain 6 Week REL** are largely comprised of secondary wall material while a

significant portion of the **Rotary Porcelain 6 Week MWL** is from the middle lamella lignin. These results suggest that it is necessary to consider the REL portion when attempting to determine the structure of native lignin or more importantly to study the whole lignin.

Table 7.1 Comparison of the unit composition and total molar yields of lignin preparations analyzed by the modified DFRC and thioacidolysis methods.

	Modified DFRC				Modified Thioacidolysis		
	Unit Composition (mol %)			Total Yield (mol%)	Unit Composition (mol %)		Total Yield (mol%)
	Unit A	Unit B	Unit C		Unit A	Units B+C	
Wiley Wood	21.6	6.8	71.6	13.2	25.1	74.9	23.6
Rotary Porcelain 6 Week Wood	26.7	7.8	65.5	14.8	21.8	78.2	21.8
Rotary Porcelain 6 Week MWL	41.3	7.7	51.0	14.5	33.4	66.6	18.1
Rotary Porcelain 6 Week REL	25.2	5.3	69.5	12.9	23.3	76.7	25.5

The REL portion has been largely ignored because of its relative insolubility in typical solvents. The development of the DMSO/NMI solvent system by Lu and Ralph, however, has afforded the opportunity to study the lignin in the REL and also in the finely milled wood by solution-state NMR.

7.2 Comments on Milling

It is well known that the yield of MWL increases with milling time [13] with concomitant structural changes in the isolated lignin. [68, 71, 73, 116] As a result, it is advisable to minimize the extent of milling when preparing MWL in order to obtain a lignin structure more similar to that of native lignin.

As a result, our laboratory typically limits milling so that we obtain a MWL yield of ~20 % after purification by the Bjorkman procedure. [61] We showed previously that rotary milling for 6 weeks with porcelain balls would provide a MWL of similar yield and likely

similar chemical content to that of the Bjorkman isolation procedure. (**Section 4**) In addition, the rotary-milled wood has the advantage that the milled wood does not contain paramagnetic contamination resulting from the vibratory-milling with steel balls.

7.3 Dissolution of lignin

The **Rotary Porcelain 6 Week Wood** and **Rotary Porcelain 6 Week REL** were treated five times with an industrial cellulase (Dyadic SuperAce, Dyadic International Inc., Jupiter, FL) to remove carbohydrates, then each sample was dissolved using the DMSO/NMI procedure described by Lu and Ralph. [21, 22] The **Rotary Porcelain 6 Week Wood** and **Rotary Porcelain 6 Week REL** did not dissolve within the prescribed time, therefore as a precaution several hours of mixing and acetylation overnight were performed in order to obtain dissolution. Only the MWL was completely soluble in the DMSO/NMI solution prior to acetylation. In the case of our lignins, the **Rotary Porcelain 6 Week Wood** and **REL** were difficult to dissolve at significant concentration in NMR solvents even after the extensive dissolution and acetylation procedures.

7.4 ^{1}H-^{13}C Two-Dimensional HMQC NMR

Lu and Ralph recently reported a two-dimensional NMR spectrum of whole acetylated cell wall dissolved using DMSO/NMI. [21] They did not remove the carbohydrates prior to NMR analysis and as a result the lignin exhibits a very low intensity compared to the carbohydrate signals. We removed the bulk of the carbohydrates in our samples and as a result our spectra show a higher intensity for the structural moieties in the lignin. **Figure 7.1** shows the expanded oxygenated aliphatic region for **Rotary Porcelain 6**

Week Wood, **MWL**, and **REL**. Although the spectra are only qualitative due to varying carbohydrate contents, they are nevertheless informative in the comparison of the lignins. Specifically, all the major lignin structural moieties are present and there are no unexplainable signals present in either the **Rotary Porcelain 6 Week Wood** or **REL** to indicate that the bonding pattern is dramatically different from the MWL. HMQC indicates that minor substructures, such as β-1', may be present only in low proportions in the milled wood, however their signal intensities may be diminished compared to the MWL due to the residual carbohydrate. (**Figure 7.1A)** Interestingly, the relatively strong signal at δ_C/δ_H 82.0/5.1-5.2 ppm may correspond to C_α/H_α correlation in the spirodienone (**XIV**) substructure. Zhang et al., suggested that these structures may be present in levels as high as 3 % in spruce MWL and confirmed this by quantitative ^{13}C NMR. [16] We have shown previously by quantitative ^{13}C NMR that these are minor structures in pine MWL (**Section 6**), but as will be seen below these substructures are not readily discernible by quantitative ^{13}C NMR of the lignin isolated from milled wood. This suggests that the signal on the 2D NMR may derive from somewhere else and that these are not major substructures in lignin.

The strong signal at δ_C/δ_H ~95/6.1-6.6 ppm may be the anomeric carbons from carbohydrates, however the proton chemical shift (typically 5.2-5.3 ppm) based upon literature data is much too far downfield to make this assignment. [21, 152, 203, 204] This signal is strong in all preparations, including MWL dissolved using this solvent system, yet it is not present in the MWL spectrum from directly dissolving the acetylated MWL in NMR solvents. [205] As a result it must be an impurity derived from the dissolution process. DMSO and N-methylimidazole, however, do not have a correlation that would appear in this region of the spectrum.

The signals in the region of δ_C/δ_H 65-75/4.7-5.4 ppm, derived from the C_2 and C_3 of acetylated carbohydrates, and correlations in the region of δ_C/δ_H 69-74/3.5-4.3 ppm are assigned to the remaining carbohydrates. [21, 152, 203, 204]

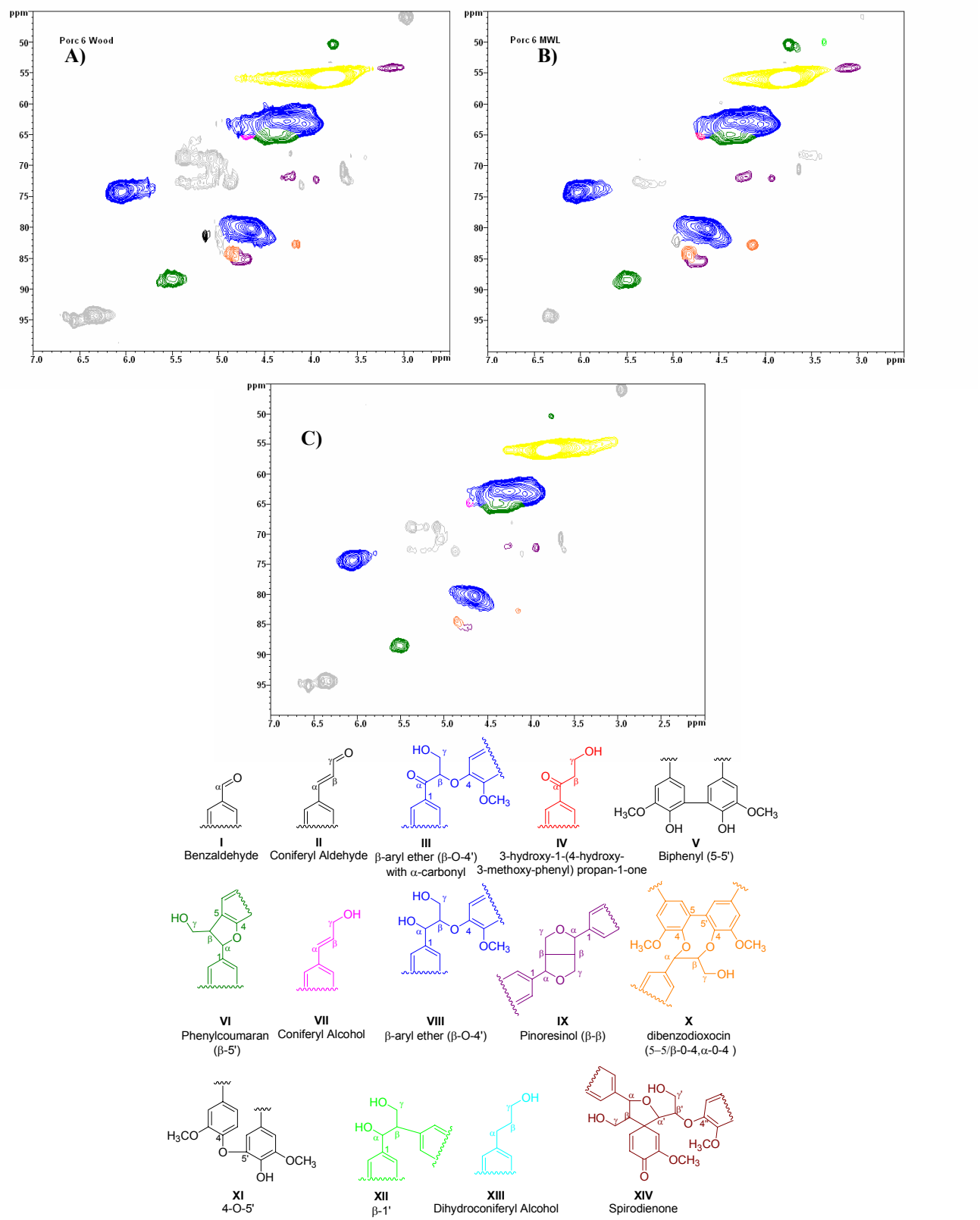

Figure 7.1 Expansions of the oxygenated aliphatic regions of the HMQC spectra: A) Rotary Porcelain 6 Week Wood; B) Rotary Porcelain 6 Week MWL; C) Rotary Porcelain 6 Week REL.

7.5 Quantitative ^{13}C NMR

In **Section 6**, we presented a solution-state NMR comparison of **Vibratory MWL** and **Vibratory CEL** prepared by the standard methods of Bjorkman and Chang. In that section data was presented using both acetylated and nonacetylated lignins enabling an in-depth comparison of the two lignin preparations. In this case, we are only able to compare acetylated lignin material because the nonacetylated wood and REL are not soluble. As a result the data presented will not be as thorough as the previous study. It is possible to solubilize these samples by milling further, however it must be ascertained whether this will cause substantial structural changes.

In order to perform quantitative ^{13}C NMR on a lignin sample, a high concentration is required to achieve good signal to noise and a relaxant is preferable to minimize the experimental time. Chromium acetoacetonate is typically added to decrease the relaxation time of the lignin carbons. [157] To increase the signal to noise ratio, a concentration on the order of 70 mg/0.25 mL is used. Due to difficulty in solubility, the **Rotary Porcelain 6 Week Wood** was dissolved at concentrations of only 60 mg/ 0.6 mL. Quantitative carbon for the **Rotary Porcelain 6 Week REL** did not yield a spectrum with enough resolution to provide any useful data. As a result a comparison between only the **Rotary Porcelain 6 Week MWL** and **Wood** will be presented.

Figure 7.2 compares the quantitative ^{13}C NMR spectra for the **Rotary Porcelain 6 Week MWL** and **Wood**. As can be seen, the resolution is higher in the MWL compared to the wood. This is easily explained by the concentrations of each of the preparations in the deuterated solvent. As a result the signal to noise is much lower for the wood compared to the MWL. In addition, the wood contains 3 % ash prior to dissolution, and while the solution

was filtered through glass wool, some insoluble porcelain material may be present in the NMR tube, thereby contributing to line broadening.

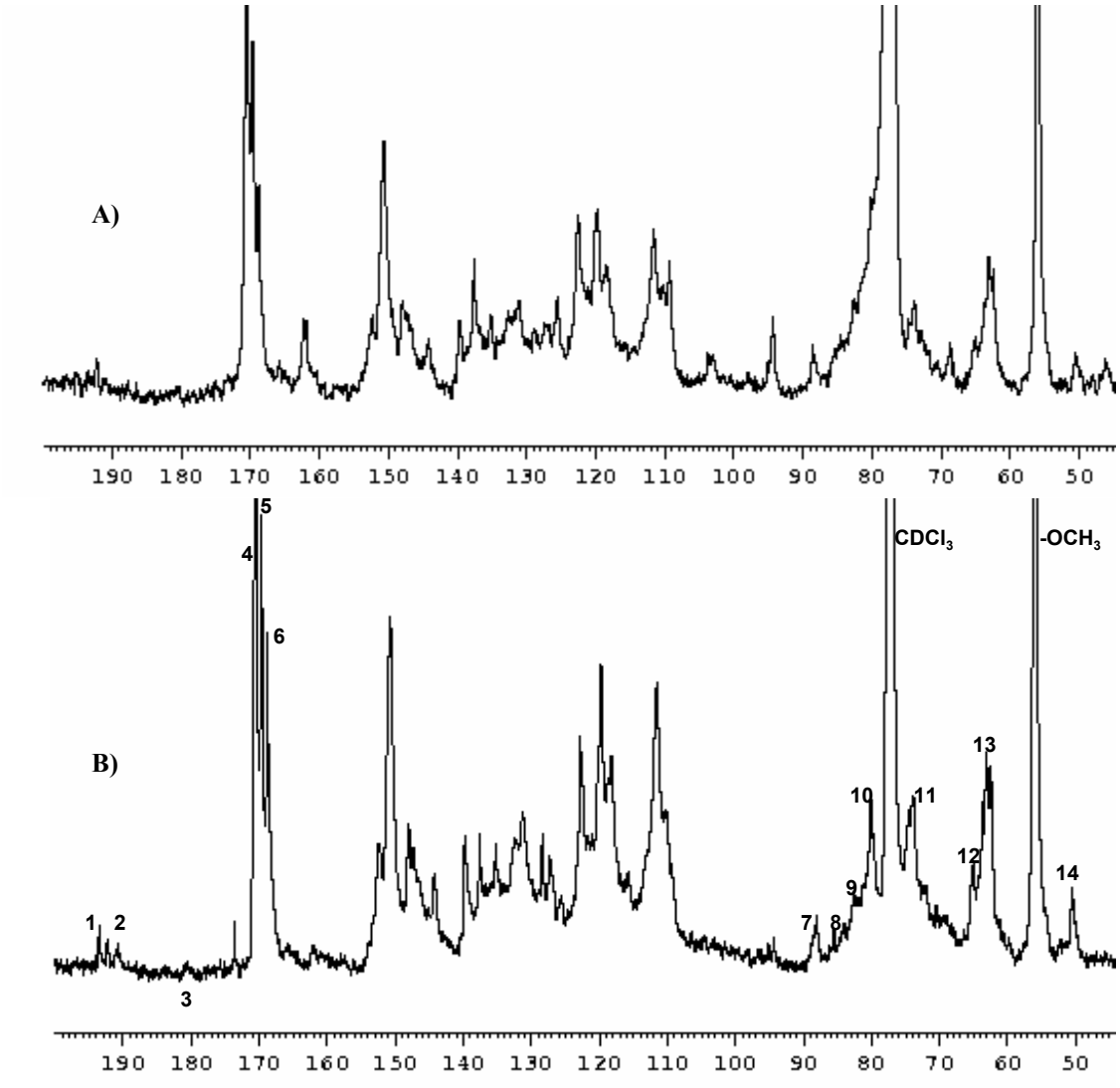

Figure 7.2 Quantitative ^{13}C NMR spectra for A) Rotary Porcelain 6 Week Wood and B) Rotary Porcelain 6 Week MWL, both dissolved and acetylated using the DMSO/NMI dissolution procedure.

Table 7.2 Peak assignments for quantitative ^{13}C NMR spectra.

Peak Number	δ (ppm)	Assignment	Peak Number	δ (ppm)	Assignment
1	194	C=O in (**II**) and (**III**)	**8**	86-85	C_α in (**IX**) and (**X**)
2	191	C=O in (**I**)	**9**	83	C_β in (**X**)
3	181	C=O in (**XIV**)	**10**	80	C_β (*e*,*t*) in (**VIII**)
4	171	C=O in aliphatic primary **–OAc**	**11**	75	C_α (*e*,*t*) in (**VIII**)
5	169.5	C=O in aliphatic secondary **–OAc**	**12**	66	Cγ in (**V**)
6	168.5	C=O in phenolic **–OAc**	**13**	64.5-61	C_γ in (**III**), (**IV**), (**VII**), (**VIII**), (**X**), (**XII**), and (**XIII**)
7	90-87	C_α in (**V**)	**14**	50	C_β in (**V**)and (**XII**)

7.5.1 Oxidized carbon region

Table 7.3 lists the data for the interunit linkages in each of the lignin preparations. The wood contained only vanillin (**I**), ~0.04 carbons per aromatic ring, with the other carbonyl moieties either absent or present in small amounts. This is not unexpected as these carbonyl structures are considered end group moieties and therefore will be represented in much smaller amounts in the higher molecular weight lignin obtained from the wood. Although the MWL portion is present in the **Rotary Porcelain 6 Week Wood**, it is roughly one-fifth of the total lignin and will be expressed to a much lower extent in the wood. Therefore the carbonyl structures may be present in the lignin isolated from milled wood but are below the detection limit of this technique.

Table 7.3 Quantitative determination of interunit linkages for Rotary Porcelain 6 Week Wood and Rotary Porcelain 6 Week MWL by ^{13}C NMR.

Spectral Region	Chemical Shift Range (ppm)	Number of Moieties per Aromatic Ring	
		Rotary Porcelain 6 Week MWL	Rotary Porcelain 6 Week Wood
Ar-CHO (I)	191	0.04	0.04
Ar-CH=CH-CHO (II) + α-C=O in β-O-4 (III)	194	0.04	negl.
Ar-CO-CH_2-CH_2OH (IV)	198	0.05	negl.
β-5' (V)	90-86	0.09	0.10
β-O-4' (VIII)+ Dibenzodioxocin (X)+ Ar-CH=CH-CH_2OH (VII)	64.5-61	0.40	0.47
β-1' (XII)	51-48	0.02	negl.
Spirodienone (XIV)	181	0.01	negl.

The MWL exhibited typical values for the 200-190 ppm region, with a total integration of 0.11 carbons per aromatic ring. Absent from this spectrum (**Figure 7.2**) is the 3-hydroxy-1-(4-hydroxy-3-methoxy-phenyl) propan-1-one (**IV**), shown in **Figure 7.1**, which was present in the MWL reported previously by direct dissolution in DMSO-d_6. (**Section 6**) This suggests that it may be solubilized during the DMSO/NMI dissolution process. Vanillin, with a chemical shift of 191 ppm, is present in levels of 0.04 carbons per aromatic ring. β-O-4' substructures with α-carbonyl (**II**) and coniferaldehyde (**III**) overlapping at 194 ppm are also present at a combined level of 0.04 carbons per aromatic ring.

Spirodienone (**XIV**) at 181 ppm is present at levels about 0.01 per aromatic ring in the **Rotary Porcelain 6 Week MWL** but not in appreciable amounts in the **Rotary**

Porcelain 6 Week Wood. A clearly resolved signal present at 193 ppm accounts for the remainder of the value of the integration for this region.

7.5.2 Aliphatic and phenolic hydroxyl content

The hydroxyl contents are represented by the acetates of the primary, secondary, and phenolic hydroxyl groups, respectively, from 171.5-167 ppm. (**Figure 7.2**) For the **Rotary Porcelain 6 Week MWL**, the aliphatic hydroxyl content (0.75 carbons per aromatic ring) is much lower than was reported for the **Vibratory MWL** prepared by the standard Bjorkman method (1.02 per aromatic ring). (**Section 6**) The aliphatic hydroxyl content for the **Rotary Porcelain 6 Week Wood** on the other hand is much higher with a value of 1.23 per aromatic ring. The difference between the two MWL preparations could be attributed to structural changes occurring within the isolatable lignin portion during milling. Interestingly the phenolic hydroxyl content of the **Rotary Porcelain 6 Week Wood** and **MWL** were quite similar with values of 0.29 and 0.28 per aromatic ring, respectively. The phenolic hydroxyl content however was much higher for the **Rotary Porcelain 6 Week MWL** (0.28 vs. 0.17 per aromatic ring) compared to the standard **Vibratory MWL** reported previously. (**Section 6**) This suggests the lignin depolymerized to a greater extent by rotary milling than vibratory milling in the standard Bjorkman procedure. A detailed comparison of different milling techniques will be presented in the following section.

7.5.3 Aliphatic side chain region

Comparison of the oxygenated aliphatic side chain regions for the two preparations is limited owing to the absence of the nonacetylated spectra. In any case estimations based upon integration of the acetylated spectra will be made where possible.

The correlations for C_α/H_α, C_β/H_β, and C_γ/H_γ for the β-O-4' substructures are centered at δ_C/δ_H 74.0/6.0, 80.0/4.6, and 62-63/4.0-4.4, respectively. Because the **Rotary Porcelain 6 Week Wood** lignin was most easily solubilized in $CDCl_3$, the correlations for the α- and β-carbons are overlapped by the solvent peak. As a result, the quantity of β-O-4' substructures (**VIII**) was calculated based upon integration of the γ-carbon region. Although this region is overlapped by the γ-carbons from other structures, most of these can be estimated based upon integration of other signals and as a result a close approximation of the β-O-4' content can be obtained.

Dibenzodioxocin (**X**) and coniferyl alcohol (**VII**) are structures that cannot be completely elucidated based on other signals. The correlations for the α- and β-carbons in the dibenzodioxocin substructure are present as seen by the C_α/H_α and C_β/H_β correlations at δ_C/δ_H 84.5/4.8 and 82.6/4.1 in the HMQC spectra. The α-carbon in the quantitative ^{13}C spectrum is overlapped by the α-carbon from the β-β' (**IX**) substructure while the β-carbon is overlapped by the β-O-4' β-carbon as well as the solvent peak. Coniferyl alcohol on the other hand will have the α- and β-carbons overlapping the aromatic region at 134 and 123 ppm,respectively, and the γ-carbon at 62-63 ppm.

The amount of coniferyl alcohol was estimated to be a maximum of 0.02 per aromatic ring in **Rotary Porcelain 6 Week MWL** (**Section 8**), but even this may be high because of the overlap of the γ-carbon from β-O-4'moieties. As coniferyl alcohol is an end group unit,

its contribution to the higher molecular weight milled wood and REL is expected to be minimal.

Integration of the γ-carbon region, 64.5-61 ppm, minus the contributions of (**III**), (**IV**), (**XII**), and (**XIV**), results in values of 0.47 and 0.40 per aromatic ring, respectively, for **Rotary Porcelain 6 Week Wood** and **MWL**. The difference in β-O-4' content is consistent with the results from the degradative techniques previously discussed.

β-5' (**V**) content can be clearly determined based upon integration of the area of 90-87.5 ppm, and is 0.10 and 0.09, respectively, for **Rotary Porcelain 6 Week Wood** and **MWL**. These values are consistent with those previously reported. (**Section 6**) Integration of the region from 51-49 ppm, comprising the β-carbons of both the β-5' and β-1' (**XII**) substructures yields a maximum value of 0.02 β-1' moieties per aromatic ring for the **Rotary Porcelain 6 Week MWL** and essentially zero for the **Rotary Porcelain 6 Week Wood**. This agrees with the HMQC spectra exhibiting a C_β/H_β correlation at δ_C/δ_H 50.0/3.4 ppm in the **Rotary Porcelain 6 Week MWL** which is not present in the **Rotary Porcelain 6 Week Wood**.

Indications based upon comparison of **Rotary Porcelain 6 Week Wood** and **MWL** by one- and two-dimensional NMR are that the β-O-4' content in the milled wood preparation is higher than that in the MWL. While phenolic hydroxyl content is nearly identical, aliphatic hydroxyl content is unexpectedly low in the **Rotary Porcelain 6 Week MWL**. All major interunit linkages expected to be present based upon the present knowledge of lignin biosynthesis are identifiable by HMQC. In addition there is not an apparent abundance of unexplainable signals in the wood or REL.

7.7 Dipolar Dephasing Solid-State ^{13}CP/MAS NMR

One of the drawbacks from the comparison of the **Rotary Porcelain 6 Week Wood** and **MWL** utilizing only the acetylated quantitative ^{13}C NMR spectra is that the degree of condensation cannot be estimated. Fortunately, this can be easily estimated by dipolar dephasing solid-state NMR. This is simply a CP/MAS experiment with a short delay period (d_2) where spin-locking is removed to allow spin-lattice relaxation to occur to the extent that the signals from carbons with directly attached protons are decayed. Removal of the protonated carbons leaves a quaternary carbon spectrum from which the degree of condensation can be estimated. While not entirely quantitative, it is a good tool for comparing the different lignin preparations.

The experiment was optimized by varying contact time from 1-5 ms and it was determined that 2 ms was optimal. Overall, contact times of 1-3 ms exhibited little difference in signal intensity. Variation of the d_1-delay from 1-10 s found little difference in signal intensity beyond a 3 s delay. An array experiment varying the d_2-delay period from 0-120 μs determined that the optimal delay was 50 ms. All results are consistent with literature reports. [169, 175, 176, 178]

The aromatic region of the nonprotonated spectrum can be divided into the condensed aromatic (141-125 ppm) and the oxygenated aromatic (160-141 ppm) regions. Thioacidolysis showed no indication of syringyl (**S**) or *p*-hydroxyphenyl (**H**) units and therefore it can be assumed that a completely uncondensed guaiacyl lignin will contain two oxygenated aromatic carbons per aromatic ring (C_3 and C_4) and one condensed aromatic carbon (C_1) per aromatic ring. Any condensed linkages in the lignin, predominately β-5' or 5-5' substructures, will shift the carbon-carbon linked aromatic carbon to the region of 141-

125 ppm. As a result, the degree of condensation can be estimated by this relationship from a ratio of **Region A** (160-141 ppm) to **Region B** (141-125 ppm). [175, 178] (**Figure 7.3**)

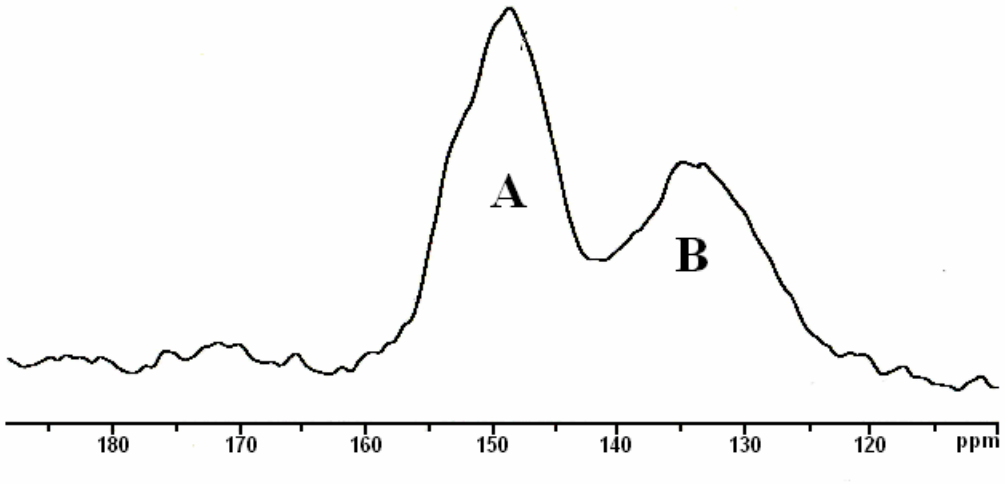

Figure 7.3 Dipolar dephasing spectrum depicting the two regions of nonprotonated carbons: the oxygenated aromatic carbons (Region A) and the condensed aromatic region (Region B).

Although this technique is not entirely quantitative, however, comparisons of samples of similar materials can still be performed. Specifically the relaxation times of all the lignin preparations will be similar. The **Rotary Porcelain 6 Week MWL** was estimated to have a degree of condensation of 0.44 per aromatic ring while the **Wiley Wood** and **Rotary Porcelain 6 Week REL** were determined to be 0.30 and 0.36 per aromatic ring, respectively. (**Table 7.4**) These results agree with those from the degradative techniques, indicating that the REL is more similar to the lignin in wood than is the MWL.

Table 7.4 Estimations of the degree of condensation for Wiley Wood, Porc 6 MWL, and Porc 6 REL, as determined by the dipolar dephasing solid-state NMR experiment.

	Estimation of Degree of Condensation
Wiley Wood	30
Rotary Porcelain 6 Week MWL	44
Rotary Porcelain 6 Week REL	36

7.8 Gel Permeation Chromatography

The relative molecular weights were determined on the acetylated lignin preparations in 0.1 N LiCl/DMF. (**Figure 7.4**) As can be seen the **Rotary Porcelain 6 Week Wood** sample has a wide distribution and as a result only the M_p, the relative molecular weight at the maximum peak height, will be reported. The **Rotary Porcelain 6 Week Wood** exhibits four possible peaks, including fairly well resolved peaks at high molecular weight (~55000 g/mol) and at very low molecular weight (~1200 g/mol). Additionally two poorly resolved peaks are present as shoulders in the range of the MWL distribution.

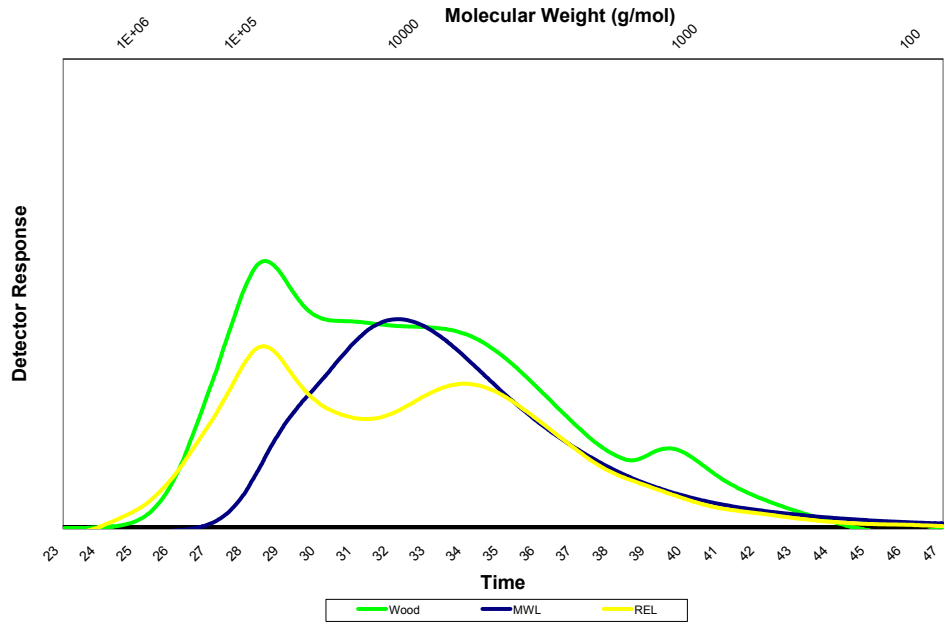

Figure7.4 GPC chromatogram of the Porc-6 Wood, Porc-6 MWL, Porc-6 REL.

The **Rotary Porcelain 6 Week MWL** is of course isolated from the **Rotary Porcelain 6 Week Wood**, and it exhibits the characteristic unimodal distribution expected from a MWL preparation. This is important because it also indicates that aggregation at higher molecular weight is not occurring, thus showing that the chromatograms of **Rotary Porcelain 6 Week Wood** and **REL** are true representations of their molecular weight distributions. [206] In addition, we have previously reported that the relative molecular weight of acetylated MWL in THF has an M_w at ~5000 g/mol (**Sections 5** and **6**), while in DMF it is closer to 10000 g/mol. This apparent increase in relative molecular weight between THF and DMF is due to the difference in retention times for the polystyrene standards, consistent with previous reports. [207, 208] The relative molecular weight as determined in DMF is closer to that originally reported in Bjorkman's sedimentation experiments, indicating the possibility that the determination of molecular weight relative to polystyrene may be underestimated in THF and that DMF is a more proper solvent for molecular weight determination. [71]

Like the **Rotary Porcelain 6 Week Wood**, the **Rotary Porcelain 6 Week REL** has a peak of high molecular weight at ~55000 g/mol and it also has a lower molecular weight peak at ~6000 g/mol. In addition it shows that the portion of MWL isolated from the **Rotary Porcelain 6 Week Wood** is clearly absent in the **Rotary Porcelain 6 Week REL**. This indicates that the GPC chromatograms are indeed representative of the MWL isolation process.

The GPC chromatograms that the **Rotary Porcelain 6 Week Wood** has a wide molecular weight distribution in the lignin portion after milling. From this the lignin that is free of carbohydrates is readily removed and purified as MWL. The very low molecular

weight portion in the wood is not present in either the MWL or the REL and is likely removed during the MWL purification process. The presence of a large portion of lower molecular weight material in the REL indicates that association with carbohydrates likely prohibits the solubilization of this lower molecular weight portion. After purification by removal of carbohydrates, the lower molecular weight portion of the REL is likely to solubilize in the aqueous dioxane.

8. Quantitative ^{13}C NMR characterization of milled wood lignins isolated by different milling techniques

KM Holtman, H-m Chang, and JF Kadla, under preparation for submission to *Biomacromolecules*.

8.1 Modified DFRC

Table 8.1 gives the data from the modified DFRC analysis for the **Vibratory MWL**, **Vibratory (Dry) MWL**, and **Rotary Porcelain 6 Week MWL**. As indicated by the Unit A composition, each of the MWL preparations are enriched in phenolic end group material with a subsequent decrease in etherified β-O-4' substructures (Unit C). This is expected as the MWLs are isolated by depolymerization involving homolytic cleavage of the β-aryl ether bonds in the wood meal. There was a slight increase in the Unit B content of the **Vibratory (Dry) MWL**, however this will not be addressed by quantitative ^{13}C NMR due to peak overlap it is difficult to differentiate an α-aryl ether bond. Previous results by HMQC have not detected these interunit linkages (**Sections 5** and **6**), consistent with literature values. [158] It is therefore questionable as to whether these structures exist.

Table 8.1. Modified DFRC unit composition and total molar yields for the different MWL preparations.

	Unit Composition (mol %)			Total Yield (mol %)
	Unit A	Unit B	Unit C	
Wiley Wood Meal	21.6	6.8	71.7	13.4
Vibratory MWL	41.3	7.7	51.0	14.5
Vibratory (Dry) MWL	40.9	10.0	49.1	11.7
Rotary Porcelain 6 Week MWL	44.0	4.7	51.3	15.5

The total yields were higher than the **Wiley Wood** for both the **Vibratory MWL** (14.5 mol %) and **Rotary Porcelain 6 Week MWL** (15.5 mol %), and lower for the

Vibratory (Dry) MWL (11.7 %). From this degradation method, it appears that the **Vibratory (Dry) MWL** has undergone substantial condensation reactions while the other two samples are relatively similar to the **Wiley Wood**.

8.2 Quantitative ^{13}C NMR

Detailed calculations of the frequency of interunit linkages in each of the milled wood lignin preparations were calculated from the nonacetylated and acetylated spectra as outlined in **Section 6**. The nonacetylated spectrum from the **Vibratory MWL** preparation is shown in **Figure 8.1** with the oxygenated aliphatic region of the acetylated spectrum shown in the inset. All peak identifications are given in **Table 8.2**. The integrations were performed by setting the aromatic region from 160-103 ppm equal to 6.12 as discussed previously (**Section 6**) and therefore all moieties are based upon equivalences per aromatic ring. [138, 143]

The spectrum can be subdivided into regions of interest in order to obtain information about the overall structure of the lignin polymer. The results are shown in **Table 8.3** and the methoxyl content can be used as a type of calibration for the spectrum. In other words, if the integration of the methoxyl peak is accurate, then the phasing and baseline of the spectrum are likely adequate. The methoxyl content for the **Vibratory MWL** and the **Rotary Porcelain 6 Week MWL** are 0.96 and 0.97 which are typical values for guaiacyl-based lignins such as those found in conifers. The **Vibratory (Dry) MWL** is slightly high at 1.00, however the value is within the 5 % error associated with this technique. [119]

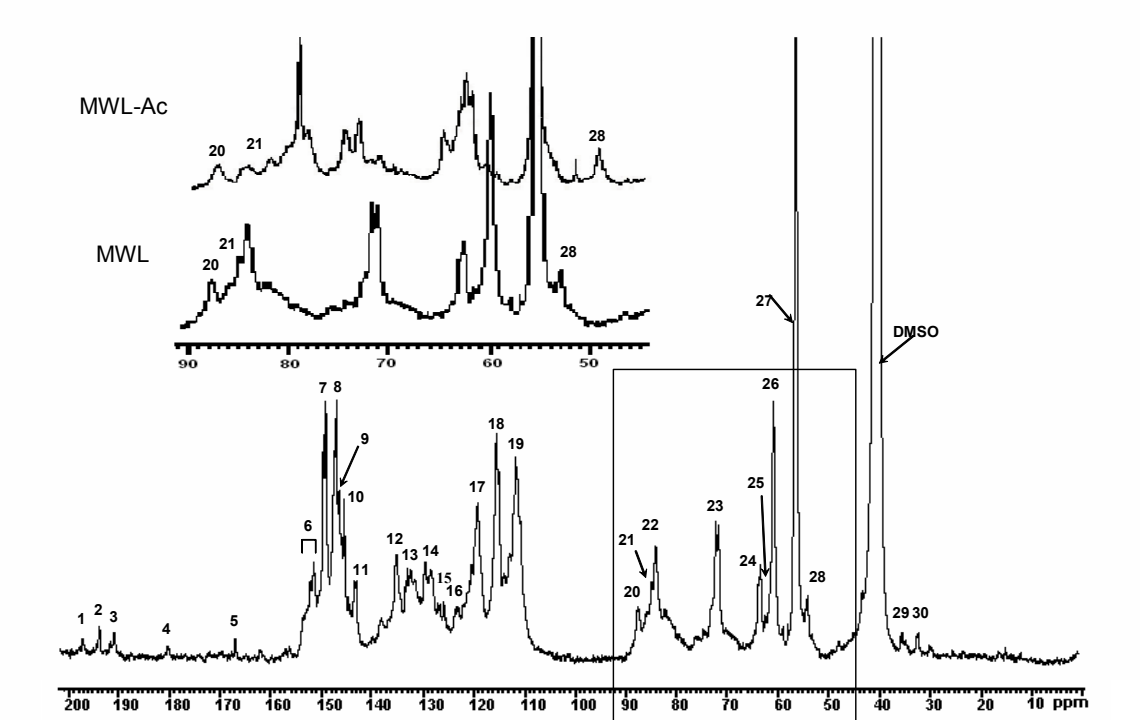

Figure 8.1 Quantitative ^{13}C NMR spectra of MWL. Included is an expansion of the oxygenated aliphatic region of the MWL and acetylated MWL (MWL-Ac).

Table 8.2 Assignment of the quantitative ^{13}C NMR spectra.

Peak Number	δ (ppm)	Assignment	Peak Number	δ (ppm)	Assignment
1	198	C=O in (**IV**)	**16**	124.5-122	C_1 and C_6 in α-C=O units
2	194	C=O in (**III**)	**17**	122-117	C_6 in G units
3	191	C=O in (**I**)	**18**	117-113	C_5 in G units
4	181	C=O in (**XIV**)	**19**	113-108	C_2 in G units
5	168	C=O in **–OAc**	**20**	87	C_α in (**V**)
6	155-151	$C_3/C_{3'}$ in etherified (**V**) C_α in (**III**) C_5 in ring B of (**XI**)	**21**	86.5-85	C_α in (**VIII**) C_α and C_β in (**IX**)
7	151-148.5	C_3 in etherified G units	**22**	85-82	C_β (*e*,*t*) in (**X**)
8	148.5-146.8	C_4 in etherified G units C_3 in nonetherified (**X**)	**23**	74-71	C_α (*e*,*t*) in (**X**) C_γ in (**VIII**)
9	146.2	C_4 in nonetherified G units C_4 in ring B of (**V**)	**24**	64-62	C_γ in (**III**), (**V**), and (**XII**)
10	145.2	$C_4/C_{4'}$ in etherified (**VI**)	**25**	61.5	C_γ in (**VII**)
11	143.5	C_3 in ring B of (**V**) $C_4/C_{4'}$ in nonetherified (**VI**)	**26**	61-59	C_γ in (**IX**) and (**X**)
12	137-134	C_1 in etherified G units	**27**	56	**$-OCH_3$**
13	134-130	C_1 in nonetherified G units $C_5/C_{5'}$ in etherified (**VI**)	**28**	54-52	C_β in (**V**), (**VIII**), and (**XII**)
14	130-127	C_β in (**II**) C_α and C_β in (**VII**)	**29**	34.5	C_α in (**XIII**)
15	127-124.5	$C_5/C_{5'}$ in nonetherified (**VI**)	**30**	31.5	C_β in (**XIII**)

Table 8.3 Quantification of the spectral regions of the ^{13}C NMR spectra.

Spectral Region	Chemical Shift Range (ppm)	Number of Moieties per Aromatic Ring		
		Vibratory MWL	Vibratory (Dry) MWL	Rotary Porcelain 6 Week MWL
Methoxyl Content	57-54	0.96	1.00	0.97
Aromatic Methine Carbons	125-103	2.57	2.56	2.46
Aromatic Carbon-Carbon Structures	141-125	1.53	1.48	1.54
Oxygenated Aromatic Carbons	160-141	2.02	2.07	2.12
Carbon from Carbonyl Type Structures	195-190	0.12	0.09	0.14
Carbon from Carboxyl Type Structures	176-163	negl.	negl.	0.05
Degree of Condensation	125-103	0.43	0.44	0.54
Aliphatic Hydroxyl Content	171-168.5	1.02	1.26	0.75
Phenolic Hydroxyl Content	168.5-166	0.17	0.29	0.30

8.2.1 Oxidized Carbon Region

Table 8.3 indicates that the **Vibratory (Dry) MWL** has a slightly lower degree of oxidation than the **Vibratory MWL**. This is exhibited by the integration of the carbonyl region from 195-190 ppm, resulting in values of 0.12 and 0.09 for the **Vibratory MWL** and **Vibratory (Dry) MWL,** respectively. The **Rotary Porcelain 6 Week MWL** sample on the other hand is slightly higher with a value of 0.14 per aromatic ring after being milled extensively over a period of weeks.

Table 8.4 indicates that the **Vibratory (Dry) MWL** contains a lower amount of vanillin (**I**), 0.02 per aromatic ring, compared to the other two preparations (0.04 per aromatic ring). The presence of the 3-hydroxy-1-(4-hydroxy-3-methoxy-phenyl) propan-1-one (**IV**) structure is higher in the **Rotary Porcelain 6 Week MWL** compared to the other two materials, 0.05 versus 0.03 and 0.02 (**Vibratory MWL** and **Vibratory (Dry) MWL**) moieties per aromatic ring. The integration of the peak at 195 ppm indicates that there is no difference in the combined amount of coniferaldehyde (**II**) and α-carbonyl structures (**III**) between the **Vibratory MWL** and **Vibratory (Dry) MWL** (0.02 per aromatic ring), but that the **Rotary Porcelain 6 Week MWL** contains a much larger amount of these units, 0.05 per aromatic ring. All structural moieties discussed are shown in **Figure 8.4** and are consistent with the labelling in **Sections 6** and **7**.

Although Zhang et al., had suggested that the spirodienone (**XIV**) structure, based upon the C_4 carbonyl signal at 181 ppm[16], may be a major contributor of β-1' moieties in native spruce lignin, our samples have not indicated it to be anything more than a minor contributor to the lignin structure. All three MWLs contain this moiety at no more than 0.01 per aromatic ring.

Table 8.4 Estimation of interunit linkages in Vibratory MWL,Vibratory (Dry) MWL, and Rotary Porcelain 6 Week MWL via quantitative ^{13}C NMR.

Spectral Region	Chemical Shift Range (ppm)	Number of Moieties per Aromatic Ring		
		Vibratory MWL	Vibratory (Dry) MWL	Rotary Porcelain 6 Week MWL
Ar-CHO (I)	191	0.04	0.02	0.05
Ar-CH=CH-CHO (II) + α-C=O in β-O-4 (III)	194	0.04	0.04	0.04
Ar-CO-CH_2-CH_2OH (IV)	198	0.03	0.02	0.05
β-5' (V)	Ac(90-86)[a]	0.09	0.07	0.09
5-5' (VI)	145-141[b]	0.16	0.17	0.18-0.19
Ar-CH=CH-CH_2OH (VII)	62	0.04	0.03	0.02
β-O-4' (VIII)	61.5-57.5[c]	0.41	0.42	0.32
β-β' (IX)	54.3-52.0[d]	0.02	0.02	0.02
Dibenzodioxocin (X)	Ac(86-83)[e]	0.08	0.06	0.03-0.04
β-1' (XII)	Ac(51-48)	<0.01	0.01	negl.
Ar-CH_2-CH_2-CH_2OH (XIII)	31	0.03	0.03	0.02
Spirodienone (XIV)	181	0.01	<0.01	0.01

[a] β-5' (V) was directly integrated from 90-86 ppm in the acetylated ^{13}C spectrum. (inset Figure 6.1)
[b] 5-5' was determined by integration of 145-141 ppm of the nonacetylated spectrum minus the value of (V).
[c] β-O-4' (VIII) calculated from region of 61.5-57.5 in the nonacetylated spectrum minus the values for (III), (IV), (X), (XII), and (XIII).
[d] β-β' (IX) calculated from integration of the region 54.3-52 in the nonacetylated spectrum minus the value of (V).
[e] Dibenzodioxocin was calculated by integration of 86-83 ppm in the acetylated ^{13}C spectrum minus the value of (IX).
[f] β-1' (XII) was calculated by integration of 51-48 ppm of the acetylated ^{13}C spectrum minus the value of (V).

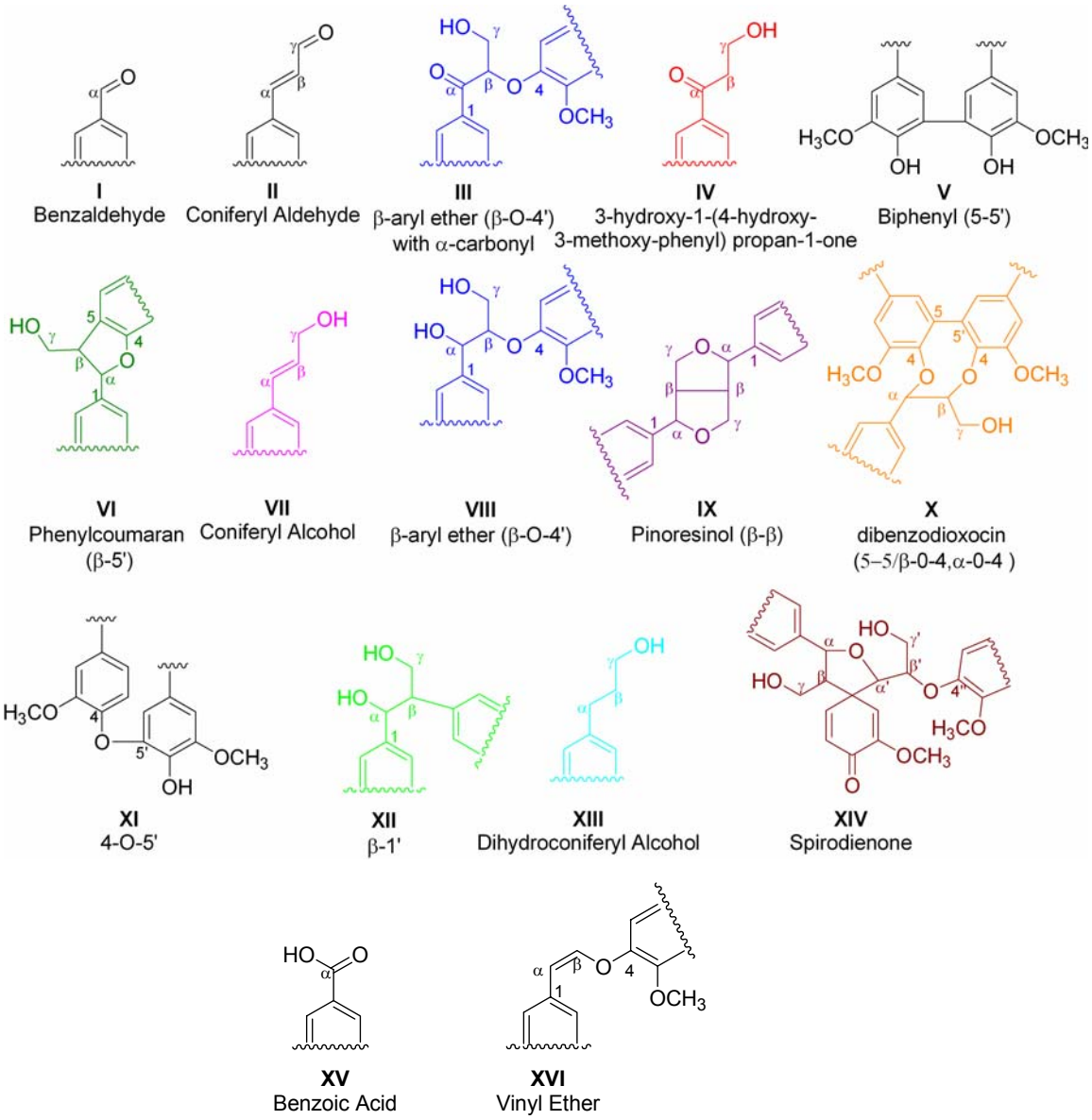

Figure 8.2 Commonly found interunit linkages in lignin preparations.

While the rest of the carbonyl region in the nonacetylated spectra of the vibratory milled lignins are basically devoid of signals, the Rotary **Porcelain 6 Week MWL** shows several small signals indicative of carboxyl structures. The total integration from 176-163 ppm yields a value of 0.05 per aromatic ring. (**Table 8.3**) The downfield signals (176-168 ppm) are likely due to aliphatic carboxyl groups, while the the upfield signals (168-163 ppm) are probably conjugated carboxyl structures. The conjugated carboxyl structures are present at levels of 0.04 per aromatic ring and are likely of the benzoic acid type (**XV**), shown in **Figure 8.2**. (**Table 8.4**)

The presence of the carboxylic structures is important because they show evidence of oxidation occurring during the milling process. Although the carbonyl content is only slightly elevated compared to the vibratory milled lignins, this is because the sidechain oxidation proceeds to a higher level of oxidation. This also confirms that suspected structures such as α-carbonyl (**III**) and 3-hydroxy-1-(4-hydroxy-3-methoxy-phenyl) propan-1-one (**IV**) are likely formed during milling and are not incorporated naturally into the lignin structure. In addition, it may indicate that vanillin (**I**) is also produced by sidechain oxidation.

8.2.2 Aliphatic and Phenolic Hydroxyl Content

Table 8.3 lists the values for the aliphatic (171-168.5 ppm) and phenolic (168.5-167 ppm) hydroxyl groups as determined for each MWL. The data for **Rotary Porcelain 6 Week MWL** supports the theory of sidechain oxidation as the aliphatic hydroxyl content (0.75 per aromatic ring) is much lower than typically reported, while the phenolic hydroxyl content is similar to literature values. [119, 153]

Comparison of the vibratory milled samples shows an unexplainable discrepancy. While both are comparable to literature values, the **Vibratory (Dry) MWL** is much higher in both aliphatic and phenolic hydroxyls, 1.26 versus 1.02 and 0.30 versus 0.17 per aromatic ring, respectively. A higher value for the phenolic hydroxyl content is consistent with more depolymerization of the lignin polymer which may be expected as the toluene is not present to stabilize radicals formed during milling. Meanwhile, a decrease in the aliphatic hydroxyl content is consistent with degradation of the sidechain, however the difference in oxidized moieties between the two preparations is not that drastic.

One might expect that an increase in phenolic hydroxyl groups would coincide with a decrease in the aliphatic hydroxyl content, however this was not observed. Furthermore the increase in phenolic hydroxyl groups does not translate into an increase in the Unit A content in the modified DFRC results for the **Vibratory (Dry) MWL**. It is a possibility that the **Vibratory MWL** was not completely acetylated although excess reagents were used and the process repeated.

8.2.3 β-O-4' Content

Prolonged milling in the rotary mill leads to a decrease in the β-O-4' (**VIII**) content as compared to the vibratory milled preparations based upon integration of the γ-carbon from 61.5-57.5 ppm. The value of β-O-4' substructures for Rotary Porcelain 6 Week MWL is 0.33 per aromatic ring while the **Vibratory MWL** and **Vibratory (Dry) MWL** were 0.42 and 0.41, respectively. These values do not coincide with the data obtained from the modified DFRC analysis. It is quite probable however that the **Rotary Porcelain 6 Week MWL** has a similar interunit linkages compared to the vibratory milled samples except that

sidechain modification has resulted in cleavage of the γ-carbon. This reaction would result in an under calculation of the β-aryl ether content and it has been reported that there is sufficient energy present in milling to cause C-C bond cleavage. [74] This theory is also supported by the discrepancy in aliphatic hydroxyls discussed in the previous section.

8.2.4 Aromatic region and the degree of condensation

The aromatic region of the nonacetylated spectrum can be divided into the protonated aromatic (125-103 ppm), the condensed aromatic (141-125 ppm), and the oxygenated aromatic (160-141 ppm) regions. In theory, the oxygenated aromatic region should contain the C_3 and C_4 carbons on the aromatic ring along with any carbons deriving from diphenyl ether structures (**XI**). The condensed aromatic region should consist of C_1 carbons plus any ring carbons involved in crosslinks such as in the 5-5' (**V**) or β-5' (**VI**) substructures. Finally the protonated aromatic region will consist of the C_2, C_6, and any uncondensed C_5 carbons. (**Table 8.3**)

As discussed in **Section 6** the oxygenated aromatic and condensed aromatic regions have some degree of overlap, making calculation of the degree of condensation less precise. Regardless the integrations of these regions are present in **Table 8.3**. The protonated aromatic region does not suffer this problem and as a result the degree of condensation can be easily estimated. Three minus the value of integration for this region will yield an estimate of the degree of condensation based upon the assumption that a completely uncondensed lignin will have protons at the C_2, C_6, and C_5 positions. The vibratory milled samples show similar integrations for this region, with values of 2.57 and 2.54, respectively for the **Vibratory MWL** and **Vibratory (Dry) MWL** samples, yielding degrees of

condensation of 0.43 and 0.44. The **Rotary Porcelain 6 Week MWL** had a degree of condensation of 0.54.

The calculation of the 5-5' content, as mentioned in the previous paper, is not precise. In the case of these samples, the 5-5' content was calculated to be 0.16-0.18 per aromatic ring. These values coincide with the degree of condensation fairly well for the vibratory milled samples, however there is a discrepancy of 0.09 carbons per aromatic ring for the **Rotary Porcelain 6 Week MWL**. While it cannot be substantiated, condensation reactions other than the formation of 5-5' substructures may be occurring. In addition there may be a greater contribution of middle lamella material to the **Rotary Porcelain 6 Week MWL.**

There may also be other side reactions occurring that will cause shifts in sidechain carbons resulting in misleading calculations. This is a potential drawback to the quantitative ^{13}C NMR analysis. A possible example is the appearance of a fairly broad signal at 141-140 ppm not present in the other NMR spectra. According to literature values, this signal may coincide with the β-carbon from vinyl ether type structures (**XVI**). (**Figure 8.2**) [148] Further support for this theory is the accumulation of oxidized material in the insoluble lignin portion as determined by solid-state NMR spectroscopy. [205]

8.2.5 Aliphatic Side Chain Region

Other interunit linkages known to be present based upon dehydrogenative polymerization show convergence between the lignin preparations and also the literature values. [198, 199] Specifically, integration for β-5' (**V**) substructures in the acetylated spectra results in values 0.09 subunits per aromatic ring each for **Vibratory MWL** and **Rotary Porcelain 6 Week MWL** and 0.07 for the **Vibratory (Dry) MWL**. [197] The β-β'

substructure (**IX**) is also present in typically reported values, 0.02 per aromatic ring, for each sample. (**Table 8.4**)

Dibenzodioxocin (**X**) structures are identified by integration of peaks from 86-83 ppm in the acetylated lignin spectra. Values of 0.08 and 0.06 per aromatic ring were obtained for the **Vibratory MWL** and **Vibratory (Dry) MWL**, respectively, while the**Rotary Porcelain 6 Week MWL** was only 0.03. It is possible that a decrease in dibenzodioxocin in the **Rotary Porcelain 6 Week MWL** could result from a shift of the sidechain carbon resonances due to cleavage of the γ-carbon or ring-opening depolymerization.

Coniferyl alcohol (**VII**) is thought to be incorporated as an end group in the lignin polymer by etherification at the 4'-position. The values obtained by integration at 62 ppm may be slightly overestimated due to overlap of the γ-carbon of the β-O-4' subunit. In any case, the values obtained per aromatic ring are 0.04 and 0.03 for the **Vibratory MWL** and **Vibratory (Dry) MWL**, respectively, and 0.02 for the **Rotary Porcelain 6 Week MWL.** (**Table 8.4**) The decrease in the **Rotary Porcelain 6 Week MWL** may be attributable to sidechain degradation or cleavage of these end groups from the lignin polymer and their subsequent loss by solubilization during the purification steps.

Finally, the contribution of minor structural moieties such as β-1' (**XII**), and dihydroconiferyl alcohol (**XIII**) should be mentioned. Dihydroconiferyl alcohol was the most prevalent of these substructures, with amounts of 0.03 per aromatic ring found in the vibratory milled samples, and 0.02 for the **Rotary Porcelain 6 Week MWL**. Again the slight decrease may be attributable to sidechain cleavage or the loss of end groups. The β-1'

were found to be relatively minor with the maximum level detected in any case was 0.01 per aromatic ring. (**Table 8.4**)

9. Solid-state NMR Spectroscopy

9.1 Experimental Plan

It was deemed necessary to study the complete lignin structure and not just the MWL in order to make an accurate assessment of the effects of milling. As a result, a quantitative evaluation of the whole lignin in the REL and the Wiley wood by solid-state NMR was attempted.

Initially the goal of the solid-state experiment was to acquire a series of spectra that would provide different types of information about the lignin structure. First, the CP/MAS experiment would provide the basic carbon spectrum of the lignin. The interrupted decoupling (also called dipolar dephasing or dipolar decoupling) experiment would supply information about the quaternary carbons in the lignin structure. Finally, a newly described experiment would selectively produce a ^{13}C spectrum containing only the methine carbons. [26] Subtraction of the latter two spectra from the CP/MAS would result in a spectrum containing predominately methylene carbons, primarily the γ-carbons in lignin. In this way, the lignin structure could be analyzed by developing an experiment similar to the solution-state ^{13}C DEPT experiment. [119]

9.1.1 CP/MAS Experiment

CP/MAS is a standard experiment used to acquire the basic carbon spectrum of solid materials and has been reported extensively for lignins. [168, 169, 171, 173, 181] **Figure 9.1** shows the CP/MAS for the **Vibratory MWL**.

Sensitivity is greatly improved by transfer of magnetization from the abundant ^{1}H to the less abundant ^{13}C through cross polarization, but this approach suffers drawbacks that can

prevent it from being quantitative. Specifically, the transfer of magnetization occurs slower with nonprotonated carbons resulting in an underestimation of the oxygenated aromatic and carbonyl carbons. Increasing contact time can improve the transfer of magnetization however too long a period will result in spin-lattice relaxation of the protonated carbons. Additionally relaxation of the nonprotonated carbons is slower than for the protonated carbons but this effect can be minimized by increasing the delay time between scans. Too long of a delay period can result in long experimental times.

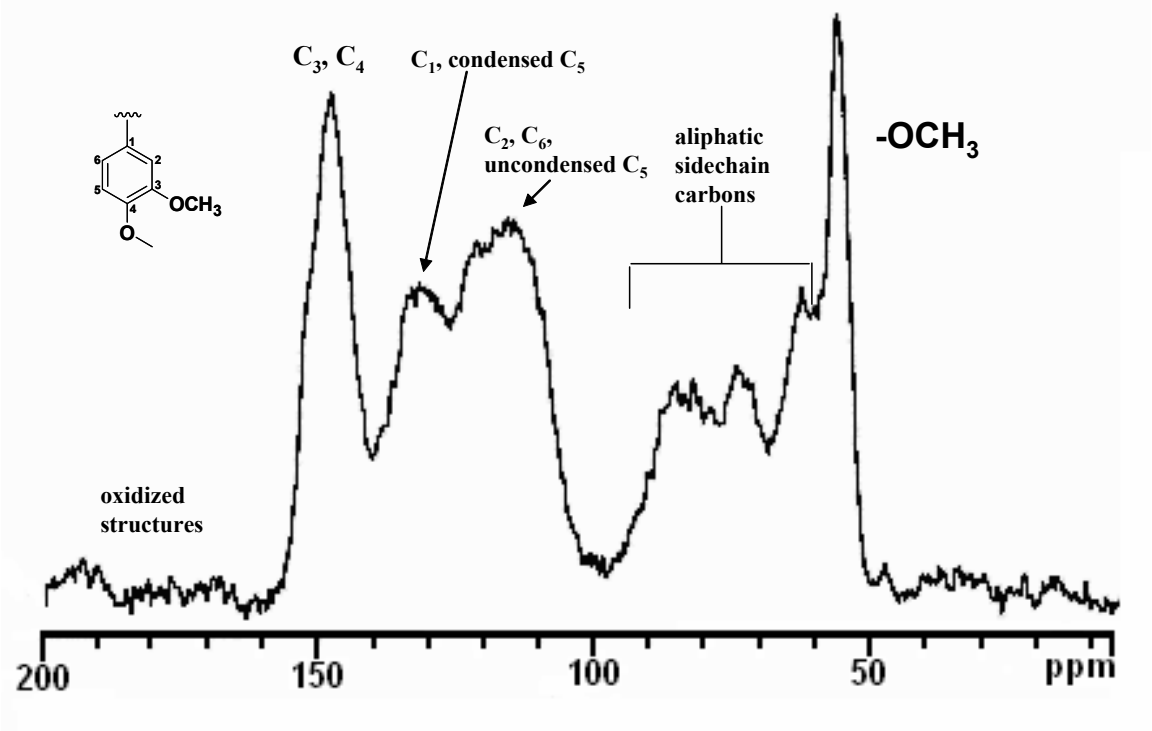

Figure 9.1 CP/MAS spectrum of Vibratory MWL.

Another problem with the CP/MAS experiment is spinning sidebands which can decrease the intensity of the centerband and overlap other areas of the spectrum. Increasing the spinning speed can reduce the overlap by pushing the sidebands outside the acquired spectrum thereby reducing overlap. However, an underestimation of the centerband still

occurs, and this is particularly prevalent for the aromatic carbons. At a 5 kHz spinning speed and a 200 MHz instrument, a 12% decrease in the intensity of the aromatic centerbands occurs in humic acid samples. [25]

9.1.2 DP/MAS (Direct Polarization/Magic Angle Spinning)

The DP/MAS or Bloch Decay experiment at high spinning speed involves direct irradiation of the carbons in the polymer and can avoid problems associated with cross polarization. The overall intensity of the spectrum is much lower but can provide a true carbon spectrum. (**Figure 9.2**) However since this experiment directly magnetizes the carbons in the spectrum, the delay time between pulses is dependent on the spin-lattice relaxation of the carbons instead of the protons. As a result, in order to obtain a quantitative spectrum the experimental time is much longer than CP/MAS. It may be possible to derive a relationship between the CP/MAS and DP/MAS spectra for lignin and use an estimation to apply the CP/MAS to analysis of sample sets.

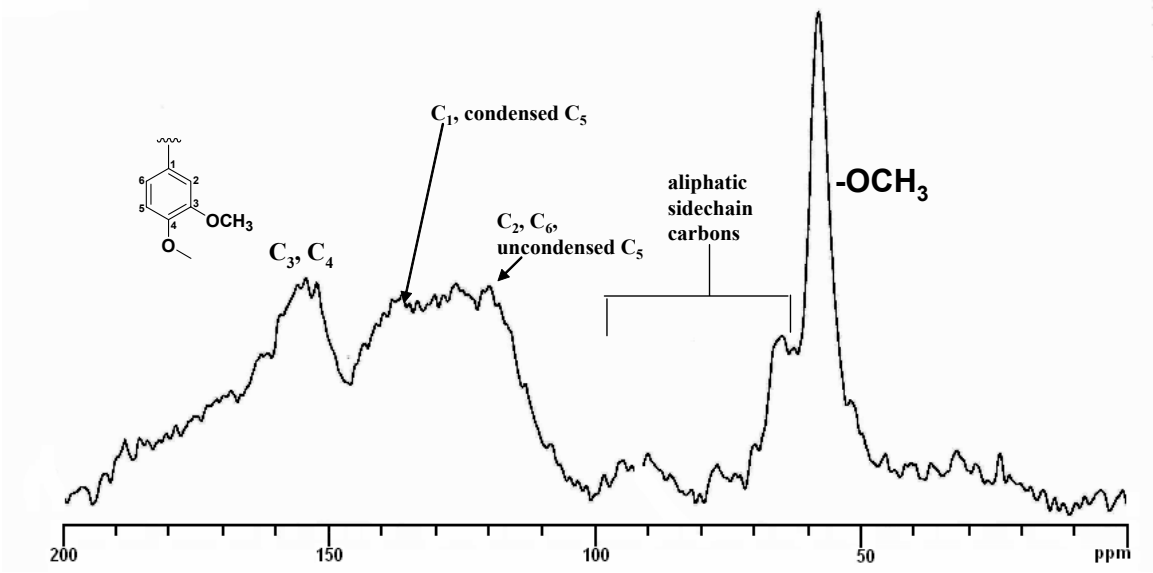

Figure 9.2 DP/MAS spectrum of Vibratory MWL.

9.1.3 Interrupted Decoupling (Dipolar Dephasing)

The quaternary carbons in the lignins were examined using the dipolar dephasing solid-state NMR technique. In this experiment the high-powered decoupler used to eliminate the carbon-proton interaction is gated off for a period of time prior to acquisition. As a result, spin-lattice relaxation can occur and the magnetization of the carbon is allowed to decompose. However, because this process occurs much more quickly if there is a directly attached proton, only the protonated carbon signals will decay and as result a spectrum containing quaternary carbons, which are exclusively located on the aromatic ring, can be obtained.

Guaiacyl lignins contain a methoxyl group at the C_3 position and a phenolic hydroxyl at the C_4 position, while the C_1 position contains the sidechain. Guaiacyl groups contain methoxyl groups at the C_3 position while syringyl groups are substituted at the C_3 and the C_5 positions. . C_3 will exhibit a chemical shift range of 147-153 ppm. The C_4 can exhibit various chemical shifts depending upon etherification and C_5 condensation. In general, the

C_4 for a guaiacyl lignin will lie in a range between 141-152 ppm. As a result the value for **Region A** (164-141 ppm) in **Figure 9.3** should be equivalent to 2 carbons per aromatic ring.

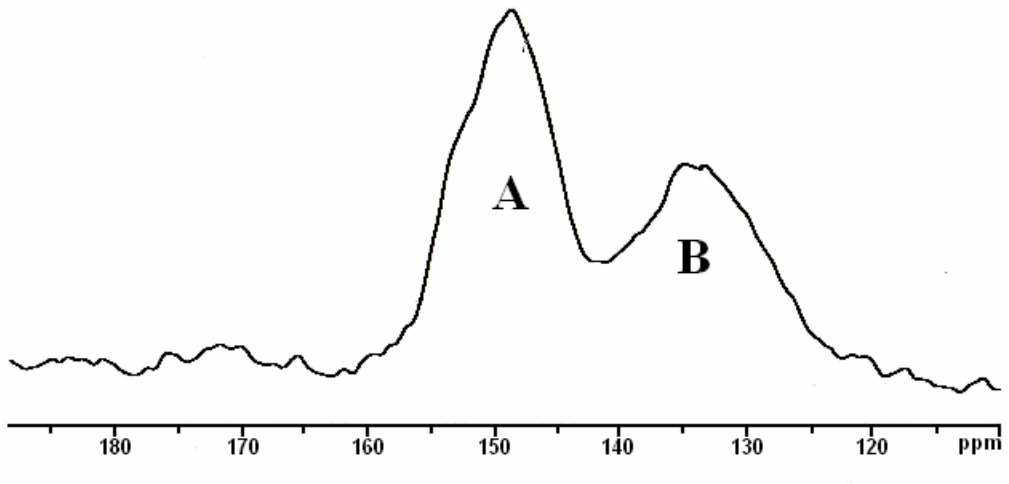

Figure 9.3 Dipolar dephasing spectrum of Vibratory MWL.

Condensed lignin structures are generally substituted at the C_5 or C_6 positions in lignin and will shift the resonance of the substituted carbon to 126 ppm. C_1 will center around 133 ppm. As a result, the integration of **Region A** and **Region B** will provide a ratio of the etherified and nonetherified aromatic protons, respectively. **Figure 9.3** shows the dipolar dephasing spectrum for **Vibratory MWL** and **Table 9.1** gives the degree of condensation data for the some of the lignins analyzed by this technique. The typical dipolar dephasing experiment is not entirely quantitative nonetheless is quite useful in comparing different lignin preparations with similar characteristics.

Table 9.1 Degree of condensation data for some lignin preparations as determined by dipolar dephasing experiment.

	Degree of Condensation per Aromatic Ring
Wiley Wood Meal	**0.30**
Vibratory MWL	**0.47**
Rotary Porcelain 6 Week MWL	**0.46**
Rotary Porcelain 6 Week REL	**0.32**

9.1.4 CH selection experiment

The CH selection experiment would isolates the methine carbons separate from the other carbon signals. Integration of the oxygenated aliphatic (90-57 ppm) and the condensed side chain carbon (~55-45 ppm) portions of the spectrum can yield additional information. Condensed sidechain carbons are predominately the C_β carbons in the β-5' (**VI**), β-β' (**IX**), and β-1' (**XII**) substructures. (**Figure 9.4**) β-1' has been shown in previous sections to be a very minor structural moiety and hence the majority of this integration likely can be attributed to the β-5' and β-β'. (**Tables 7.4** and **8.4**)

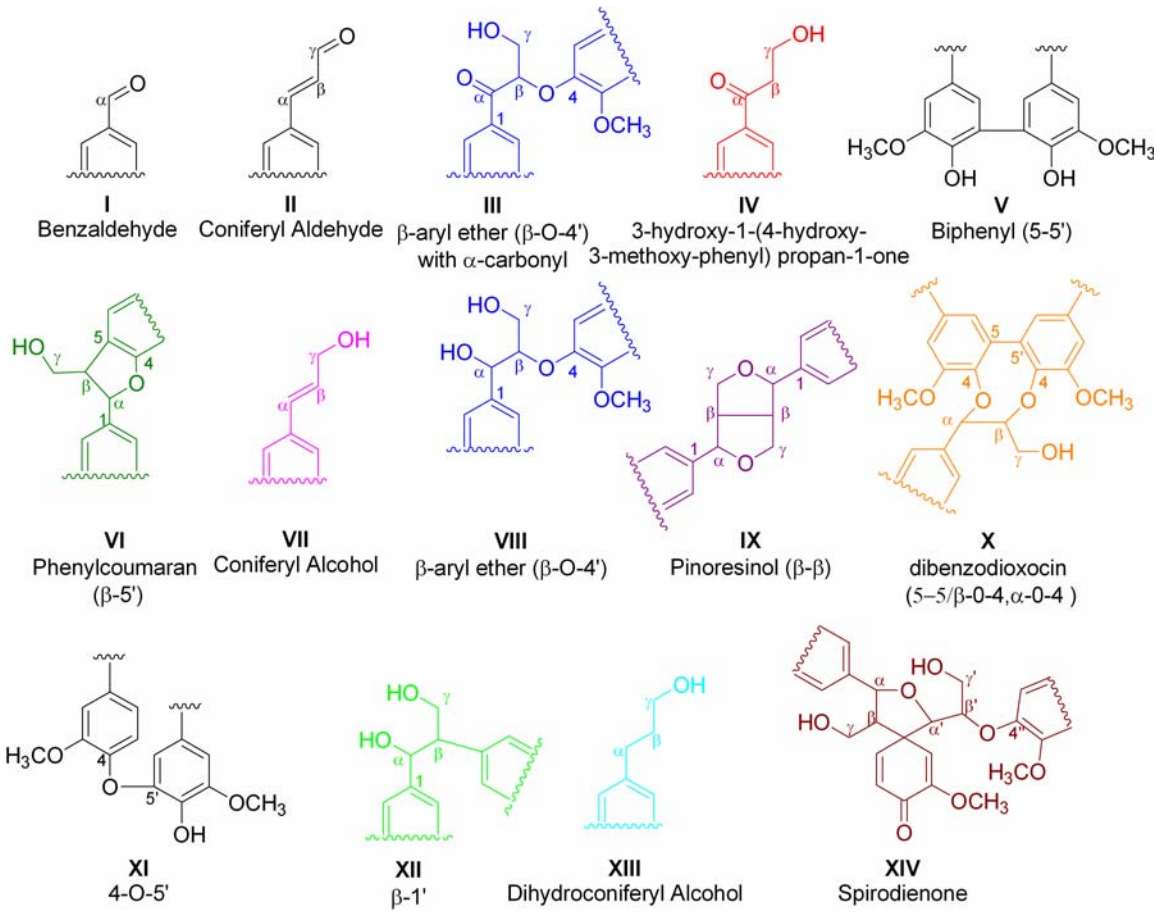

Figure 9.4 Substructures commonly found in the lignin polymer.

The region from 90-57 ppm contains the etherified (or oxygenated) sidechain carbons from most of interunit linkages shown in **Figure 9.4**. While the substructures (**VI**, **IX**, and **XII**) described above will exhibit signals in this region, they can be subtracted from the total integration based on the condensed carbon signals. Substructures **I**, **II**, **IV**, **V**, **VII**, **XI**, **XIII** do not exhibit signals in this region, and since the methylene carbons are edited out, the majority of the integration of this region will be from carbons etherified at the β-position. Specifically, we know that the β-O-4' with α-OH (**VIII**) is the predominant interunit linkage and it will contribute two carbons to this region. β-O-4' with α-carbonyl (**III**) is a minor substructure possibly produced during milling and the C_β will lie in this region.

Dibenzodioxocin (**X**) is etherified through both the α- and β-positions to form an eight-membered ring and also has two carbons that will lie in this region. Additionally, since the methylene carbons have been spectrally edited, it is easier to deconvolute the signals in this spectral region.

Minor substructures (**I**, **II**, **III**, **IV**) such as the sidechain carbonyls may be estimated simply by a total integration of the region from 200-190 ppm. The total substructures with unsaturated side chains, such as coniferyl alcohol (**VII**) and coniferaldehyde (**II**), may be estimated by integration of the aromatic region from the CH selection experiment. Integration of the region from 34-30 ppm of either the CP/MAS spectrum or CH_2 spectrum resulting from subtraction of the other spectra could also yield the total of dihydroconiferyl alcohol (**XIII**) carbons although the sensitivity likely is not high enough to make an accurate assessment. Substructures **V**, **XI**, and **XIV** are minor moieties in lignin and may be difficult to determine by solid-state NMR.

9.1.5 Comments on Experiments Using Chemagnetics 200 MHz Instrument

As can be seen from the CP/MAS spectrum of the **Vibratory REL** sample in **Figure 9.5**, paramagnetic ions have a detrimental impact on the solid-state NMR spectrum. This is well-documented, but confirms the presence of iron resulting from vibratory milling in the REL will have a detrimental effect on signal acquisition. [174] As a result, any lignin from milled wood or REL obtained by vibratory milling cannot be analyzed by solid-state NMR or for that matter by solution-state NMR.

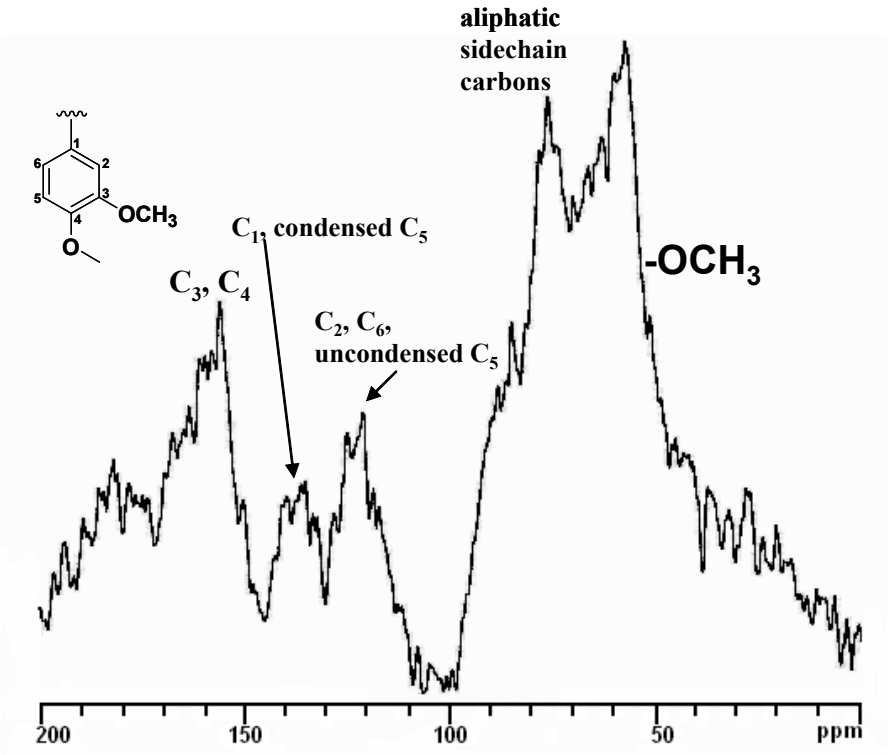

Figure 9.5 CP/MAS of Vibratory REL showing the effects of paramagnetic materials on the spectrum.

As a result, any comprehensive comparison of lignin in wood, MWL, CEL, and REL requires use of the rotary milled samples. Therefore the solid-state NMR study of lignin structure in these samples must be performed using the **Rotary Porcelain 6 Week** preparations.

The CH selection experiment is a complex experiment that has been recently developed at Iowa State University. [26] As a result it is not among the basic experiments that are provided with the spectrometer software. Upon Dr. White's suggestion, I sent **Wiley Wood**, **Rotary Porcelain 6 Week Wood**, **Rotary Porcelain 6 Week MWL**, and **Rotary Porcelain 6 Week REL** samples to their laboratory for analysis.

9.2 Solid-state NMR analysis of thermally treated kraft lignins [209]

This section is a presentation of the CP/MAS analysis of thermally treated kraft lignins performed at the NCSU Solid-State NMR laboratory. This work was done to assess the effects of heating rate and temperatures on the carbonization process. Lignin has a glass transition temperature (T_g) below the temperature required for carbonization and as a result the lignin must be thermostabilized. Results found that structural changes including crosslinking, side chain oxidation, and subsequent loss CO_2 occurred in all cases. Lower heating rates, at rates approaching 0.06 ^oC/min allowed the glass transition temperature to increase faster than the temperature thereby preventing thermal softening of the lignin.

Figure 9.6 shows the ^{13}C/CPMAS NMR spectra for a hardwood kraft lignin that has been oxidized to different temperatures at a heating rate of 0.6 ^oC/min. The methoxyl peak, centered at 57 ppm, drastically decreases with heating to higher temperatures, indicating that demethoxylation is a major reaction occurring in kraft lignin oxidation. The regions from 50-20 ppm and 90-57 ppm represent aliphatic C-C and aliphatic C-H moieties, respectively. It is anticipated that kraft lignins will contain both of these type structures and this is apparent from the CP/MAS spectrum of the pellets. However these structures disappear even at heating to lower temperatures, consistent with the oxidation reactions discussed in the paper. [209]

Oxidized lignins exhibit chemical shifts anywhere from 200-160 ppm depending upon the type of structural moieties present. The pellets contain spectral signals in the range of 180-170 ppm, indicative of carboxylic acid-type structures. Despite the fact that a high degree of oxidation is occurring, carbonyl and carboxylic acid structures persist in only modest amounts in the sample heated to 200 ^oC and very little in the lignin heated to 340 ^oC.

However, the region from 170-160 ppm, representing esters and anhydrides, increases in intensity throughout heating of the lignin. This indicates that oxidized lignin structures undergo fairly rapid crosslinking reactions involving formation of esters and anhydrides as well as probable decomposition resulting in the loss of CO_2 and H_2O. This is consistent with the decrease in C=O and the increase in anhydrides and esters as presented earlier in the XPS and FTIR data. [209]

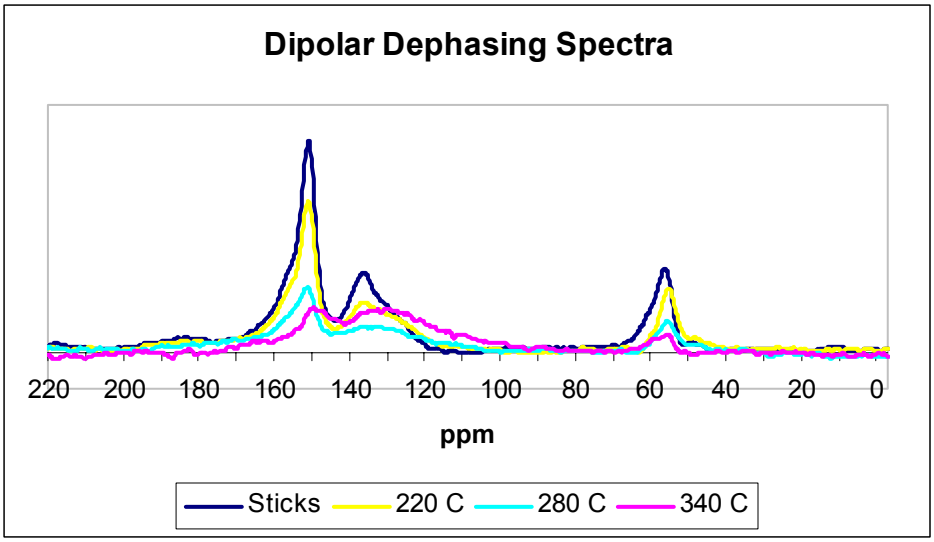

Figure 9.6 CP/MAS spectra of the unheated sticks and the lignin preparations heated to 220 °C, 280 °C, and 340 °C at a heating rate of 0.6 °C/min.

The aromatic carbons lie in the region from 160-103 ppm and can be divided into the aromatic C-O (160-141 ppm), the aromatic C-C (141-125 ppm), and the protonated aromatic regions (125-103 ppm). Lignin is built from phenylpropanoid precursors containing methoxyl groups at the C_3 position in the case of guaiacyl structures and the C_3 and C_5 positions in syringyl structures. The aromatic C-O region contains predominately etherified aromatic carbons, e.g. C_3 in guaiacyl structures, C_3 and C_5 in syringyl structures, and the

phenolic position (C_4) in guaiacyl structures. The C_4 in syringyl structures will be shifted upfield to 138-135 ppm. The peaks in this region rapidly decrease with heating to higher temperatures. This indicates that demethoxylation probably occurs primarily with the loss of formaldehyde over homolytic cleavage of the methoxyl C-O bond. In addition, β-aryl ethers present in the kraft lignin are likely to be highly degraded.

The region from 141-125 ppm contains aromatic C-C structures (C-C condensation linkages) in addition to the syringyl C_4 carbons. The shoulder at 138-135 ppm in the pellets disappears rapidly, indicating demethoxylation of syringyl structures. As is expected, the aromatic C-C structures already present in the lignin are stable and their proportion relative to the other aromatic regions in the kraft lignin increases significantly. The increase in C-C bonds from the XPS data is likely to be expressed in this region due to the reaction described in (5). [209]

The region from 125-103 ppm contains the protonated aromatic carbons and in the case of a kraft lignin the vinylic carbons shown in (4). [209] During oxidation these vinylic carbons will be rapidly oxidized and the signals should disappear. Additionally, some protonated carbons should be lost due to crosslinking reactions described in (5). [209] Signals in this region decrease somewhat with heating to 220 ^{o}C, possibly indicating oxidation of vinylic moieties. Further decrease of spectral intensity in this region upon heating of lignin to 340 ^{o}C may indicate the occurrence of aromatic C-C condensation reactions resulting in crosslinking of the aromatic rings in the lignin polymer.

9.3 Quantitative experiments performed at Iowa State University

The CH selection experiment involves suppression of the methylene carbons by multiple quantum coherence dephasing. [26] The spectrum will still contain quaternary and methyl carbons, both of which are easily removed. The same pulse sequence with an added dipolar dephasing interval will produce a spectrum with only quaternary carbons. Similarly a T_{1C} filter can be added to remove the signals deriving from the methyl carbons. Subtraction of these spectra from the CH selection spectra will result in only methine signals being present.

Since these experiments are being performed on the spectrometer at Iowa State University, it was decided that it would be preferable to perform all the experiments on the same spectrometer. Rather than using the CP/MAS experiment with its drawbacks as described above, they instead employ the CP/TOSS (TOtal Sideband Suppression) experiment. This is a CP/MAS experiment with the TOSS pulse sequence applied prior to the start of acquisition to suppress sidebands. It is not entirely quantitative because of the large sidebands of the sp^2 carbons cannot be totally added back to the centerbands. A correction factor can be acquired by comparison of the CP/TOSS and DP/MAS spectra to provide essentially a quantitative spectrum.

Subtraction of the dipolar dephased and CH only spectra from the CP/TOSS spectrum can then provide a spectrum with only the CH_2 and CH_3 signals present. As can be seen in **Figure 2.37**, with the exception of the methoxyl peak, the contribution from methyl groups in lignin is minor and as a result this spectrum will contain predominately methylene carbons.

9.4 Two-dimensional HETCOR

The laboratory at Iowa State University also employs HETCOR experiments in which it is hoped will provide high resolution two-dimensional spectra of lignin comparable to the solution-state HMQC experiment. Additionally, application of variable spin diffusion times can detect two and three bond correlations, in essence producing a spectrum similar to that of the solution-state HMBC experiment.

9.5 Final notes on Solid-State NMR

The experiments discussed in **Section 9.3** have been performed and are currently in the data analysis stages. Because this is a collaboration, time schedules do not always coincide sometimes resulting in a delay in the publication of data. Therefore, time permitting the data from these experiments will be included in this dissertation. In any case, this data will be published in peer reviewed journals and if it does not appear in this dissertation, it can be considered supplementary data. My co-chairs, Dr. Kadla and Dr. Jameel, are in agreement that the data provided in the prior sections is sufficient to fulfill the requirements for graduation.

It is planned that the data acquired in **Section 9.3** will be summarized in at least one publication and that the data from **Section 9.4** will also be a standalone paper. Provided that these experiments are deemed successful, these experiments are intended to be applied to a solid wood exhibiting a natural mutation, a transgenic wood sample, and the oxidized kraft lignin samples described in **Section 9.2**.

10. Conclusions

The modified DFRC method is a simple degradative procedure that can be performed to analyze the aryl ether content of low molecular weight lignin materials. If it assumed that the relative inefficiency should be similar based upon similar molecular weights, then a comparison of different lignin preparations can be performed.

Two-dimensional NMR has shown that DFRC does not completely degrade the β-O-4' linkages in MWL while thioacidolysis completely degrades these structures.

As a result, for quantitative analysis of the aryl ether content, thioacidolysis is the preferred degradative method. In addition the modified thioacidolysis method can be used to assess the free phenolic β-O-4' content (Unit A).

It is likely that the differences in total molar yield between the degradative techniques are associated with the mechanism by which β-O-4' cleavage is achieved. Specifically, in a complex polymer such as lignin, it may be difficult to achieve the orientation required for zinc cleavage due to a lack of molecular mobility.

The decrease in yield for the DFRC method is greatest at the highest molecular weights, indicating the rigidity of the polymer or accessibility may have an impact on its efficiency.

NMR is by far the most effective technique for analyzing soluble lignin samples. Quantitative ^{13}C NMR can be used to estimate the interunit linkages in lignin. Two-dimensional NMR techniques can be used to analyze lignins to determine the structural moieties present and identify minor structures.

Initial inspection of the MWL from different milling techniques suggests that the use of the standard Bjorkman technique (1 week rotary milling followed by 2 days vibratory milling) is better than a long rotary milling method. The rotary milling showed a decrease in β-O-4' content and an increase in oxidized sidechain structures. Dibenzodioxocin structures also showed a decrease.

While it requires further investigation, these results suggest that a highly efficient milling is beneficial. The new planetary mill should therefore be utilized to make this determination. It may be that a quick reduction of particle size is preferrable, however it may be found that a slower, more efficient route to milled wood may be obtained. In either case, it may give a comparable or an improved MWL as compared to the milled wood.

Although differences in DFRC total molar yield initially indicated a dramatic difference between **Vibratory MWL** and **Vibratory (Dry) MWL**, NMR analysis showed little difference. This indicates that milling in toluene may not be necessary.

All MWL preparations had similar biphenyl content, indicating that condensation at the 5-position on the aromatic rings is probably not occurring to a significant extent.

Initial examination by solid-state NMR indicated that the MWL had a higher degree of condensation than either the wood or the REL. This likely suggests that the MWL does in fact originate to a significant extent from the middle lamella. It also suggests that the REL is insoluble likely due to molecular weight and less because it has a structure significantly different from MWL.

MWL and CEL are similar in structure with the CEL being moderately higher in β-O-4' content and lower in condensed structures. This is likely due to the morphological origin of each of the samples, as the CEL is likely predominately from the secondary wall due to its association with carbohydrates. It is therefore not a mistake to combine these samples to increase "MWL yield" but likely alters the ratio of middle lamella and secondary wall contributions.

Treatment of REL to mostly remove carbohydrates, followed by dioxane extraction would likely isolate an additional amount of lignin that could further increase this yield. It is paramount to move towards analysis of lignin structure, therefore this type of suggestion may be counterproductive.

The newly described method for dissolution of cell walls is highly dependent upon the degree of milling in order to achieve complete solubilization. Contrary to the reports by Ralph et al., our lignins were difficult to solubilize, indicating that depolymerization greatly effects this procedure. Therefore it is questionable how useful this method may become. It

is definitely a step towards analysis of the whole lignin and therefore alone has made a positive impact.

It is time to look more closely at solid-state NMR analysis of lignin structure and our group is already quickly moving in this direction. We are collaborating with a group of NMR specialists at Iowa State University who are also interested in structural characterization of materials. Through different experiments they have recently devised, we will be able to similar determinations described in the NMR results on Wiley Wood and hopefully whole wood without interference from carbohydrates.

11. Future Work

In order to make a comparison of milling techniques, it is necessary to include the planetary mill as part of the study. Specifically, a MWL with a total yield of ~20 % should be prepared from wood ground in this mill. A comparison of the MWL with the MWLs described above would validate the use of this new mill.

Since wood can be ground much more quickly in this mill, optimization of the milling technique should be performed. It should be determined the precise amount of time required to reduce the particle size of the milled wood in order to obtain dissolution. From this point, the carbohydrates can be degraded in order to isolate the whole lignin from wood.

It would be interesting to study the correlation between the radical formation and structural changes in MWL. The radical content in wood can be measured by electron spin resonance (ESR) spectroscopy while the MWL structure can be analyzed by NMR.

Analysis of the effect of temperature on milling can also be performed. Contradictory reports have previously been given on the effect of temperature and the techniques used here could provide an unambiguous comparison of low and room temperature milling.

A systematic study of the impact of milling versus the dissolution of whole wood lignin using the DMSO/N-methylimidazole method should be performed. Specifically, how does milling effect solubility and what type of structural changes occur over various time

periods. Included in this should be particle size analysis (and also above) to determine the correlation to solubility.

Although milling and subsequent solvent extraction provides a highly utilizable lignin, the attempts to unequivocably determine lignin structure should be migrating toward analysis in solid wood. To this end, we have performed an analysis of Wiley Wood, milled wood, MWL, and REL using various solid-state techniques. These experiments developed by Drs. Jingdong Mao and Klaus Schmidt-Rohr at the Dept. of Chemistry, Iowa State University, allow us to perform a solid-state DEPT analysis of the lignins. As a result we should be able to obtain very close approximation of different interunit linkages in the lignins as well as estimate a more precise degree of condensation. Analysis of the data is currently being performed.

12. Literature Cited

1. Sarkanen, K.V. and C.H. Ludwig, *Definition and Nomenclature*, in *Lignins : occurrence, formation, structure and reactions*, K.V. Sarkanen and C.H. Ludwig, Editors. 1971, Wiley-Interscience: New York. p. 1-18.

2. Higuchi, T., *Biosynthesis of Lignin*. Biosynthesis and Biodegradation of Wood Components, ed. T. Higuchi. 1985, New York, NY: Academic Press. p. 141-160.

3. Terashima, N. and K. Fukushima, *Biogenesis and Structure of Macromolecular Lignin in the Cell Wall of Tree Xylem as Studied by Microautoradiography*, in *Plant Cell Wall Polymers, Biogenesis and Biodegradation*, N.G. Lewis and M.G. Paice, Editors. 1989, American Chemical Society: Washington, D.C. p. 160-181.

4. Terashima, N., et al., *Forage cell wall structure and digestibility*, ed. H.G. Jung. 1993, Madison, Wisc.: American Society of Agronomy Inc. : Crop Science Society of America Inc. : Soil Science Society of America Inc. p. 247-270.

5. Sederoff, R.R. and H.M. Chang, *Lignin Biosynthesis*, in *Wood Structure and Composition*, M. Lewin and I.S. Goldstein, Editors. 1991, Marcel Dekker: New York, NY. p. 263-286.

6. Smook, G.A., *Handbook for pulp and paper technologists*, ed. M.J. Kocurek. 1982, Atlanta, GA: TAPPI.

7. Fengel, D., *Ideas on the Ultrastructural Organization of the Cell Wall Components.* Journal of Polymer Science: Part C, 1971. 36: p. 383-392.

8. Yamamoto, E., G.H. Bokelman, and N.G. Lewis, *Phenylpropanoid Metabolism in Cell Walls*, in *Plant Cell Wall Polymers, Biogenesis and Biodegradation*, N.G. Lewis and M.G. Paice, Editors. 1989, American Chemical Society: Washington, D.C. p. 68-88.

9. Bjorkman, A., *Studies on finely divided wood. Part 5. The effect of milling.* Svensk Papperstidning-Nordisk Cellulosa, 1957. 60(9): p. 329-335.

10. Hon, D.N.S., *Mechanochemical Reactions of Lignocellulosic Materials.* Journal of Applied Polymer Science, 1983. 37: p. 461-481.

11. Assarsson, A., B. Linderg, and O. Theander, *Studies on mechanically degraded cellulose.* Acta Chemica Scandinavica, 1959. 13: p. 1231-1234.

12. Rex, R.W., *Electron Paramagnetic Resonance Studies of Stable Free Radicals in Lignins and Humic Acids.* Nature, 1960. 188: p. 1185-1186.

13. Lai, Y.Z. and K.V. Sarkanen, *Isolation and structural studies*, in *Lignins : occurrence, formation, structure and reactions*, K.V. Sarkanen and C.H. Ludwig, Editors. 1971, Wiley-Interscience: New York. p. 165-240.

14. Karhunen, P., et al., *Dibenzodioxocins - a Novel Type of Linkage in Softwood Lignins.* Tetrahedron Letters, 1995. 36(1): p. 169-170.

15. Ralph, J., J.P. Peng, and F.C. Lu, *Isochroman structures in lignin: a new beta-1 pathway.* Tetrahedron Letters, 1998. 39(28): p. 4963-4964.

16. Zhang, L.M. and G. Gellerstedt, *NMR observation of a new lignin structure, a spiro-dienone.* Chemical Communications, 2001(24): p. 2744-2745.

17. Ralph, J., et al., *Elucidation of new structures in lignins of CAD- and COMT-deficient plants by NMR.* Phytochemistry, 2001. 57(6): p. 993-1003.

18. Hardell, H.-L., et al., *Variations in lignin structure in defined morphological parts of spruce.* Svensk Papperstidning-Nordisk Cellulosa, 1980. 83(2): p. 44-49.

19. Lapierre, C., J.Y. Lallemand, and B. Monties, *Evidence of Poplar Lignin Heterogeneity by Combination of ^{13}C and ^{1}H NMR Spectroscopy.* Holzforschung, 1982. 36(6): p. 275-282.

20. Hori, K. and G. Meshitsuka, *Structural Heterogeneity of Hardwood Lignin: Characteristics of End-Wise Lignin Fraction*, in *Lignin and lignan biosynthesis*, N.G. Lewis and S. Sarkanen, Editors. 1996, American Chemical Society: Washington, DC. p. 173-185.

21. Lu, F.C. and J. Ralph, *Non-degradative dissolution and acetylation of plant cell walls: High-resolution solution-state NMR.* Plant Journal, 2003. 35: p. 535-544.

22. Lu, F.C. and J. Ralph. *Non-degradative dissolution and acetylation of plant cell walls; High-resolution solution-state NMR*. in *12th International Symposium on Wood and Pulping Chemistry*. 2003. Yokohama, Japan.

23. Mao, J.D., et al., *Quantitative Characterization of Humic Substances by Solid-State Carbon-13 Nuclear Magnetic Resonance.* Soil Science Society of America Journal, 2000. 64: p. 873-884.

24. Mao, J.D., B. Xing, and K. Schmidt-Rohr, *New structural information on a humic acid from two-dimensional H-1-C-13 correlation solid-state nuclear magnetic resonance.* Environmental Science and Technology, 2001. 35(10): p. 1928-1934.

25. Mao, J.D., et al., *Suitability of different C-13 solid-state NMR techniques in the characterization of humic acids.* International Journal of Environmental Analytical Chemistry, 2002. 82(4): p. 183-196.

26. Schmidt-Rohr, K. and J.D. Mao, *Efficient CH-group selection and identification in C-13 solid-state NMR by dipolar DEPT and H-1 chemical-shift filtering.* Journal of the American Chemical Society, 2002. 124(46): p. 13938-13948.

27. Mao, J.D. and K. Schmidt-Rohr, *Recoupled long-range C-H dipolar dephasing in solid-state NMR, and its use for spectral selection of fused aromatic rings.* Journal of Magnetic Resonance, 2003. 162(1): p. 217-277.

28. Payen, A., Comptes Rendus De L Academie Des Sciences Serie Iii-Sciences De La Vie-Life Sciences, 1838. 7: p. 1052.

29. Sjostrom, E., *Wood chemistry: fundamentals and applications*. 1981, New York, NY: Academic Press.

30. Prade, R.A., *Xylanases: From biology to biotechnology.* Biotechnology and Genetic Engineering Reviews, Vol 13, 1996. 13: p. 101-131.

31. Monties, B., *Lignins*. Methods in Plant Biochemistry, ed. P.M. Dey and J.B. Harborne. 1985, San Diego, CA: Academic Press. p. 284.

32. Horton, R.H., et al., *Photosynthesis*, in *Principles of Biochemistry*. 2002, Prentice Hall: Upper Saddle River, NJ. p. 462-487.

33. Ye, Z.H., et al., *An Alternative Methylation Pathway in Lignin Biosynthesis in Zinnia.* The Plant Cell, 1994. 6: p. 1427-1439.

34. Hu, W.J., et al., *Repression of lignin biosynthesis promotes cellulose accumulation and growth in transgenic trees.* Nature Biotechnology, 1999. 17(8): p. 808-812.

35. Osakabe, K., et al., *Coniferyl aldehyde 5-hydroxylation and methylation direct syringyl lignin biosynthesis in angiosperms.* Proceedings of the National Academy of Sciences of the United States of America, 1999. 96(16): p. 8955-8960.

36. Li, L., et al., *5-Hydroxyconiferyl aldehyde modulates enzymatic methylation for syringyl monolignol formation, a new view of monolignol biosynthesis in angiosperms.* Journal of Biological Chemistry, 2000. 275(9): p. 6537-6545.

37. Li, L., et al., *The last step of syringyl monolignol biosynthesis in angiosperms is regulated by a novel gene encoding sinapyl alcohol dehydrogenase.* Plant Cell, 2001. 13: p. 1567-1585.

38. Ralph, J., et al., *Abnormal lignin in a loblolly pine mutant.* Science, 1997. 277: p. 235-239.

39. Sederoff, R.R., et al., *Unexpected variation in lignin.* Current Opinion in Plant Biology, 1999. 2(2): p. 145-152.

40. Boudet, A.-M., *Lignins and lignification: Selected issues.* Plant Physiology and Biochemistry, 2000. 38(1/2): p. 81-96.

41. Douglas, C.J., *Phenylpropanoid Metabolism and Lignin Biosynthesis: From Weeds to Trees.* Cell Biology, 1996. 1(6): p. 171-178.

42. Herrmann, K.M., *The Shikimate Pathway: Early Steps in the Biosynthesis of Aromatic Compounds.* The Plant Cell, 1995. 7: p. 907-919.

43. *KEGG (Kyoto Encyclopedia of Genes and Genomes) Database.* http://www.genome.ad.jp/kegg/. 2001, Bioinformatics Center, Institute for Chemical Research.

44. Brown, S.A. and A.C. Neish, *Shikimic acid as a precursor in lignin biosynthesis.* Nature, 1955. 175: p. 688-689.

45. Whetten, R.W. and R.R. Sederoff, *Lignin Biosynthesis.* The Plant Cell, 1995. 7: p. 1001-1013.

46. Gross, G., *Biosynthesis and metabolism of phenolic acids and monolignols.* Biosynthesis and Biodegradation of Wood Components, ed. T. Higuchi. 1985, New York, NY: Academic Press. p. 229-271.

47. Sarkanen, K.V., *Precursors and their Polymerization*, in *Lignins : occurrence, formation, structure and reactions*, K.V. Sarkanen and C.H. Ludwig, Editors. 1971, Wiley-Interscience: New York. p. 95-163.

48. Erdtmann, H., *Oversikt over naturprodukter av diaryl-butan-typ.* Svensk Papperstidning-Nordisk Cellulosa, 1939. 42: p. 115-122.

49. Freudenberg, K., *Lignin- Its constitution and formation from p-hydroxycinnnamyl alcohols.* Science, 1965. 148(3670): p. 595-600.

50. Sarkanen, K.V. and H.L. Hergert, *Classification and Distribution*, in *Lignins : occurrence, formation, structure and reactions*, K.V. Sarkanen and C.H. Ludwig, Editors. 1971, Wiley-Interscience: New York. p. 43-94.

51. Freudenberg, K., *Entwerf eines konstitutionsschemas fer das lignin der fichte.* Holzforschung, 1964. 18: p. 3-9.

52. Sakakibara, A., *A Structural Model of Softwood Lignin.* Wood Science and Technology, 1980. 14(2): p. 89-100.

53. Glasser, W.G. and H.R. Glasser, *Evaluation of lignin's chemical structure by experimental and computer simulation techniques.* Paperi ja Puu, 1981. 63: p. 71-83.

54. Fergus, B.J., et al., *The distribution of lignin in sprucewood as determined by ultraviolet microscopy.* Wood Science and Technology, 1969. 3: p. 117-138.

55. Brauns, F.E., *Native lignin I. Its isolation and methylation.* Journal of the American Chemical Society, 1939. 61(8): p. 2120-2127.

56. Schubert, W.J. and F.F. Nord, *Investigations on Lignin and Lignification. I. Studies on Softwood Lignin.* Journal of the American Chemical Society, 1950. 72(2): p. 977-981.

57. Nord, F.F. and W.J. Schubert, *Enzymatic Studies on Cellulose, Lignin, and the Mechanism of Lignification.* Holzforschung, 1951. 5: p. 1-9.

58. Brauns, F.E., *The Chemistry of Lignin*. 1952, New York, NY: Academic Press. p. 688.

59. Pew, J.C., *Properties of Powdered Wood and Isolation of Lignin by Cellulytic Enzymes.* Tappi, 1957. 40(7): p. 553-558.

60. Bjorkman, A., *Isolation of lignin from finely divided wood with neutral solvents.* Nature, 1954. 174(4440): p. 1057-1058.

61. Bjorkman, A., *Studies on finely divided wood. Part I. Extraction of lignin with neutral solvents.* Svensk Papperstidning-Nordisk Cellulosa, 1956. 59(13): p. 477-485.

62. Hermans, P.H. and A. Weidinger, *On the Recrystallization of Amorphous Cellulose.* Journal of the American Chemical Society, 1947. 68(12): p. 2547.

63. Glasser, W.G. and G. Sandermann, *The Catalytic Effect of Lignin Radicals and Chemical Reactions.* Holzforschung, 1970. 24: p. 73-76.

64. Lee, Z.Z., et al., *Characteristics of Milled Wood Lignins Isolated with Different Milling Times.* Mokuzai Gakkaishi, 1981. 27(9): p. 671-677.

65. Glasser, W.G. and C.A. Barnett, *The Structure of Lignin in Pulps II. A comparative evaluation of isolation methods.* Holzforschung, 1979. 33: p. 78-86.

66. Brownell, H.H., *Isolation of milled wood lignin and lignin-carbohydrate complex. Part II of a study on the lignin-carbohydrate bond.* Tappi, 1965. 48(9): p. 513-519.

67. Brownell, H.H., *Improved Ball Milling in the Isolation of Milled Wood Lignin.* Tappi, 1968. 51(7): p. 298-300.

68. Whiting, P. and D.A.I. Goring, *The morphological origin of milled wood lignin.* Svensk Papperstidning-Nordisk Cellulosa, 1981. 84(15): p. R120-R122.

69. Maurer, A. and D. Fengel, *On the Origin of Milled Wood Lignin Part 1. The Influence of Ball-Milling on the Ultrastructure of Wood Cell Walls and the Solubility of Lignin.* Holzforschung, 1992. 46(5): p. 417-423.

70. Lapierre, C., *C. Lapierre's milled wood lignin isolation method*.

71. Bjorkman, A. and B. Person, *Studies on finely divided wood. Part 2. The properties of lignins extracted with neutral solvents from softwoods and hardwoods.* Svensk Papperstidning-Nordisk Cellulosa, 1957. 60(5): p. 158-169.

72. Pew, J.C., *Fine Grinding, Enzyme Digestion, and the Lignin-Cellulose Bond in Wood.* Tappi, 1962. 45(3): p. 247-256.

73. Chang, H.M., et al., *Comparative studies on cellulolytic enzyme lignin and milled wood lignin of sweetgum and spruce.* Holzforschung, 1975. 29(5): p. 153-159.

74. Kleinert, T.N. and J.R. Morton, *Electron Spin Resonance in Wood-grinding and Wood-pulping.* Nature, 1962. 196: p. 334-336.

75. Ranby, B., et al., *The Free Radical Content in Wood and Lignins.* Acta Chemica Scandinavica, 1969. 23: p. 3257-3259.

76. Steelink, C., *Stable free radicals in lignin and lignin oxidation products.* Advances in Chemistry Series, 1966. 59: p. 51-63.

77. Hon, D.N.S., *ESR studies of the photodegradation of cellulose graft-copolymers.* Journal of Applied Polymer Science, 1979. 23: p. 1487.

78. Steenken, S. and P. O'Neill, *Oxidative demethoxylation of methoxylated phenols and hydroxybenzoic acids by OH radical- in situ electron-spin resonance, conductometric pulse-radiolysis, and product analysis study.* Journal of Physical Chemistry, 1977. 81: p. 505.

79. Zhang, L.M. and G. Gellerstedt. *Detection and Determination of Carbonyls and Quinones by Modern NMR Techniques*. in *10th International Symposium on Wood and Pulping Chemistry*. 1999. Yokohama, Japan.

80. Larsson, S. and G.E. Miksche, *Gas chromatographic analysis of lignin oxidation products. Evidence of new linking principle of phenylpropane units.* Acta Chemica Scandinavica, 1969. 23: p. 917.

81. Bjorkman, A., *Studies on finely divided wood. Part 3. Extraction of lignin-carbohydrate complexes with neutral solvents.* Svensk Papperstidning-Nordisk Cellulosa, 1957. 60(7): p. 243-251.

82. Lu, F.C. and J. Ralph, *Derivatization followed by reductive cleavage (DFRC method), a new method for lignin analysis: Protocol for analysis of DFRC monomers.* Journal of Agricultural and Food Chemistry, 1997. 45: p. 2590-2592.

83. Lu, F.C. and J. Ralph, *DFRC method for lignin analysis. 1. New method for beta aryl ether cleavage: Lignin model studies.* Journal of Agricultural and Food Chemistry, 1997. 45: p. 4655-4660.

84. Lu, F.C. and J. Ralph, *The DFRC method for lignin analysis. 2. Monomers from isolated lignins.* Journal of Agricultural and Food Chemistry, 1998. 46: p. 547-552.

85. Lu, F.C. and J. Ralph, *The DFRC method for lignin analysis. Part 3. NMR studies.* Journal of Wood Chemistry and Technology, 1998. 18: p. 219-233.

86. Peng, J.P., F.C. Lu, and J. Ralph, *The DFRC method for lignin analysis. 4. Lignin dimers isolated from DFRC-degraded loblolly pine wood.* Journal of Agricultural and Food Chemistry, 1998. 46(2): p. 553-560.

87. Peng, J.P., F.C. Lu, and J. Ralph, *The DFRC method for lignin analysis - Part 5 - Isochroman lignin trimers from DFRC-degraded Pinus taeda.* Phytochemistry, 1999. 50(4): p. 659-666.

88. Ikeda, T., et al., *Studies on the effect of ball milling on lignin structure using a modified DFRC method.* Journal of Agricultural and Food Chemistry, 2002. 50(1): p. 129-135.

89. Tohmura, S. and D.S. Argyropoulos, *Determination of arylglycerol-beta-aryl ethers and other linkages in lignins using DFRC/P-31 NMR.* Journal of Agricultural and Food Chemistry, 2001. 49(2): p. 536-542.

90. Argyropoulos, D.S., et al., *Abundance and reactivity of dibenzodioxocins in softwood lignin.* Journal of Agricultural and Food Chemistry, 2002. 50(4): p. 658-666.

91. Holtman, K.M., et al., *Elucidation of lignin structure through degradative methods: Comparison of modified DFRC and thioacidolysis.* Journal of Agricultural and Food Chemistry, 2003. 51(12): p. 3535-3540.

92. Lundquist, K., *Acidolysis*, in *Methods in lignin chemistry*, S.Y. Lin and C.W. Dence, Editors. 1992, Springer-Verlag: Berlin ; New York. p. 289-299.

93. Lundquist, K., *Low-molecular weight lignin hydrolysis products.* Applied Polymer Symposium, 1976. 28: p. 1393-1407.

94. Ede, R.M., et al., *A 2D NMR investigation of the heterogeneity of distribution of diarylpropane structures in extracted Pinus radiata lignins.* Holzforschung, 1996. 50(2): p. 161-164.

95. Lapierre, C., B. Monties, and C. Rolando, *Preparative Thioacidolysis of Spruce Lignin: Isolation and Identification of Main Monomeric Products.* Holzforschung, 1986. 40(1): p. 47-50.

96. Lapierre, C., B. Monties, and C. Rolando, *Thioacidolysis of Lignin - Comparison with Acidolysis.* Journal of Wood Chemistry and Technology, 1985. 5(2): p. 277-292.

97. Rolando, C., B. Monties, and C. Lapierre, *Thioacidolysis*, in *Methods in lignin chemistry*, S.Y. Lin and C.W. Dence, Editors. 1992, Springer-Verlag: Berlin ; New York. p. 334-349.

98. Lapierre, C., et al., *Thioacidolysis of Spruce Lignin - GC-MS Analysis of the Main Dimers Recovered After Raney-Nickel Desulfuration.* Holzforschung, 1991. 45(1): p. 61-68.

99. Onnerud, H., M. Palmblad, and G. Gellerstedt, *Investigation of lignin oligomers using electrospray ionisation mass spectrometry.* Holzforschung, 2003. 57(1): p. 37-43.

100. Lapierre, C. and C. Rolando, *Thioacidolyses of Pre-Methylated Lignin Samples from Pine Compression and Poplar Woods.* Holzforschung, 1988. 42(1): p. 1-4.

101. Freudenberg, K., *Uber lignin.* Angew Chemie, 1939. 52: p. 362-363.

102. Leopold, B., *Aromatic Keto-Polyethers and Hydroxy-Polyethers as Lignin Models .3.* Acta Chemica Scandinavica, 1950. 4(10): p. 1523-1537.

103. Marton, J., *Reactions in Alkaline Pulping*, in *Lignins : occurrence, formation, structure and reactions*, K.V. Sarkanen and C.H. Ludwig, Editors. 1971, Wiley-Interscience: New York. p. 639-694.

104. Leopold, B. and I.L. Marmstrom, *Studies on lignin. IV. Investigation on the nitrobenzene oxidation products of lignin from different woods by paper partition chromatography.* Acta Chemica Scandinavica, 1952. 6: p. 49-54.

105. Chang, H.M. and G.G. Allan, *Oxidation*, in *Lignins : occurrence, formation, structure and reactions*, K.V. Sarkanen and C.H. Ludwig, Editors. 1971, Wiley-Interscience: New York. p. 433-485.

106. Schultz, T.P. and M.C. Templeton, *Proposed mechanism for the nitrobenzene oxidation of lignin.* Holzforschung, 1986. 40: p. 93-97.

107. Leopold, B. and I.L. Marmstrom, *Nitrobenzene oxidation of model compounds of the lignin type.* Acta Chemica Scandinavica, 1951. 5: p. 936-940.

108. von Wacek, A. and K. Kratzl, *Constitution of the side chains of lignin.* Journal of Polymer Science, 1948. 3(4): p. 539-548.

109. Chen, C.-L., *Nitrobenzene and cupric oxide oxidation*, in *Methods in lignin chemistry*, S.Y. Lin and C.W. Dence, Editors. 1992, Springer-Verlag: Berlin ; New York. p. 301-321.

110. Freudenberg, K., et al., *Zur Kenntnis des Lignins (15. Mitteil.).* Ber Dtsch Chem Ges, 1936. 69: p. 1415-1425.

111. Gellerstedt, G., *Chemical Degradation Methods: Permanganate Oxidation*, in *Methods in lignin chemistry*, S.Y. Lin and C.W. Dence, Editors. 1992, Springer-Verlag: Berlin ; New York. p. 322-333.

112. Freudenberg, K. and A.C. Neish, *Constitution and Biosynthesis of Lignin*, ed. A. Kleinzeller, G.F. Springer, and H.G. Wittman. 1968, New York, NY: Springer-Verlag. p. 78-82.

113. Larsson, S. and G. Miksche, *Gas chromatographic analysis of lignin oxidation products. The diphenyl ether linkage in lignin.* Acta Chemica Scandinavica, 1967. 21: p. 1970-1971.

114. Holtman, K.M. and J.F. Kadla, *A solution-state NMR study of the similarities between MWL and CEL.* Journal of Agricultural and Food Chemistry, under review.

115. Gellerstedt, G. and E. Lindfors, *Structural changes in lignin during kraft pulping.* Holzforschung, 1984. 38: p. 151-158.

116. Gellerstedt, G. and R.A. Northey, *Analysis of Birch Wood Lignin by Oxidative Degradation.* Wood Science and Technology, 1989. 23(1): p. 75-83.

117. Morohoshi, N. and W.G. Glasser, *The structure of lignins in pulps. Part 4. Comparative evaluation of five lignin depolymerization reactions.* Journal of Wood Science and Technology, 1979. 13: p. 165-178.

118. Larsson, S. and G. Miksche, *Gaschromatografische Analyse von Ligninoxydationsprodukten. IV. Zur Struktur des Lignins der Birke.* Acta Chemica Scandinavica, 1971. 25: p. 647-662.

119. Robert, D., *Carbon 13 nuclear magnetic resonance spectroscopy*, in *Methods in lignin chemistry*, S.Y. Lin and C.W. Dence, Editors. 1992, Springer-Verlag: Berlin ; New York. p. 250-273.

120. Lapierre, C., et al., *Photosynthetic C-13 enrichment of poplar lignins- preliminary studies by acidolysis and C-13 NMR.* Holzforschung, 1983. 37(5): p. 217.

121. Bardet, M., et al., *Use of C-13 enriched wood for structural NMR investigation of wood and wood components, cellulose and lignin, in solid and in solution.* Holzforschung, 1986. 40(Suppl.): p. 17-24.

122. Kilpelainen, I., et al., *Application of 3-Dimensional HMQC-HOHAHA NMR-Spectroscopy to Wood Lignin, a Natural Polymer.* Tetrahedron Letters, 1994. 35(49): p. 9267-9270.

123. Ammalahti, E., et al., *Identification of side-chain structures in a poplar lignin using three-dimensional HMQC-HOHAHA NMR spectroscopy.* Journal of Agricultural and Food Chemistry, 1998. 46(12): p. 5113-5117.

124. Liitia, T.M., et al., *Analysis of technical lignins by two- and three-dimensional NMR spectroscopy.* Journal of Agricultural and Food Chemistry, 2003. 51(8): p. 2136-2143.

125. Zhang, L.M. and G. Gellerstedt. *Achieving quantitative assignment of lignin structure by combining ^{13}C and HSQC NMR techniques*. in *Proceedings of the 6th European Workshop on Lignocellulosics and Pulp*. 2000. Bordeaux, France.

126. Heikkinen, S., et al., *Quantitative 2D HSQC (Q-HSQC) via suppression of J-dependence of polarization transfer in NMR spectroscopy: Application to wood lignin.* Journal of the American Chemical Society, 2003. 125: p. 4362-4367.

127. Lambert, J.B., et al., *Ch. 2. Introduction and Experimental Methods*, in *Organic Structural Spectroscopy*. 1998, Prentice Hall: Upper Saddle River, NJ. p. 8-37.

128. Ludwig, C.H., B.J. Nist, and J.L. McCarthy, *Lignin XII. The high resolution nuclear magnetic resonance spectroscopy of protons in compounds related to lignin.* Journal of the American Chemical Society, 1964. 86: p. 1186-1196.

129. Ludwig, C.H., B.J. Nist, and J.L. McCarthy, *Lignin XIII. The high resolution nuclear magnetic resonance spectroscopy of protons in acetylated lignins.* Journal of the American Chemical Society, 1964. 86: p. 1196-1202.

130. Ludwig, C.H., *Magnetic Resonance Spectra*, in *Lignins : occurrence, formation, structure and reactions*, K.V. Sarkanen and C.H. Ludwig, Editors. 1971, Wiley-Interscience: New York. p. 299-344.

131. Adler, E., G. Brunow, and K. Lundquist, *Investigation of the acid-catalyzed alkylation of lignins by means of NMR spectroscopic methods.* Holzforschung, 1987. 41: p. 199-207.

132. Bland, D.E. and S. Sternhell, *Estimation of aromatic protons in methanol lignins of Pinus radiata and Eucalyptus regnans from proton magnetic resonance spectra.* Australian Journal of Chemistry, 1965. 18: p. 401-410.

133. Lundquist, K., *NMR studies of lignins 4. Investigation of spruce lignin by ^{1}H NMR spectroscopy.* Acta Chemica Scandinavica B, 1980. 34: p. 21-26.

134. Lundquist, K., *NMR studies of lignins 2. Interpretation of the ^{1}H NMR spectrum of acetylated birch.* Acta Chemica Scandinavica B, 1979. 33: p. 27-30.

135. Gagnaire, D. and D. Robert, *A Polymer Model of Lignin (D.H.P.) ^{13}C Selectively Labelled at the Benzylic Positions: Synthesis and NMR Study.* Makromolecular Chemie, 1977. 178: p. 1477-1495.

136. Lundquist, K., *NMR Studies of Lignins. 3. ^{1}H NMR Spectroscopic Data for Lignin Model Compounds.* Acta Chemica Scandinavica B, 1979. 33: p. 418-420.

137. Brunow, G. and K. Lundquist, *Comparison of a Synthetic Dehydrogenation Polymer of Coniferyl Alcohol with Milled Wood Lignin from Spruce, using 1H NMR Spectroscopy.* Paperi ja Puu, 1980. 62(11): p. 669-671.

138. Chen, C.-L. and D. Robert, *Characterization of lignin by ^{1}H and ^{13}C NMR spectroscopy*, in *Methods in enzymology*, W.A. Wood and S.T. Kellogg, Editors. 1988, Academic Press: San Diego. p. 2 v.

139. Lundquist, K., *Proton (^{1}H) NMR Spectroscopy*, in *Methods in lignin chemistry*, S.Y. Lin and C.W. Dence, Editors. 1992, Springer-Verlag: Berlin ; New York. p. 242-249.

140. Karhunen, P., *Studies on the Syntheses and Reactions of Lignin Model Compounds with Biphenyl, Diaryl Ether and Dibenzodioxocin Structures*, in *Dept. of Chemistry*. 1999, University of Helsinki: Helsinki, Finland. p. 44.

141. Ralph, S.A., L.L. Landucci, and J. Ralph, *NMR database of lignin and cell wall model compounds.* http://www.dfrc.ars.usda.gov/nmrDatabase.html. 2001.

142. Gunther, H., *NMR Spectroscopy. Basic principles, concepts, and applications in chemistry.* 2nd ed. 1995, New York, NY: John Wiley and Sons.

143. Chen, C.-L., *Characterization of MWL and dehydrogenative polymerization from monolignols by carbon 13 NMR spectroscopy*, in *Lignin and lignan biosynthesis*, N.G. Lewis and S. Sarkanen, Editors. 1996, American Chemical Society: Washington, DC. p. 255-275.

144. Capanema, E.A., M.Y. Balakshin, and J.F. Kadla, *A comprehensive approach for quantitative lignin characterization by NMR spectroscopy.* Journal of Agricultural and Food Chemistry, in publication.

145. Ludemann, H.-D. and H.H. Nimz, *C-13-NMR Spectra of Lignins. 2. Beech and Spruce Bjorkman Lignin.* Makromolecular Chemie, 1974. 175: p. 2409-2422.

146. Ludemann, H.-D. and H.H. Nimz, *C-13-NMR Spectra of Lignins.* Makromolecular Chemie, 1974. 175: p. 2393.

147. Nimz, H.H., et al., *Carbon-13 NMR Spectra of Lignins, 8. Structural Differences between Lignins of Hardwoods, Softwoods, Grasses, and Compression Wood.* Holzforschung, 1981. 35: p. 16-26.

148. Kringstad, K.P. and R. Morck, *^{13}C-NMR Spectra of Kraft Lignins.* Holzforschung, 1983. 37: p. 237-244.

149. Ralph, J., et al., *Solution-State NMR of Lignins*, in *Advances in Lignocellulosics characterization*, D.S. Argyropoulos, Editor. 1999, TAPPI Press: Atlanta, GA. p. 55-108.

150. Nimz, H.H. and H.-D. Ludemann, *C-13-NMR Spectra of Lignins. 5. Oligomeric Model Substances of Lignin.* Makromolecular Chemie, 1974. 175: p. 2577-2583.

151. Nimz, H.H. and H.-D. Ludemann, *C-13 NMR-Spectra of Lignins. 6. Lignin and DHP Acetates.* Holzforschung, 1976. 30(2): p. 33-40.

152. Nimz, H.H., et al., *Carbon-13 NMR Spectra of Lignins, 10. Comparison of Structural Units in Spruce and Beech Lignin.* Journal of Wood Chemistry and Technology, 1984. 4(3): p. 265-284.

153. Robert, D. and G. Brunow, *Quantitative Estimation of Hydroxyl Groups in Milled Wood Lignin from Spruce and in a Dehydrogenation Polymer from Coniferyl Alcohol Using ^{13}C NMR Spectroscopy.* Holzforschung, 1984. 38(2): p. 85-90.

154. Morck, R. and K.P. Kringstad, *^{13}C-NMR Spectra of Kraft Lignins II. Kraft Lignin Acetates.* Holzforschung, 1985. 39: p. 109-119.

155. Landucci, L.L., S.A. Ralph, and K.E. Hammel, *^{13}C NMR Characterization of Guaiacyl, Guaiacyl/Syringyl and Syringyl Dehydrogenation Polymers.* Holzforschung, 1998. 52: p. 160-170.

156. Bardet, M., M.F. Foray, and D. Robert, *Use of the DEPT sequence to facilitate the ^{13}C NMR structural analysis of lignins.* Makromolecular Chemie, 1985. 186: p. 1495-1504.

157. Xia, Z., L.G. Akim, and D.S. Argyropoulos, *Quantitative ^{13}C NMR Analysis of Lignins with Internal Standards.* Journal of Agricultural and Food Chemistry, 2001. 49: p. 3573-3578.

158. Ede, R.M. and G. Brunow, *Application of 2-Dimensional homonuclear and heteronuclear correlation NMR-spectroscopy to wood lignin structure determination.* Journal of Organic Chemistry, 1992. 57(5): p. 1477-1480.

159. Kilpelainen, I., et al., *Application of Two-Dimensional NMR Spectroscopy to Wood Lignin Structure Determination and Identification of Some Minor Structural Units of*

Hard- and Softwood Lignins. Journal of Agricultural and Food Chemistry, 1994. 42(12): p. 2790-2794.

160. Quideau, S. and J. Ralph, *A biomimetic route to lignin model compounds via Silver (I) Oxide oxidation.2. NMR characterization of noncylcic benzyl aryl ether trimers and tetramers.* Holzforschung, 1994. 48(2): p. 124-132.

161. Ede, R.M. and J. Ralph, *Assignment of 2D TOCSY spectra of lignins: The role of lignin model compounds.* Magnetic Resonance in Chemistry, 1996. 34(4): p. 261-268.

162. Lambert, J.B., et al., *Ch. 5. Further Topics in One-Dimensional NMR*, in *Organic Structural Spectroscopy*. 1998, Prentice Hall: Upper Saddle River, NJ. p. 8-37.

163. Fukagawa, N., G. Meshitsuka, and A. Ishizu, *A 2-Dimensional NMR-Study of birch milled wood lignin.* Journal of Wood Chemistry and Technology, 1991. 11(3): p. 373-396.

164. Capanema, E.A., et al., *Structural analysis of residual and technical lignins by H-1-C-13 correlation 2D NMR-spectroscopy.* Holzforschung, 2001. 55(3): p. 302-308.

165. Chen, C.L., E.A. Capanema, and H.S. Gracz, *Reaction mechanisms in delignification of pine Kraft-AQ pulp with hydrogen peroxide using Mn(IV)-Me4DTNE as catalyst.* Journal of Agricultural and Food Chemistry, 2003. 51(7): p. 1932-1941.

166. Ralph, J., et al., *Lignin Feruloyl Ester Cross-links in Grasses .1. Incorporation of Feruloyl Esters into Coniferyl Alcohol Dehydrogenation Polymers (21): 2961-2969 NOV 7 1992.* Journal of the Chemical Society-Perkins Transactions 1, 1992. 21: p. 2961-2969.

167. Ralph, J., J.H. Grabber, and R.D. Hatfield, *Lignin-Ferulate cross-links in grasses - active incorporation of ferulate polysaccharide esters into ryegrass lignins.* Carbohydrate Research, 1995. 275(1): p. 167-178.

168. Schaefer, J. and E.O. Stejskal, *Carbon-13 NMR of polymers spinning at the magic angle.* Journal of the American Chemical Society, 1976. 98: p. 1031-1032.

169. Leary, G.J. and R.H. Newman, *Cross Polarization/Magic Angle Spinning Nuclear Magnetic Resonance (CP/MAS) Spectroscopy*, in *Methods in lignin chemistry*, S.Y. Lin and C.W. Dence, Editors. 1992, Springer-Verlag: Berlin ; New York. p. 146-161.

170. Bartuska, V.J., et al., *Structural studies of lignin isolation by ^{13}C NMR.* Holzforschung, 1980. 34: p. 214-217.

171. Hemmingson, J.A. and R.H. Newman, *A CP/MAS ^{13}C NMR study of the effect of steam explosion processes on wood composition and structure.* Journal of Wood Chemistry and Technology, 1985. 5: p. 159-188.

172. Haw, J.F., G.E. Maciel, and H.A. Schroeder, *Carbon-13 nuclear magnetic resonance spectroscopic study of wood pulping with cross polarization and magic angle spinning.* Analytical Chemistry, 1984. 56: p. 1323-1329.

173. Manders, W.F., *Solid state ^{13}C NMR determination of the syringyl/guaiacyl ratio in hardwoods.* Holzforschung, 1987. 41: p. 13-18.

174. Gerasimowicz, W.V., K.B. Hicks, and P.E. Pfeffer, *Evidence for the existence of associated lignin-carbohydrate polymers as revealed by carbon-13 CPMAS solid-state NMR spectroscopy.* Macromolecules, 1984. 17: p. 2597-2603.

175. Hatcher, P.G., *Chemical structural studies of natural lignin by dipolar dephased solid state ^{13}C nuclear magnetic resonance.* Organic Geochemistry, 1987. 11: p. 31-39.

176. Love, G.D., C.E. Snape, and M.C. Jarvis, *Determination of the aromatic lignin content in oak wood by quantitative C-13 solid-state NMR.* Biopolymers, 1992. 32(9): p. 1187-1192.

177. Hawkes, G.E., et al., *A comparison of solution and solid-state ^{13}C NMR spectra of lignins and lignin model compounds.* Holzforschung, 1993. 47: p. 302-312.

178. Liitia, T.M., et al., *Application of solid-state C-13 NMR spectroscopy and dipolar dephasing technique to determine the extent of condensation in technical lignins.* Solid State Nuclear Magnetic Resonance, 2002. 21(3-4): p. 171-186.

179. Dixon, W.T., et al., *Total suppression of sidebands in CPMAS C-13 NMR.* Journal of Magnetic Resonance, 1982. 49(2): p. 341-345.

180. Burum, D.P., *HETCOR in Organic Solids*.

181. Liitia, T.M., S.L. Maunu, and B. Hortling, *Solid-state NMR studies of residual lignin and its association with carbohydrates.* Journal of Pulp and Paper Science, 2000. 26(9): p. 323-330.

182. Brownell, H.H. and K.L. West, *The nature of the lignin-carbohydrate linkage in wood. Fractionation of ball-milled wood solubilized with ethylene oxide.* Pulp and Paper Magazine of Canada, 1961. 62: p. T374-T384.

183. Lin, S.Y., *Ultraviolet Spectroscopy*, in *Methods in lignin chemistry*, S.Y. Lin and C.W. Dence, Editors. 1992, Springer-Verlag: Berlin ; New York. p. 350-365.

184. Lapierre, C., B. Monties, and C. Rolando, *Structural Studies of Lignins - Estimation of Arylglycerol-Arylether Bonds by Means of Thioacidolysis.* Comptes Rendus De L Academie Des Sciences Serie III-Sciences De La Vie-Life Sciences, 1984. 299(11): p. 441-444.

185. Viebock , F. and A. Schwappach, *Eine neue Methode zur massanalytischen Bestimmung der Methoxyl- und Athoxylgruppe. Makro-Analyse.* Ber Dtsch Chem Ges, 1930. 63: p. 2818-2823.

186. Mansfield, S.D. and R. Meder, *Cellulose hydrolysis - the role of monocomponent cellulases in crystalline cellulose degradation.* Cellulose (Dordrecht, Netherlands), 2003. 10(2): p. 159-169.

187. Hon, D.N.S. and W.G. Glasser, *Effect of mechanical action on wood and fiber components.* Tappi, 1979. 62: p. 107-110.

188. Onnerud, H. and G. Gellerstedt. *Inhomogeneities in the chemical structure of spruce lignin*. in *11th International Symposium of Wood and Pulping Chemistry Proceedings*. 2001. Nice, France: Association Technique de L'Industrie Papetiere.

189. Terashima, N., K. Fukushima, and T. Imai, *Morphological origin of milled wood lignin studied by radiotracer method.* Holzforschung, 1992. 46: p. 271-275.

190. Ralph, J. and F.C. Lu, *The DFRC method for lignin analysis. 6. A simple modification for identifying natural acetates on lignins.* Journal of Agricultural and Food Chemistry, 1998. 46: p. 4616-4619.

191. Pasco, M.F. and I.D. Suckling, *Lignin removal during kraft pulping - An investigation by thioacidolysis.* Holzforschung, 1994. 48: p. 504-508.

192. Marques, A.V., et al., *Structural characterization of cork lignin by thioacidolysis and permanganate oxidation.* Holzforschung, 1999. 53: p. 167-174.

193. Ralph, J. and J.H. Grabber, *Dimeric beta-ether thioacidolysis products resulting from incomplete ether cleavage.* Holzforschung, 1996. 50: p. 425-428.

194. Iiyama, K. and A.F.A. Wallis, *Dissolution of wood with acetyl bromide solutions - Reactions of lignin model compounds.* Journal of Wood Chemistry and Technology, 1990. 10: p. 39-58.

195. Lu, F.C. and J. Ralph, *The DFRC method for lignin analysis. 7.Behavior of cinnamyl end groups.* Journal of Agricultural and Food Chemistry, 1999. 47: p. 1981-1987.

196. Ralph, J., *personal communication*.

197. Balakshin, M.Y. and E.A. Capanema, *personal communication*.

198. Adler, E., *Lignin chemistry - past, present and future.* Wood Science and Technology, 1977. 11(3): p. 169-218.

199. Erickson, M., S. Larsson, and G.E. Miksche, *Analysis Using Gas-Chromatography of Lignin Oxidation-Products .8. Structure of Spruce Lignin.* Acta Chemica Scandinavica, 1973. 27(3): p. 903-914.

200. Argyropoulos, D.S., *Quantitative P-31 NMR analysis of 6 soluble Lignins.* Journal of Wood Chemistry and Technology, 1994. 14(1): p. 65-82.

201. Pew, J.C., *Evidence of a Biphenyl Group in Lignin.* Journal of Organic Chemistry, 1963. 28(4): p. 1048.

202. Drumond, M., et al., *Substituent Effects on C-13 Chemical-Shifts of Aromatic Carbons in Biphenyl Type Lignin Model Compounds.* Journal of Wood Chemistry and Technology, 1989. 9(4): p. 421-441.

203. Teleman, A., et al., *Characterization of O-acetyl-(4-O-methylglucurono)xylan isolated from birch and beech.* Carbohydrate Research, 2002. 337: p. 373-377.

204. Evtuguin, D.V., et al., *Characterization of an acetylated heteroxylan from Eucalyptus globulus Labill.* Carbohydrate Research, 2003. 338: p. 597-604.

205. Holtman, K.M. unpublished results.

206. Connors, W.J., S. Sarkanen, and J.L. McCarthy, *Gel Chromatography and Association Complexes of Lignin.* Holzforschung, 1980. 34(3): p. 80-85.

207. Sjoholm, E., K. Gustafsson, and A. Colmsjo, *Size exclusion chromatography of lignins using Lithium Chloride/N,N-Dimethylacetamide as mobile phase. I. Dissolved and residual pine kraft lignins.* Journal of Liquid Chromatography & Related Technologies, 1999. 22(11): p. 1663-1685.

208. Sjoholm, E., K. Gustafsson, and A. Colmsjo, *Size exclusion chromatography of lignins using Lithium Chloride/N,N-Dimethylacetamide as mobile phase. II. Dissolved and residual pine kraft lignins.* Journal of Liquid Chromatography & Related Technologies, 1999. 22(18): p. 2837-2854.

209. Braun, J.L., K.M. Holtman, and J.F. Kadla, *Lignin-based carbon fibers 2. Oxidative thermostabilization of kraft lignin.* Carbon, under review.